The Earth's Lowermost Mantle: Compositional Effects on the Post-Perovskite Transition

Krystle Catalli

Sang-Heon Shim, Brent Grocholski, Vitali Prakapenka

SSGF STEWARDSHIP SCIENCE GRADUATE FELLOWSHIP

NSF

COMPRES

EAPS Earth, Atmospheric and Planetary Sciences

Outline

- Earth structure
- Perovskite and post-perovskite
- Experiments
- Results
  - Binary and ternary systems
  - Multi-mineral systems
- Geophysical implications

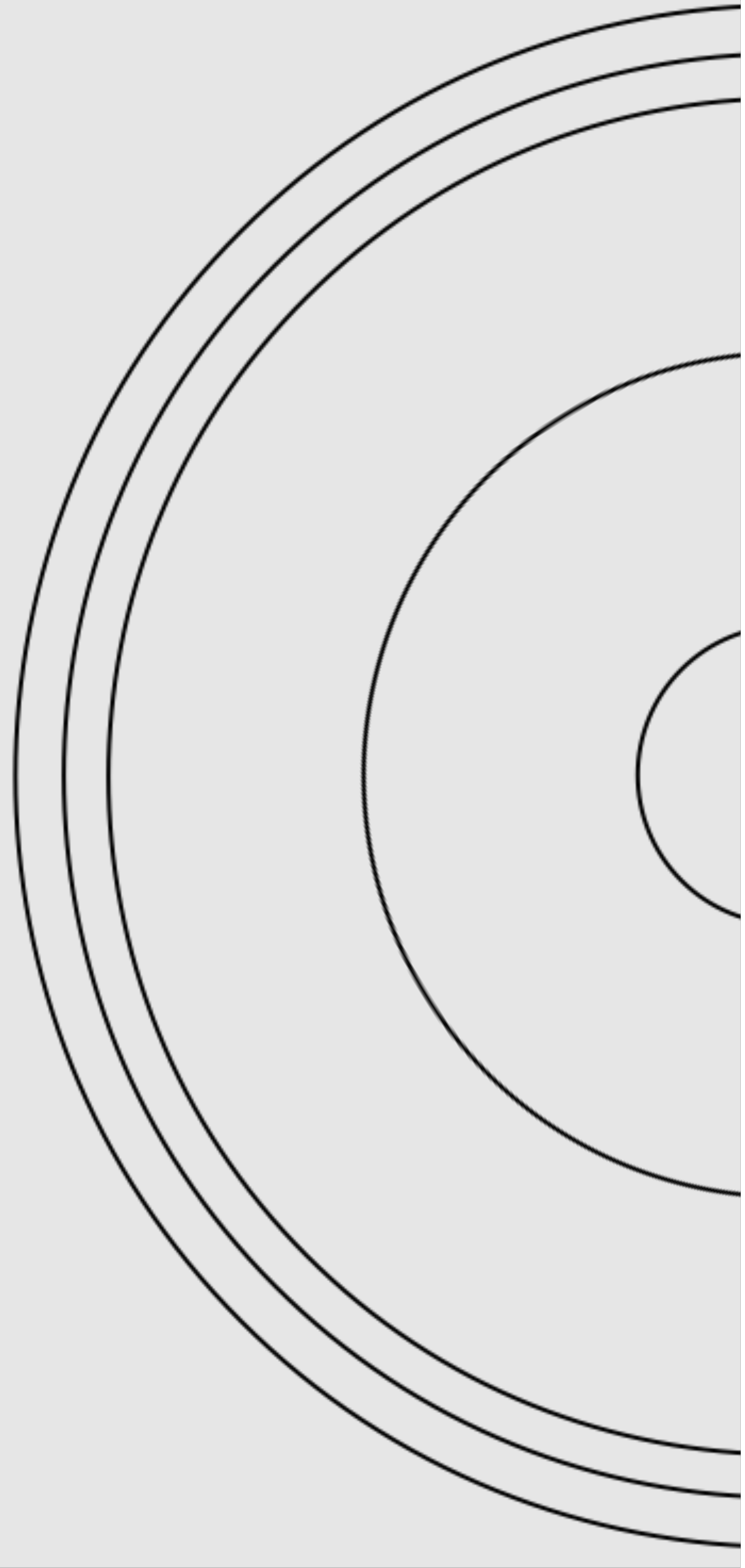

The Earth

The layered structure of the Earth is known from seismology:

- 410 and 660 are due to structural transitions in minerals
- CMB is a chemical transition
- ICB is a liquid-solid transition

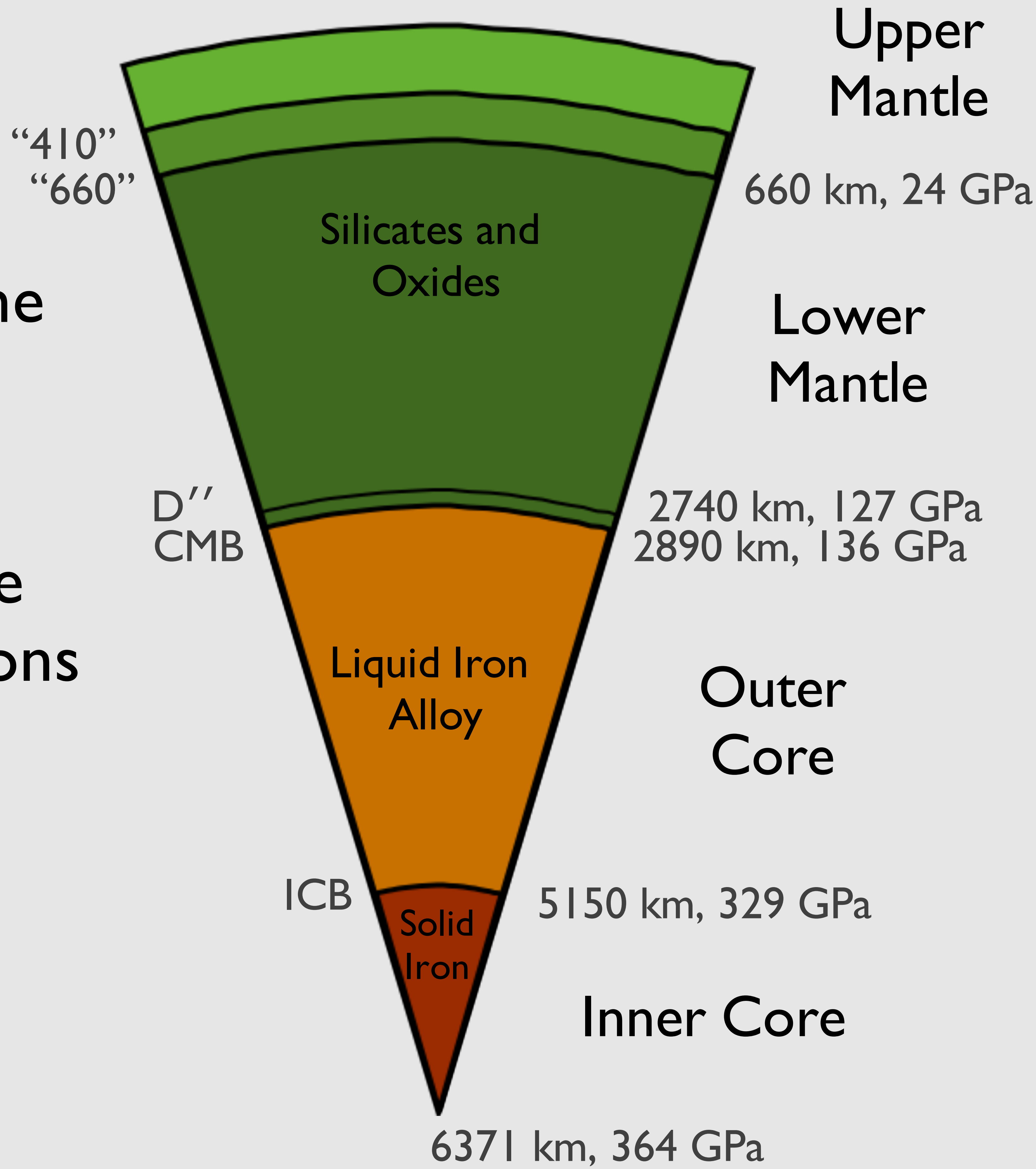

Depth/pressure values from PREM

The D′′ layer

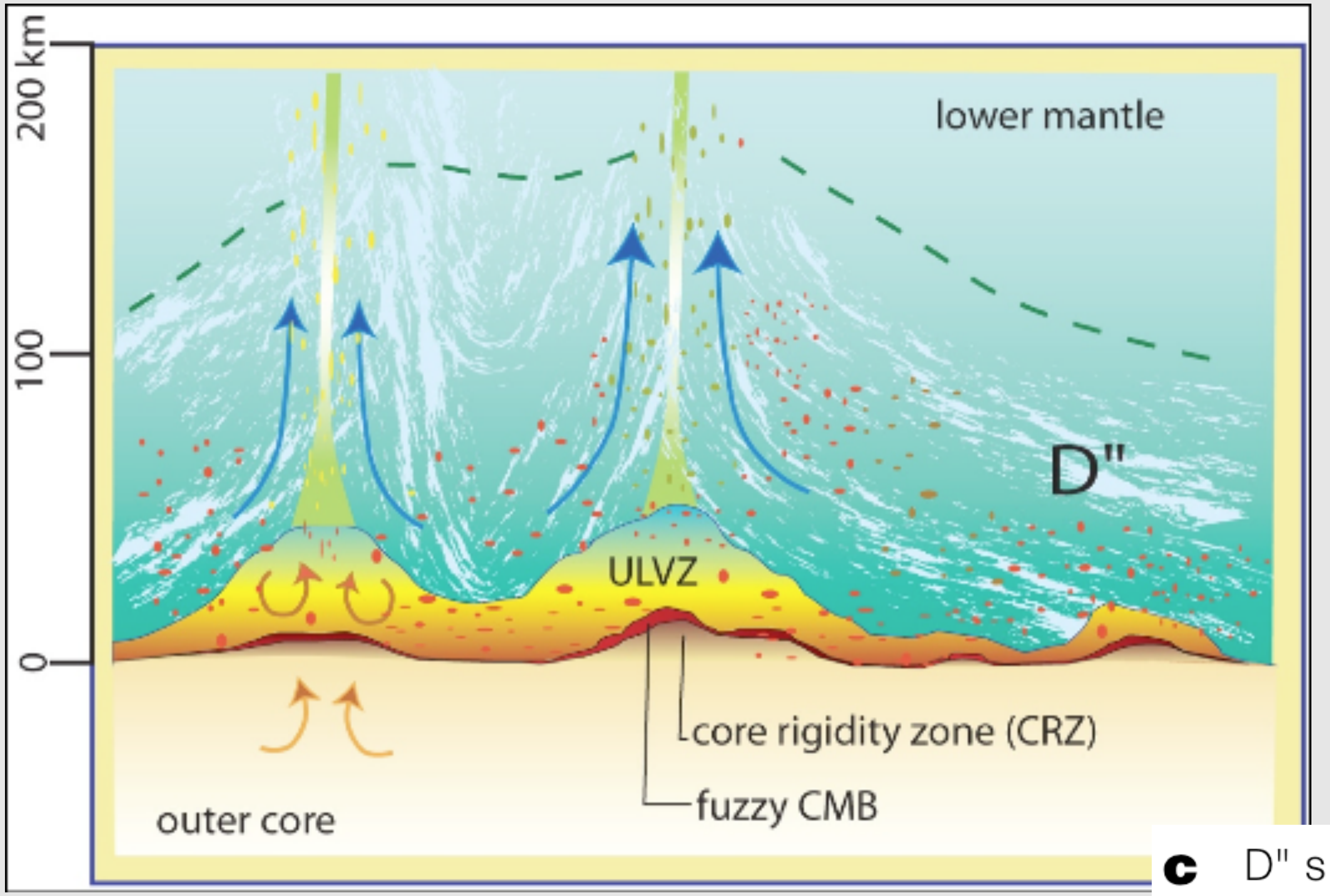

garnero.asu.edu

seismic discontinuity of varying depth

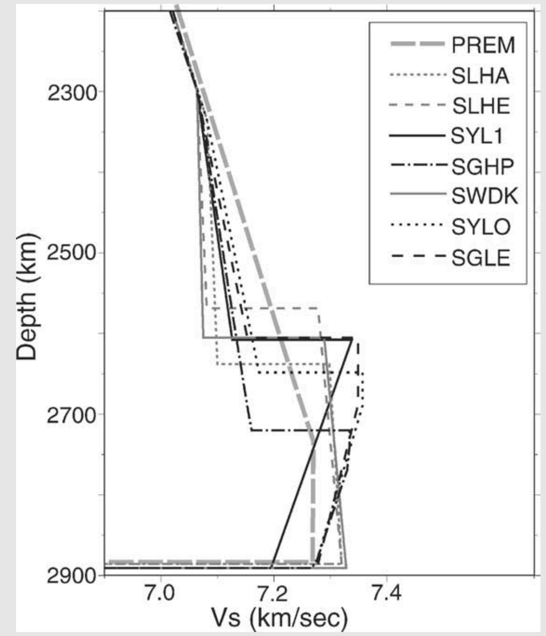

anisotropic seismic wavespeeds

regions of ultra low velocities

unclear if it occurs globally

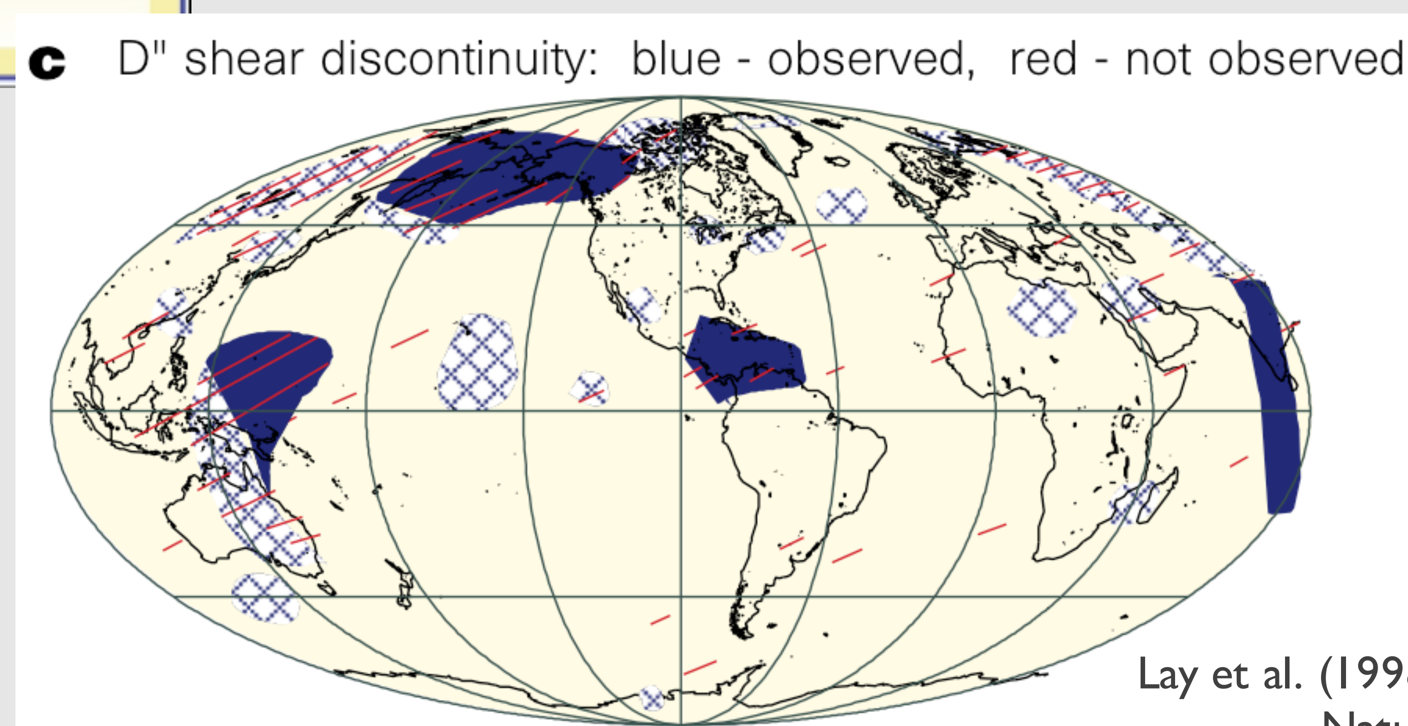

Lay et al. (1998) Nature

$MgSiO_3$ Perovskite

~125 GPa →

$MgSiO_3$ Post-Perovskite

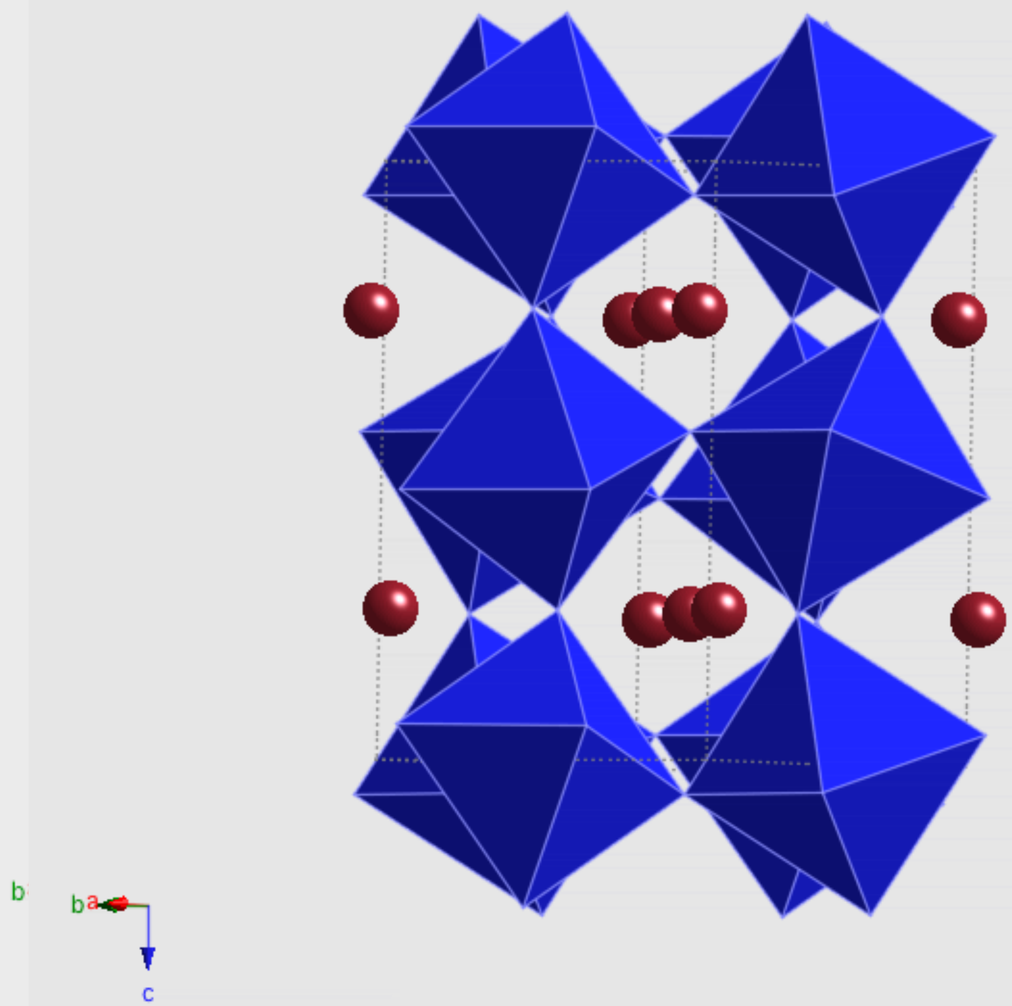

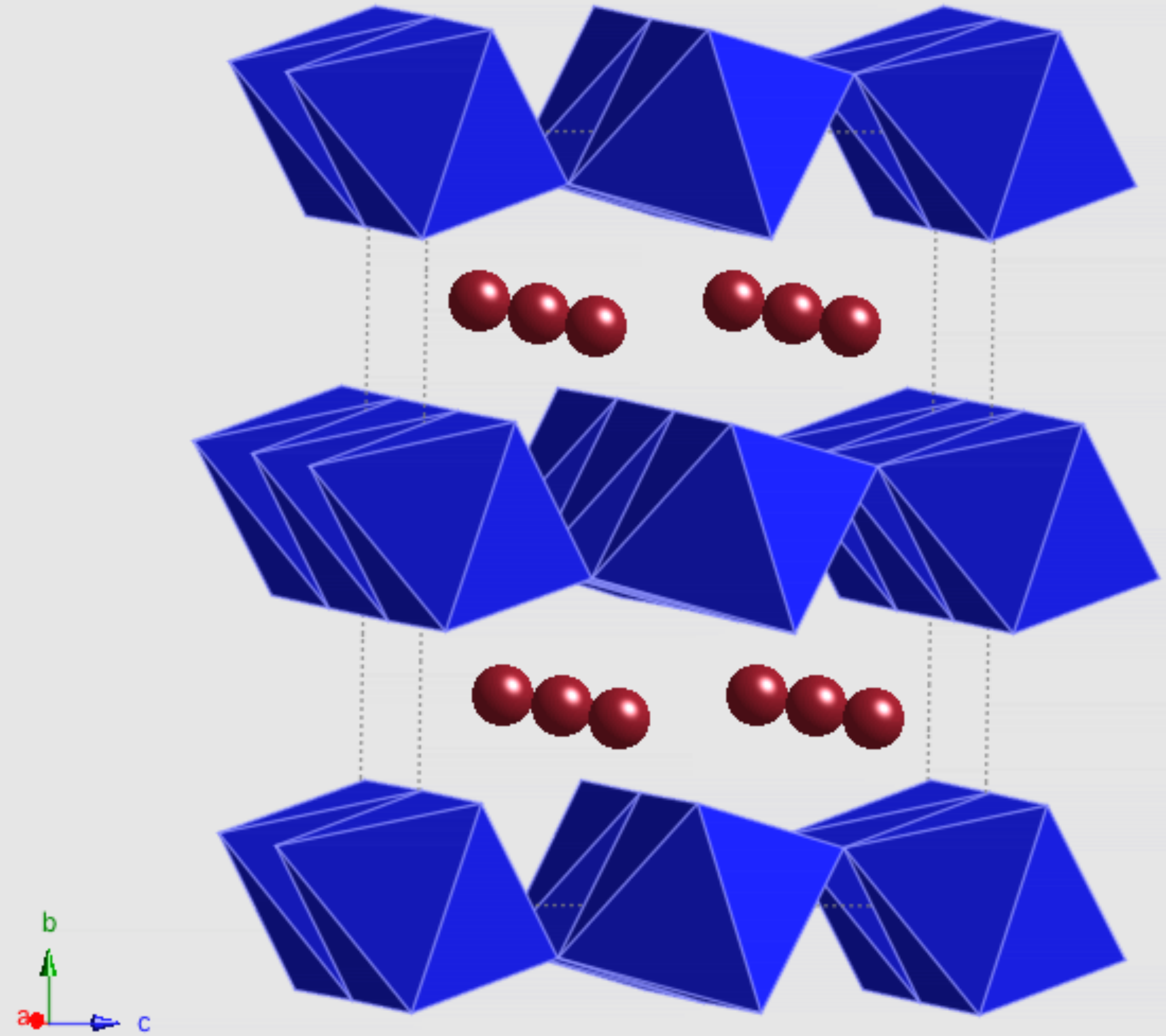

Si 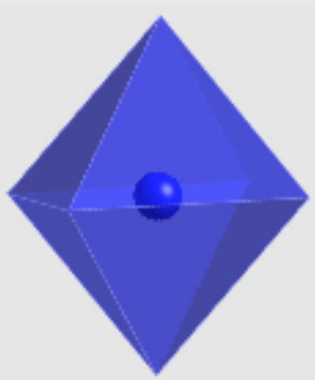 Mg 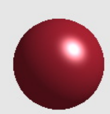

Transition discovered in 2004: Murakami et al. (2004) Science; Oganov and Ono (2004) Nature; Shim et al. (2004) GRL

Using PPv to explain seismic observations

- Seismic discontinuity → phase transition

e.g. Murakami et al, 2004, Science

- Anisotropy → deformation of PPv

e.g. Miyagi et al, 2010, Science

- ULVZ → Fe enrichment of PPv

Mao et al, 2006, Science

- Intermittent detection of D′′ and varying depth. . .

Models for pure $MgSiO_3$

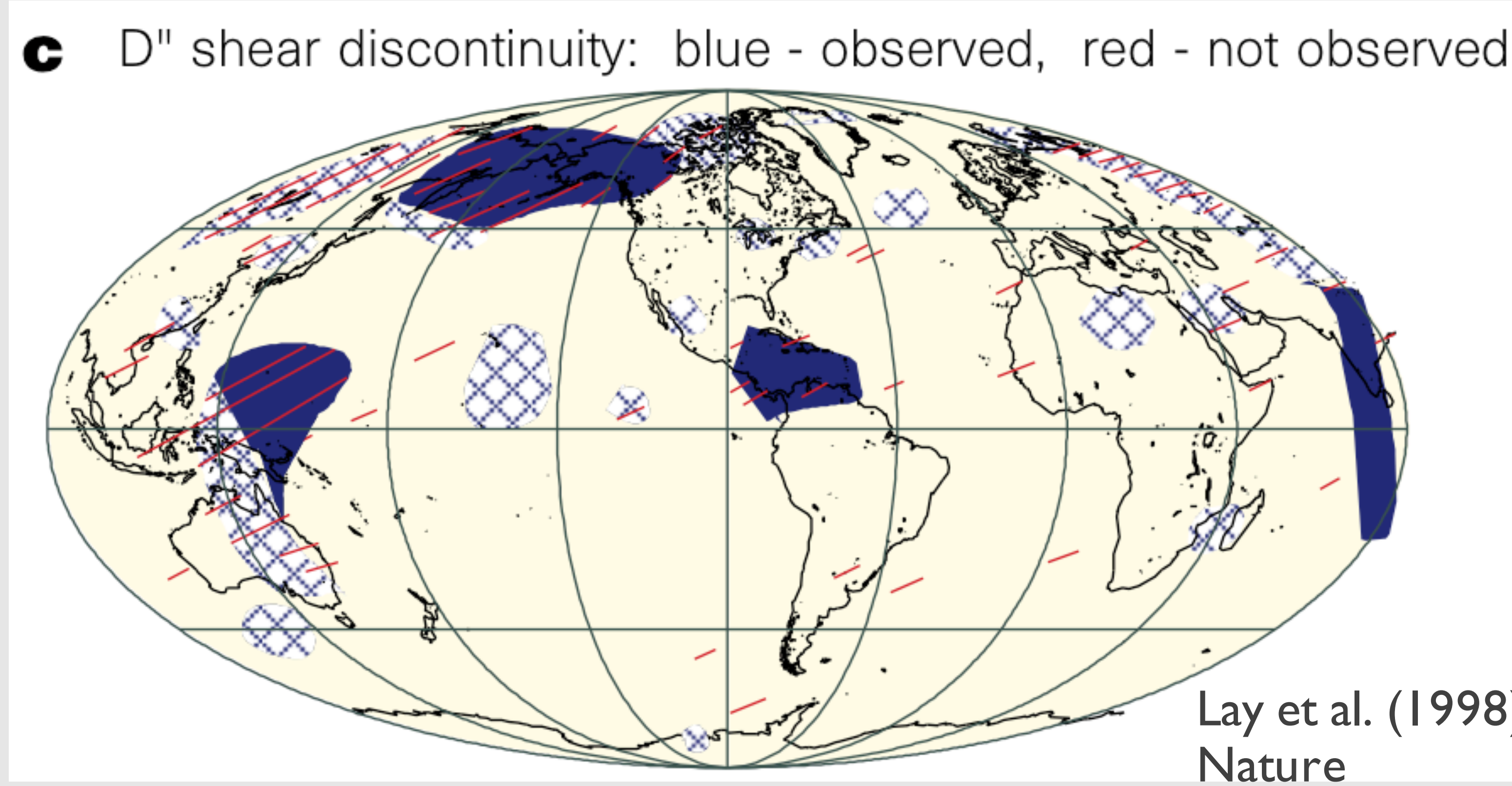

Lay et al. (1998) Nature

PPv

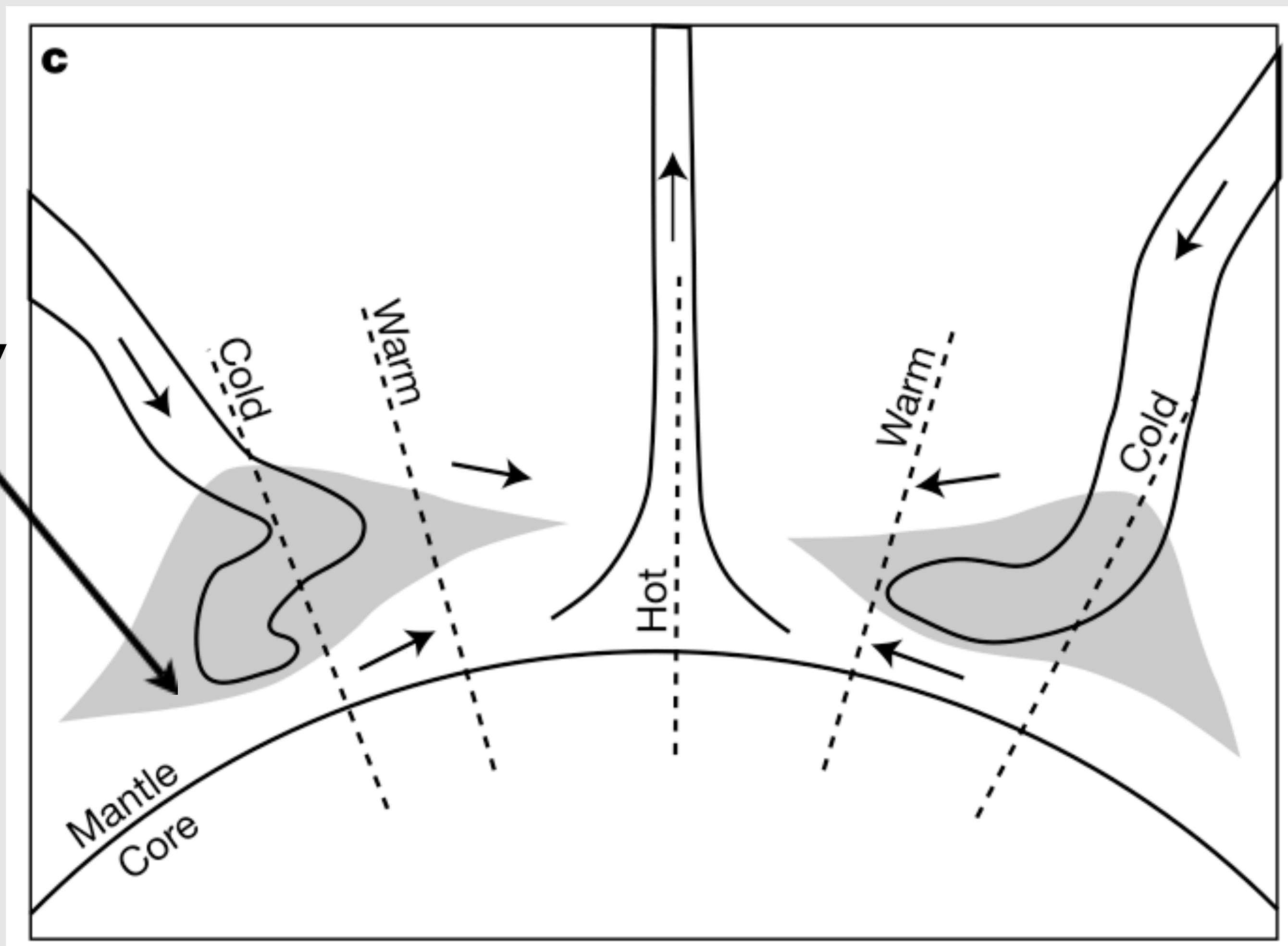

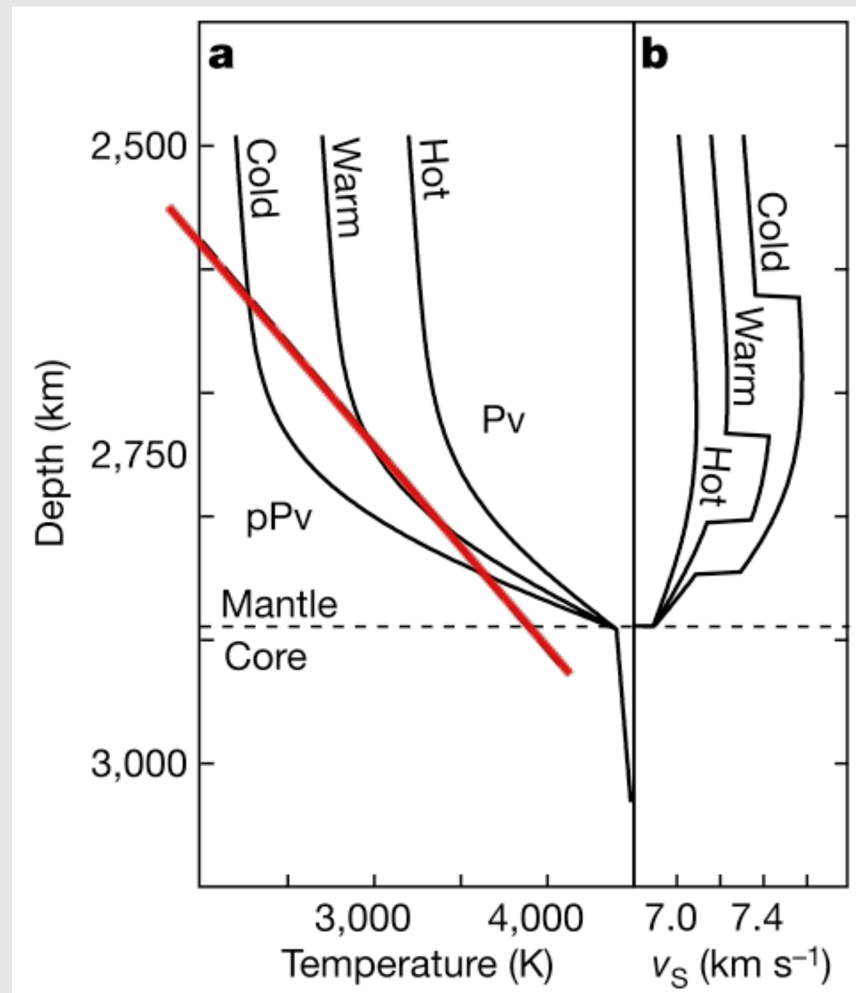

Hernlund et al. (2005) Nature

What about compositional effects?

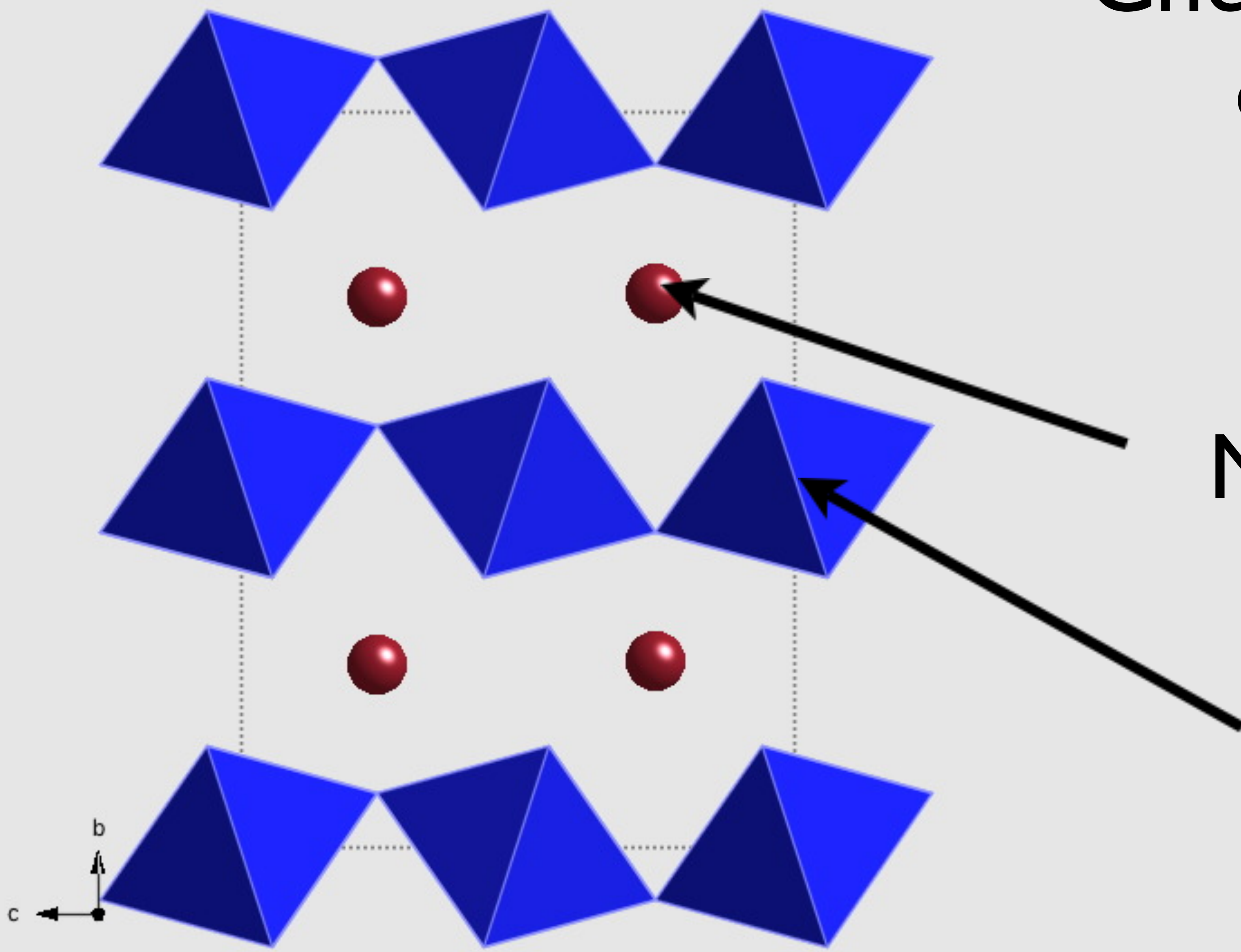

Chemical composition of PPv (and Pv)

Mg: Fe^{2+}, Fe^{3+}, Al

Si: Al, Fe^{3+}

Thickness of mantle phase boundaries

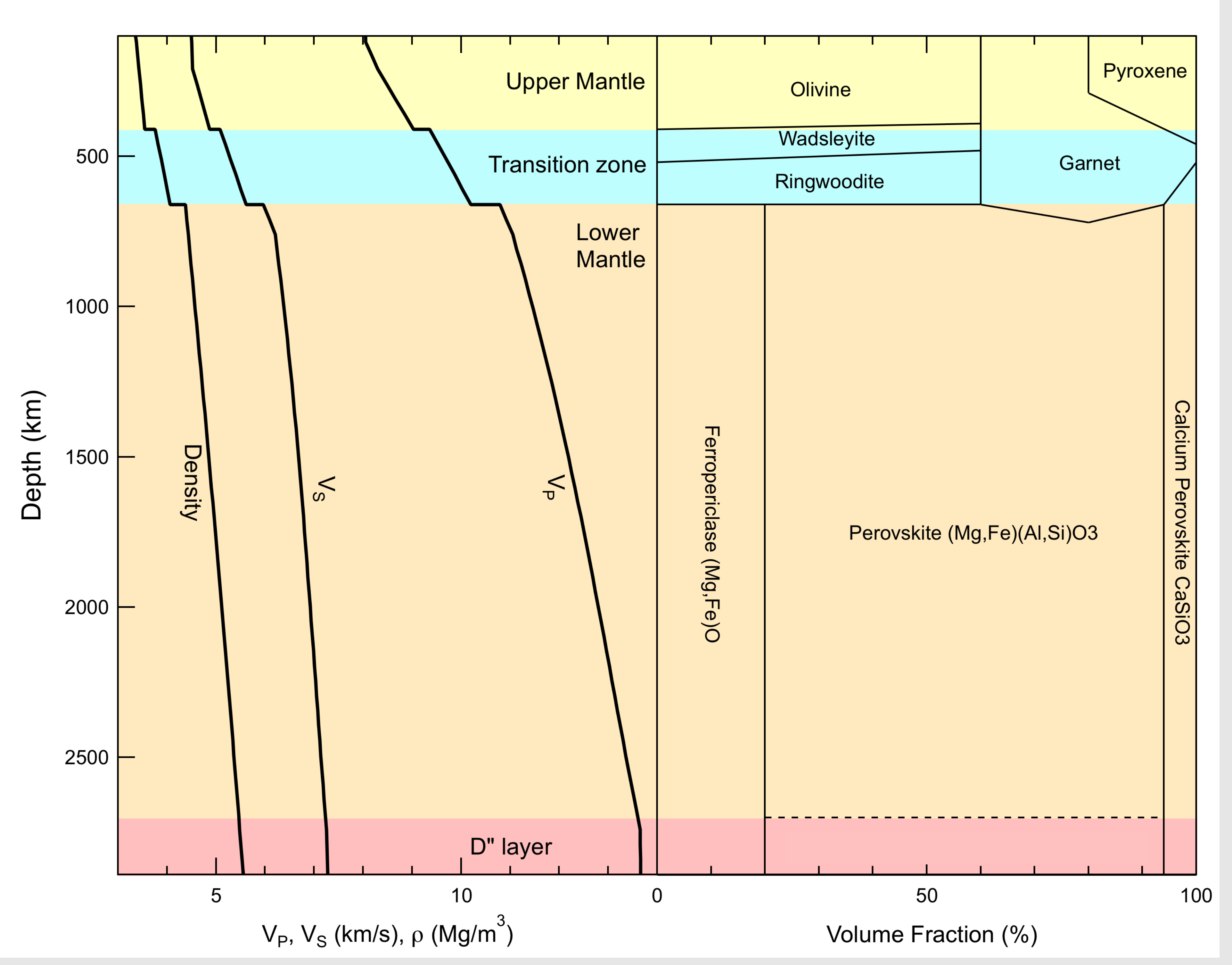

Seismology Mineralogy

Thickness of mantle phase boundaries

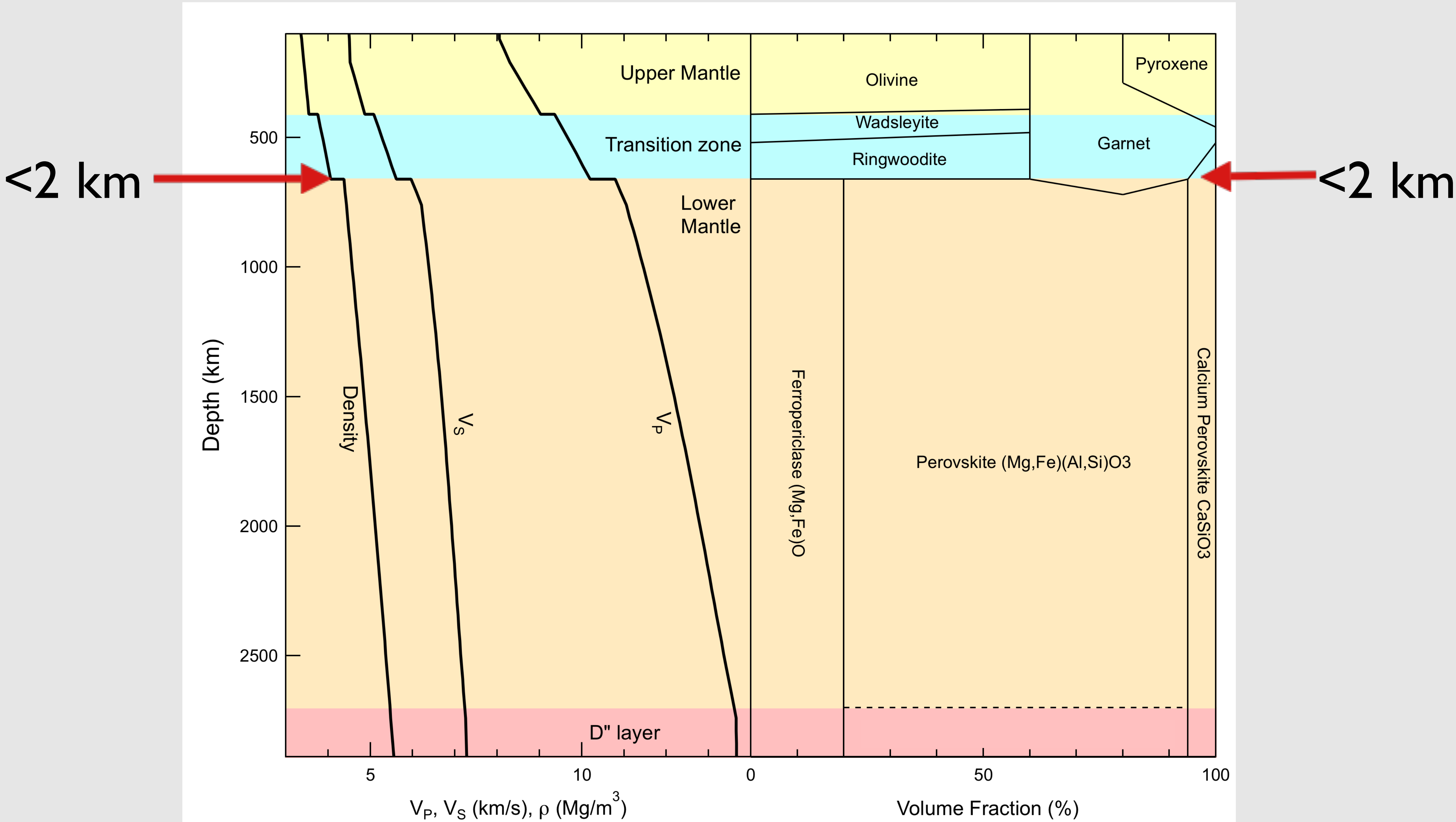

Seismology Mineralogy

Thickness of mantle phase boundaries

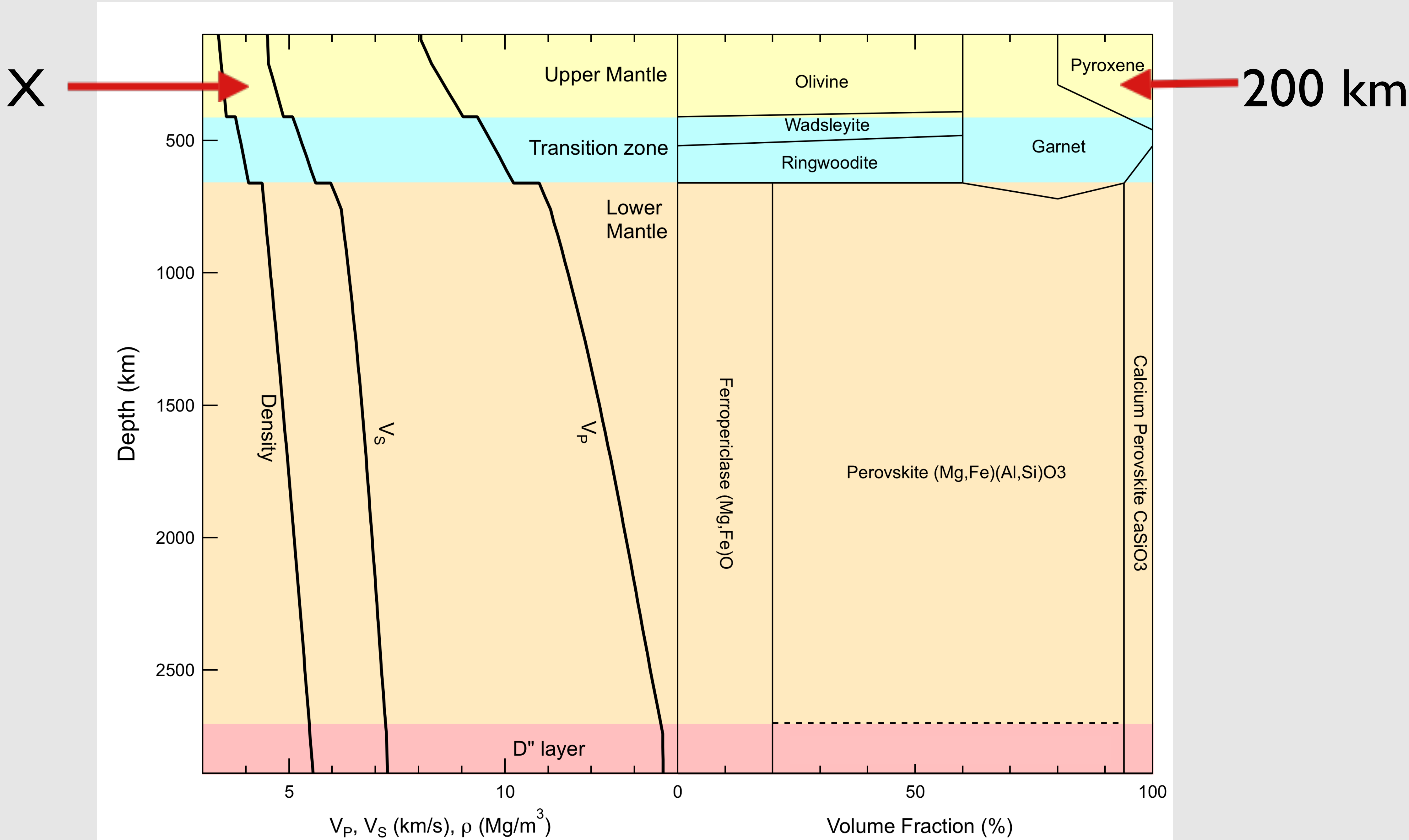

Seismology Mineralogy

Thickness of mantle phase boundaries

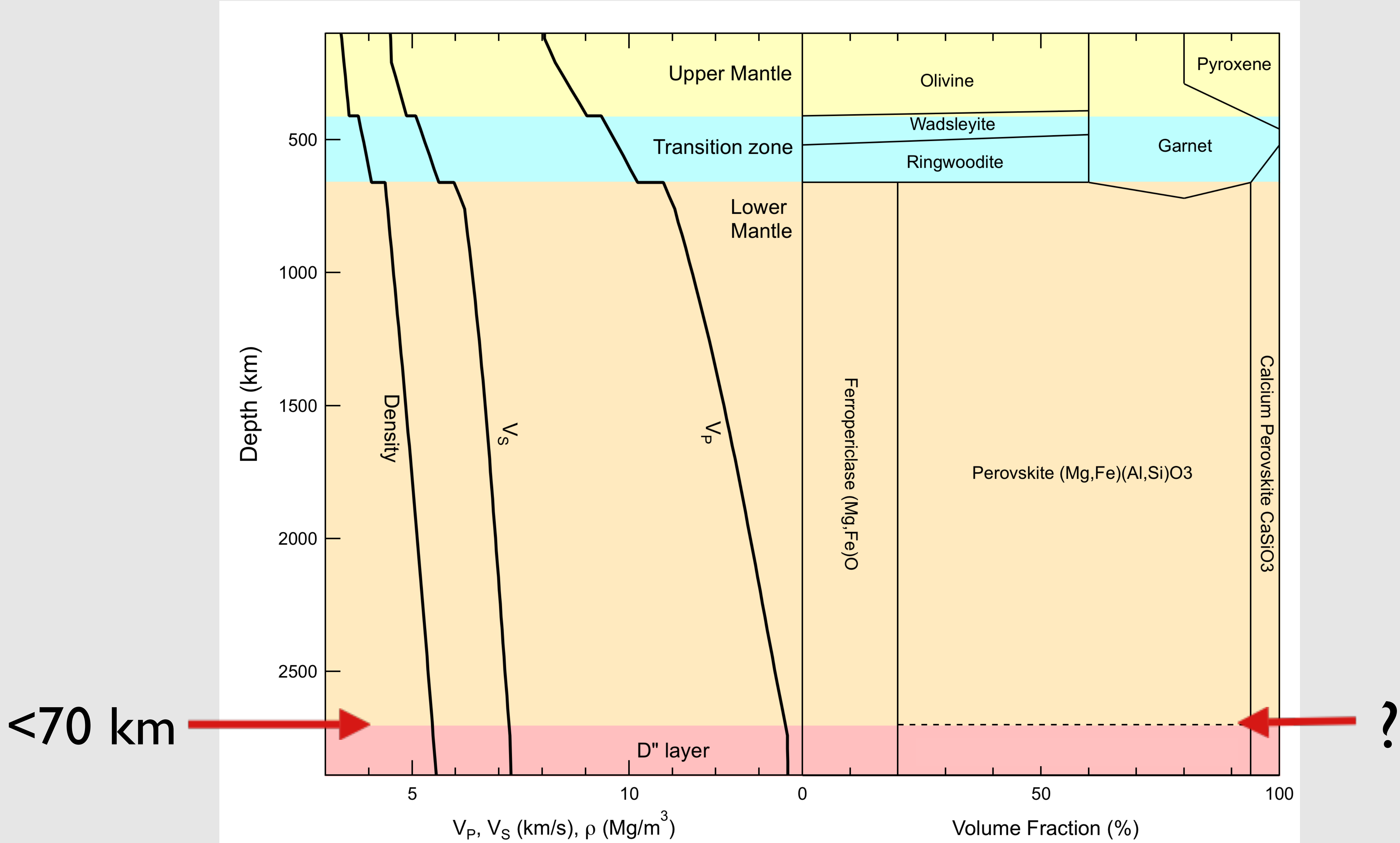

Seismology Mineralogy

Diamond anvil cell

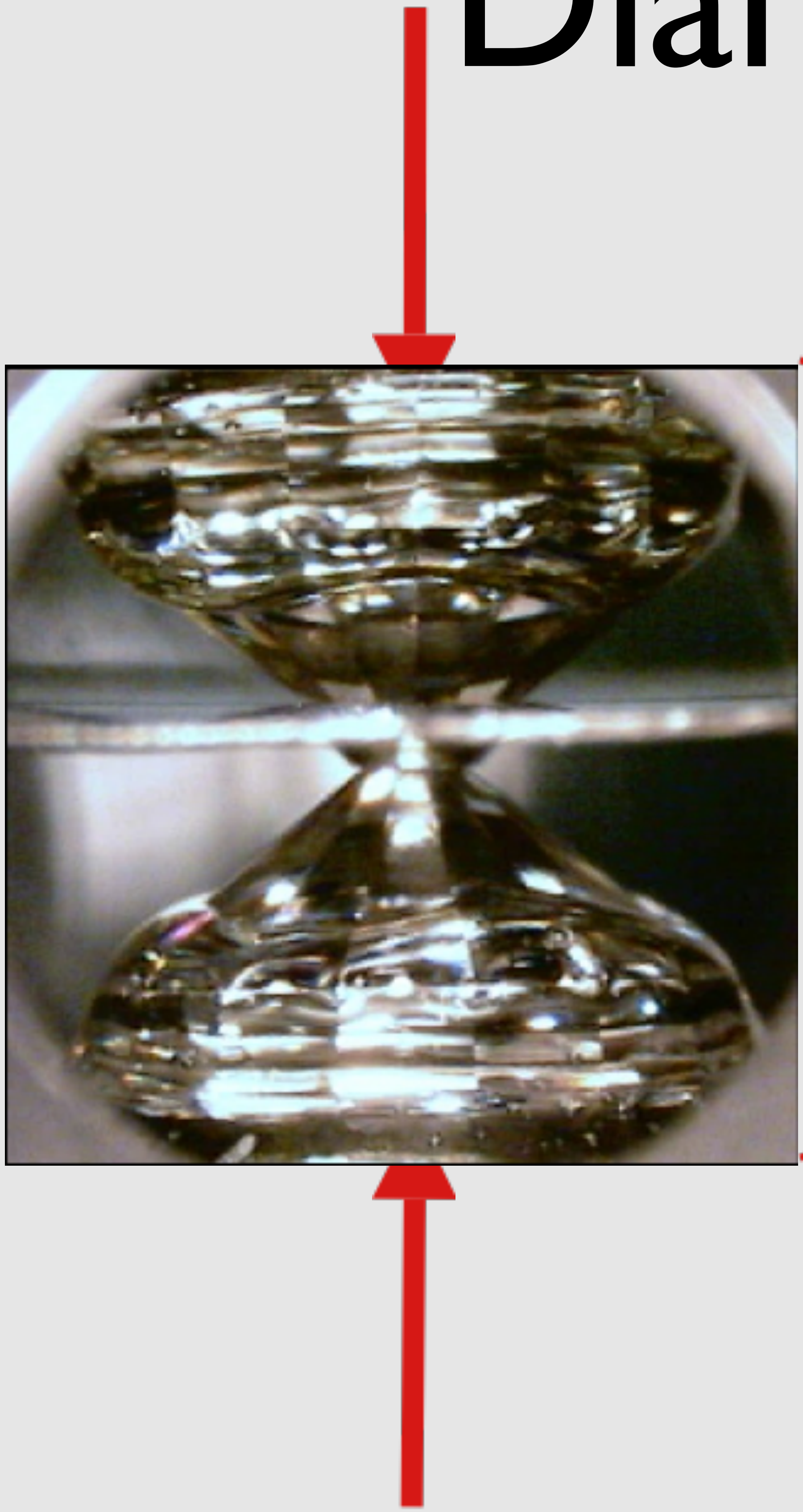

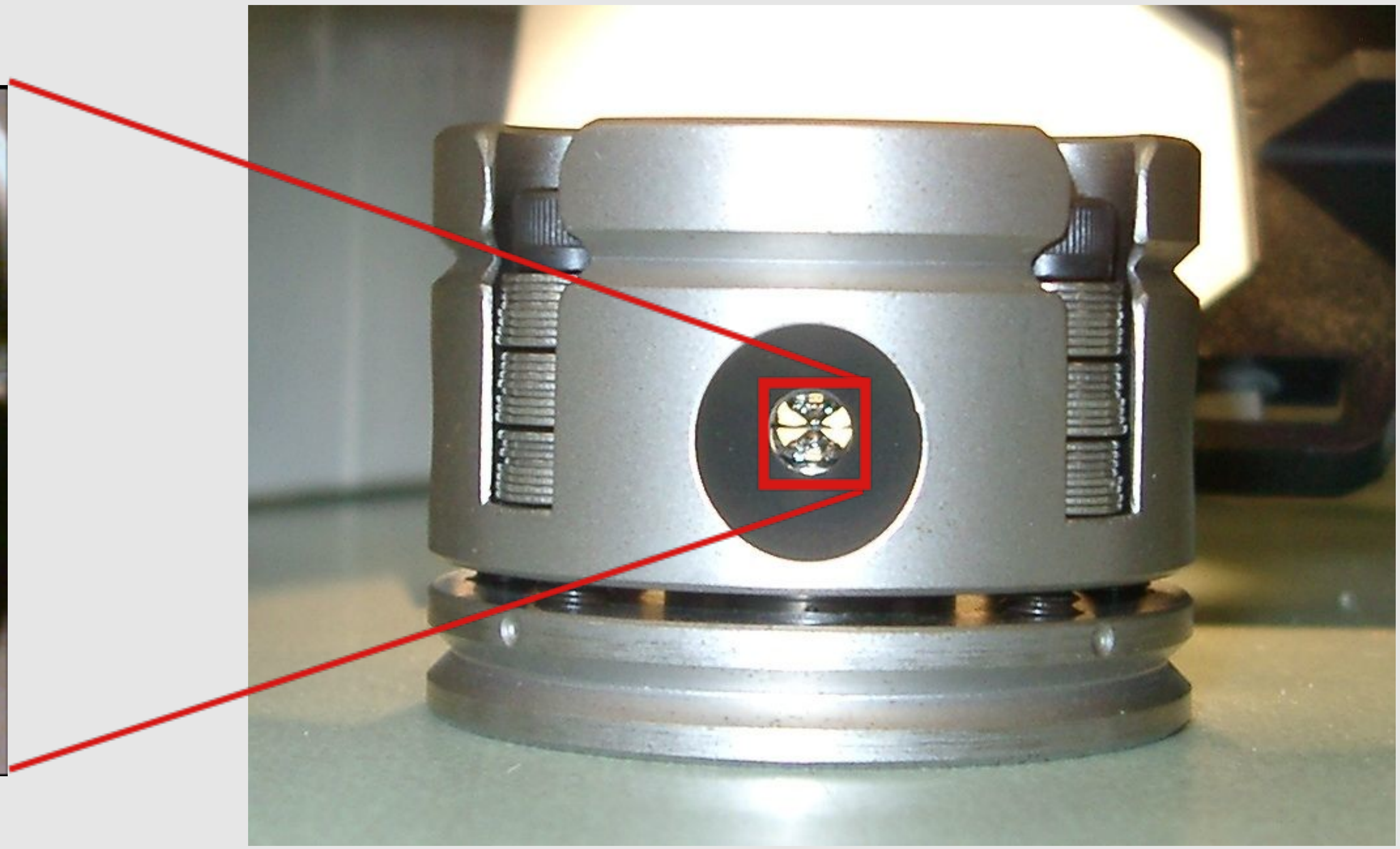

- Brilliant cut, internally flawless, natural 0.25 carat diamonds

Diamond anvil cell

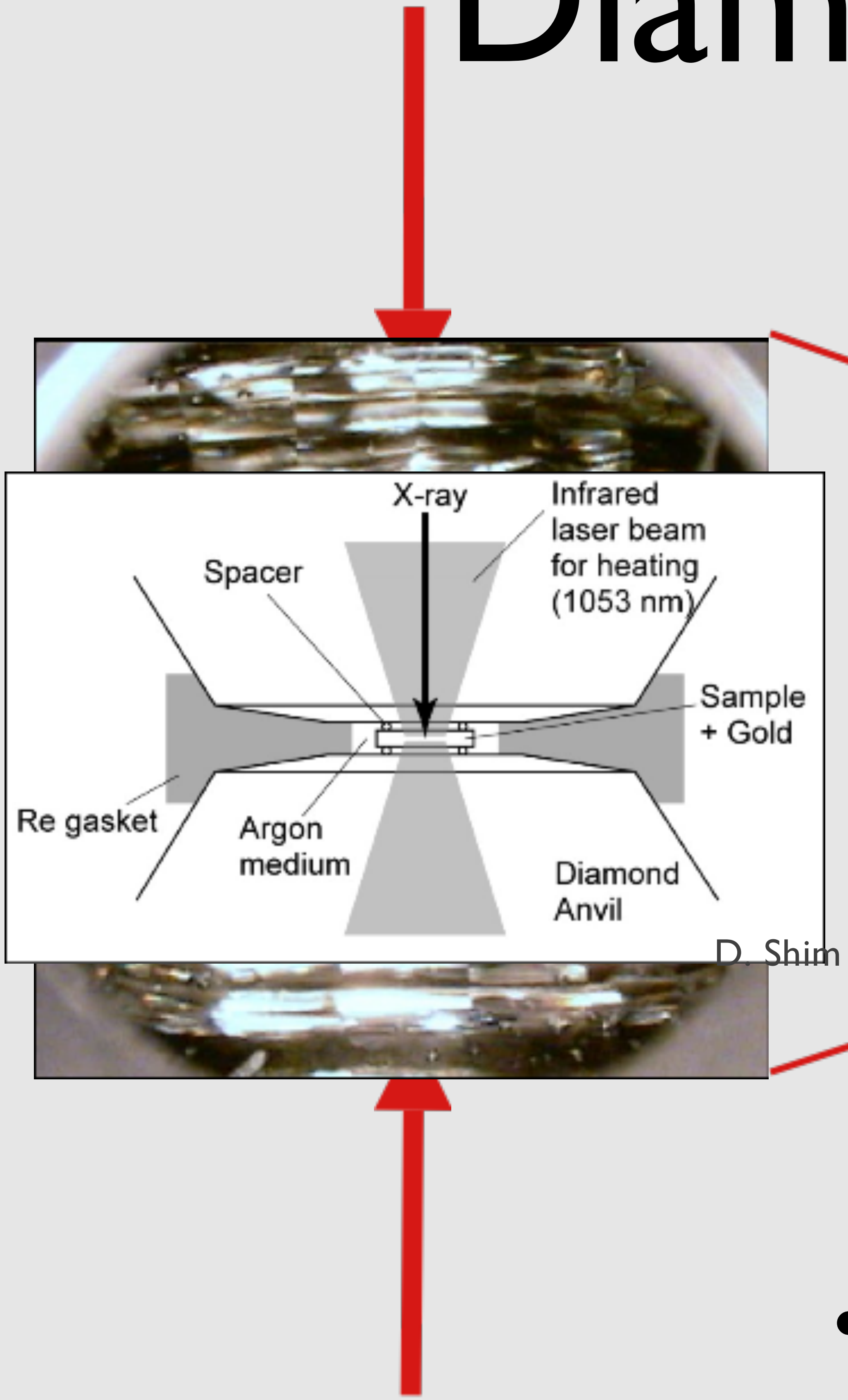

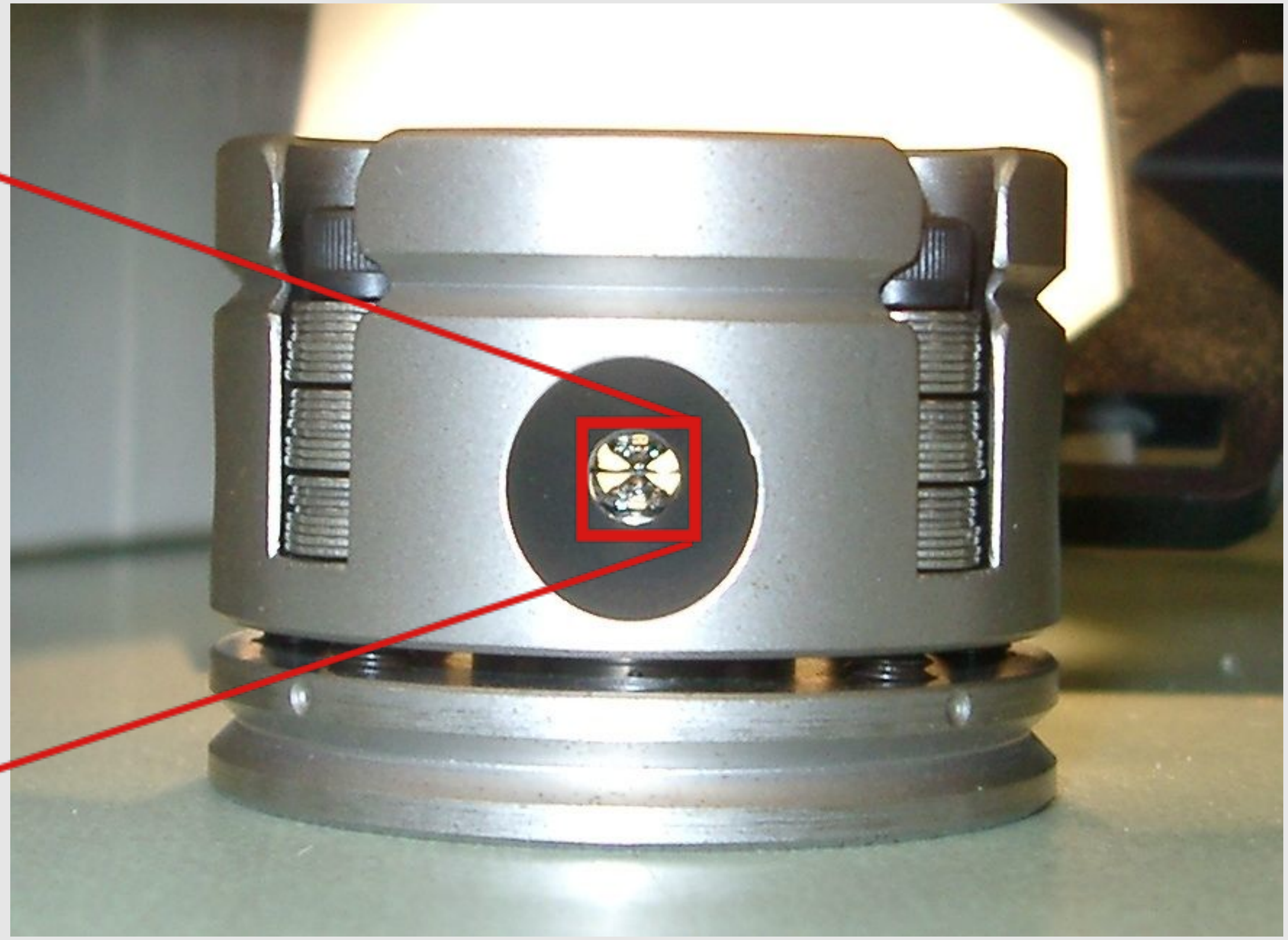

- Transparent to a wide range of wavelengths of light

Advanced Photon Source, Argonne National Lab

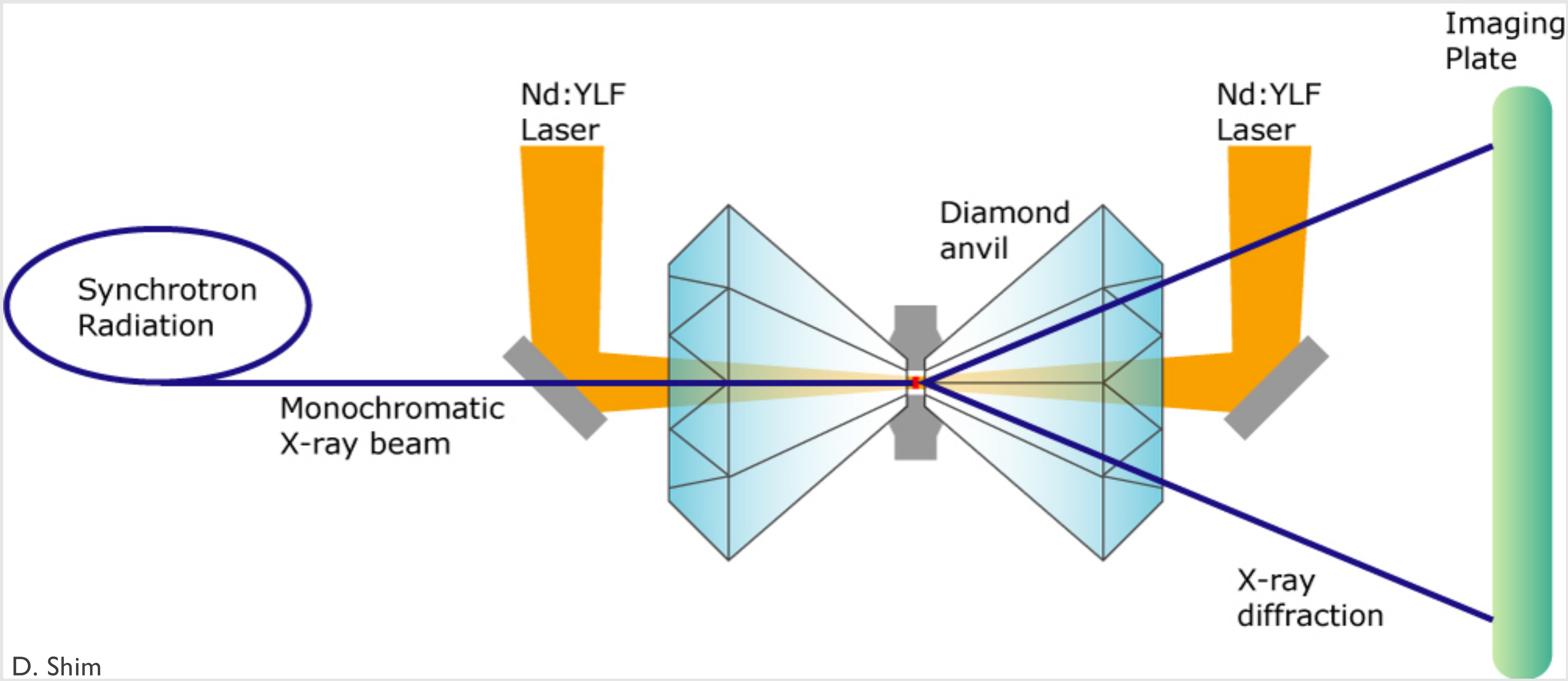

Pv → PPv

- Ternary and binary systems
- Multi-mineral systems

Starting materials

- Homogenous glasses synthesized using the laser levitation method
  - $0.9\ MgSiO_3 - 0.1\ Fe_2O_3$ **Fe^{3+}**
  - $0.9\ MgSiO_3 - 0.05\ Fe_2O_3 - 0.05\ Al_2O_3$ **Fe^{3+} and Al^{3+}**
- Natural enstatite crystal
  - $(Mg_{0.91},Fe_{0.09})_2Si_2O_6$ **Fe^{2+}**

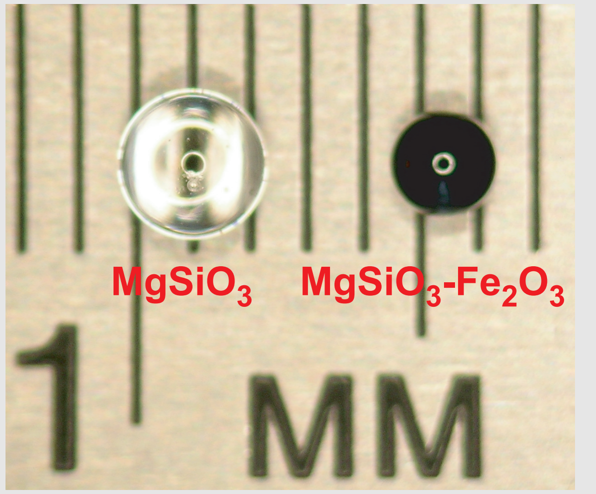

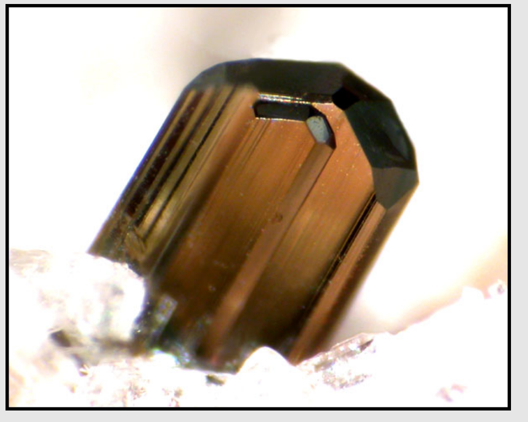

mindat.org

Assess the effects of Fe^{2+}, Fe^{3+} and Al^{3+} on the Pv→PPv phase transition

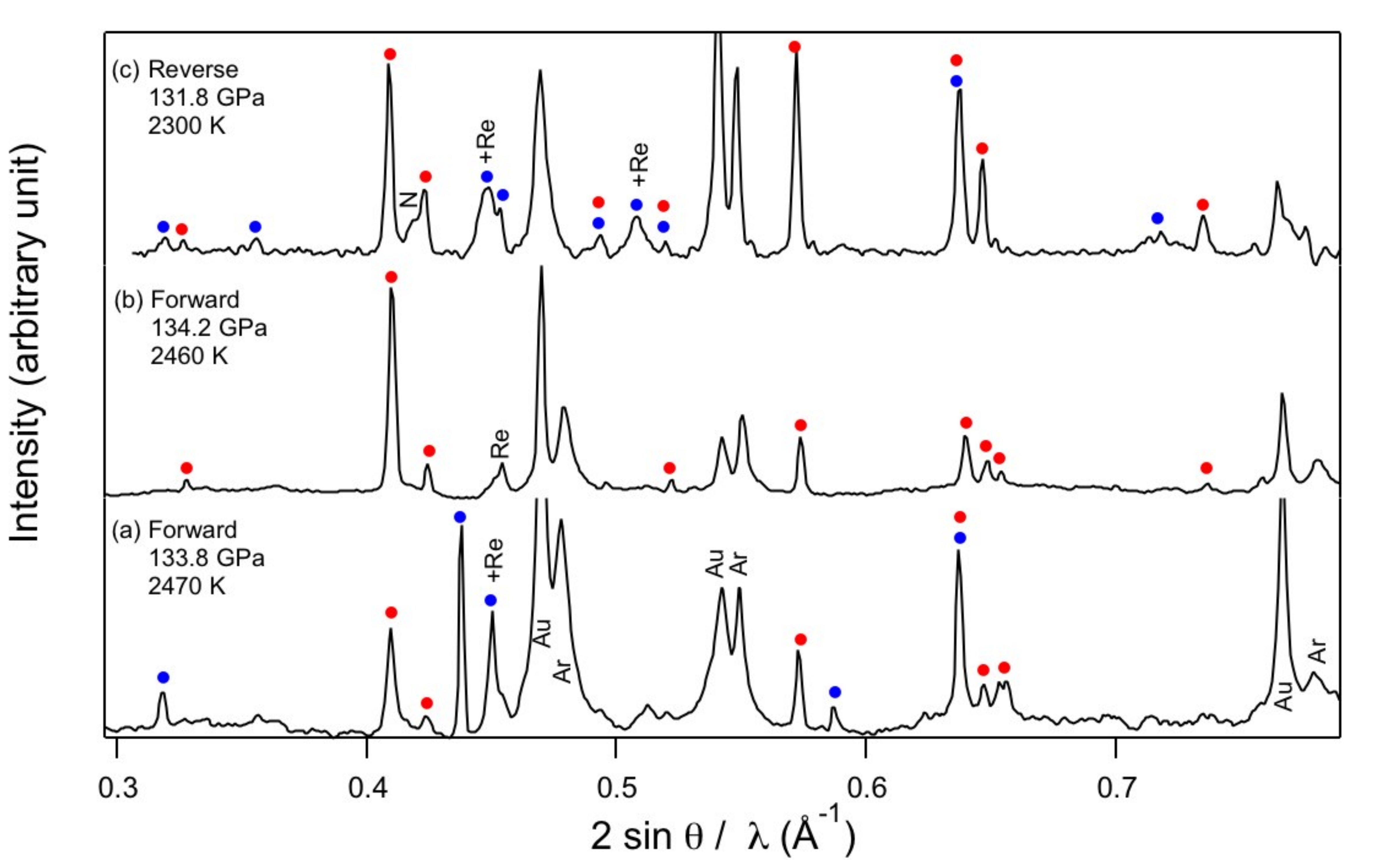

Catalli et al., 2009, Nature

● post-perovskite ● perovskite

$(Mg_{0.91},Fe^{2+}_{0.09})SiO_3$

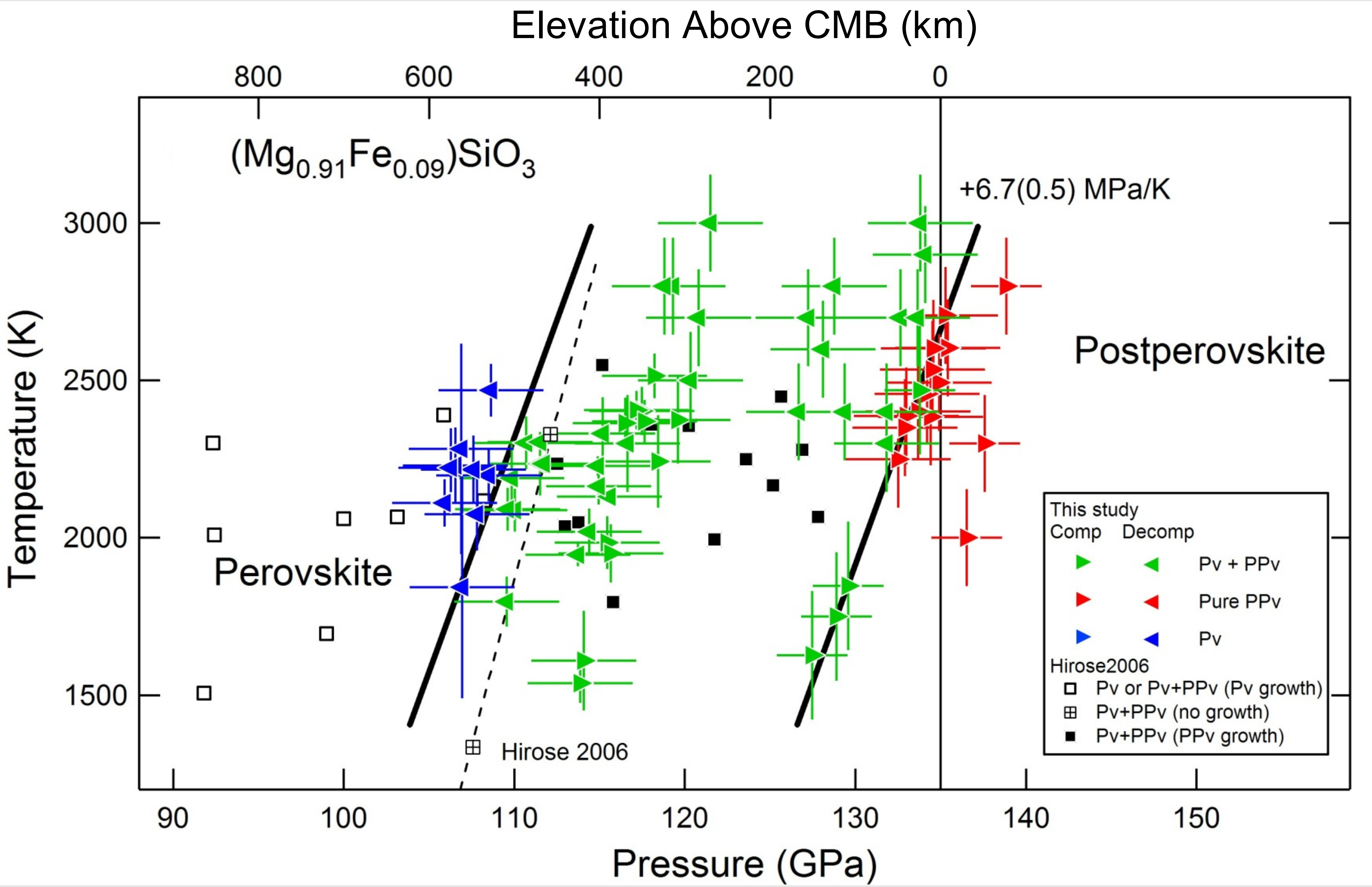

Catalli et al., 2009, Nature

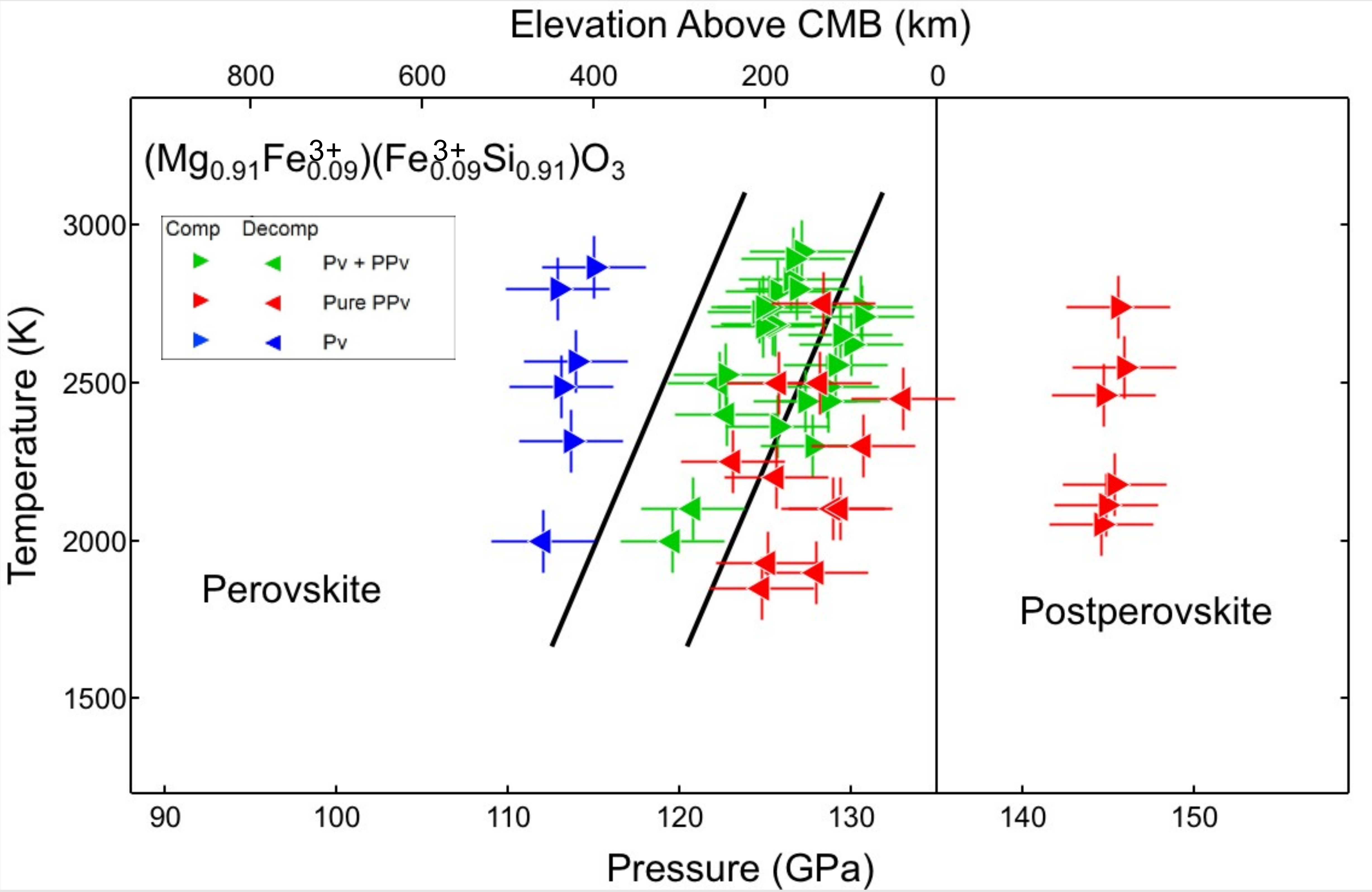

Catalli et al., 2009, Nature

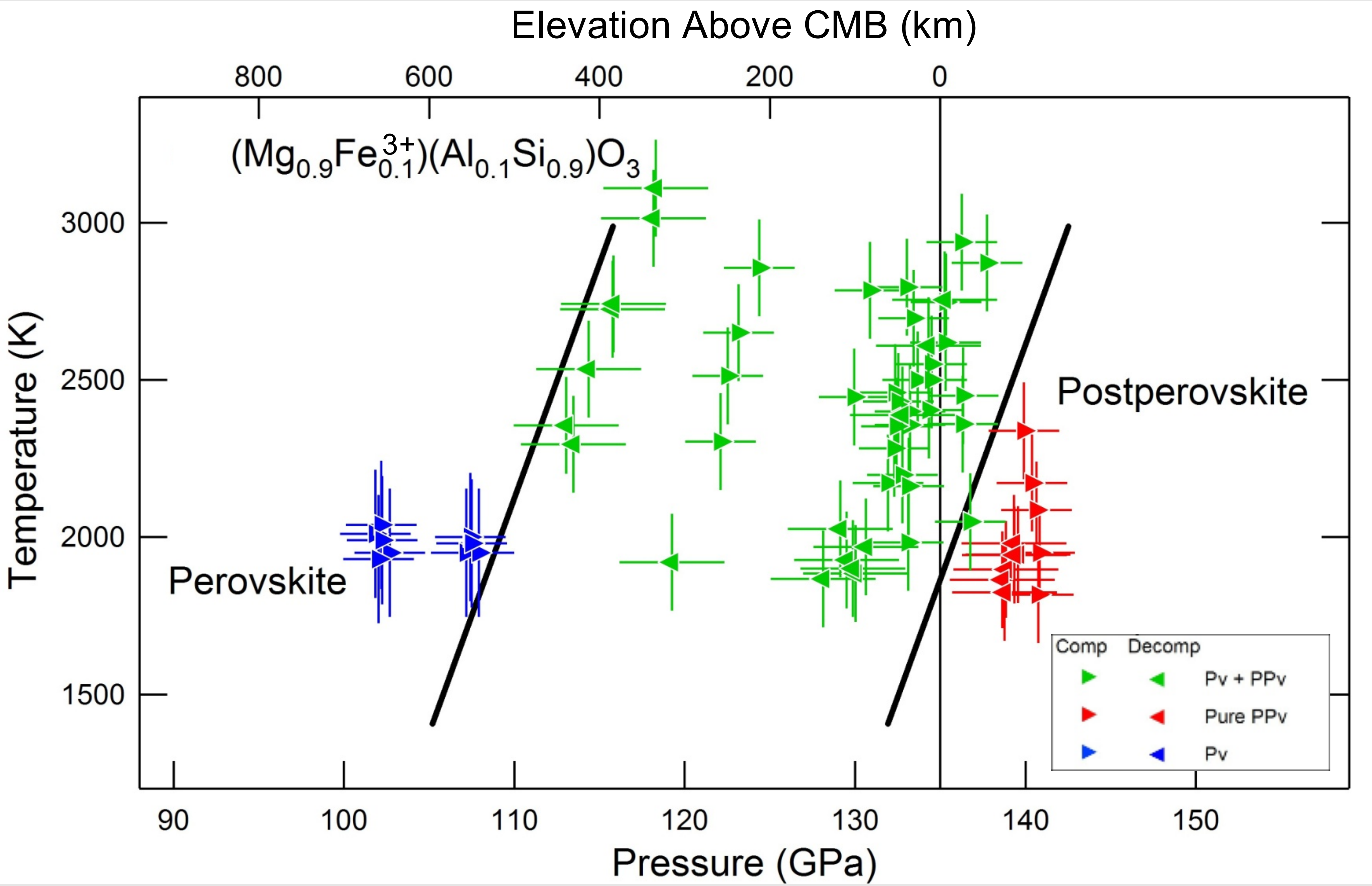

Catalli et al., 2009, Nature

Summary of binary and ternary systems

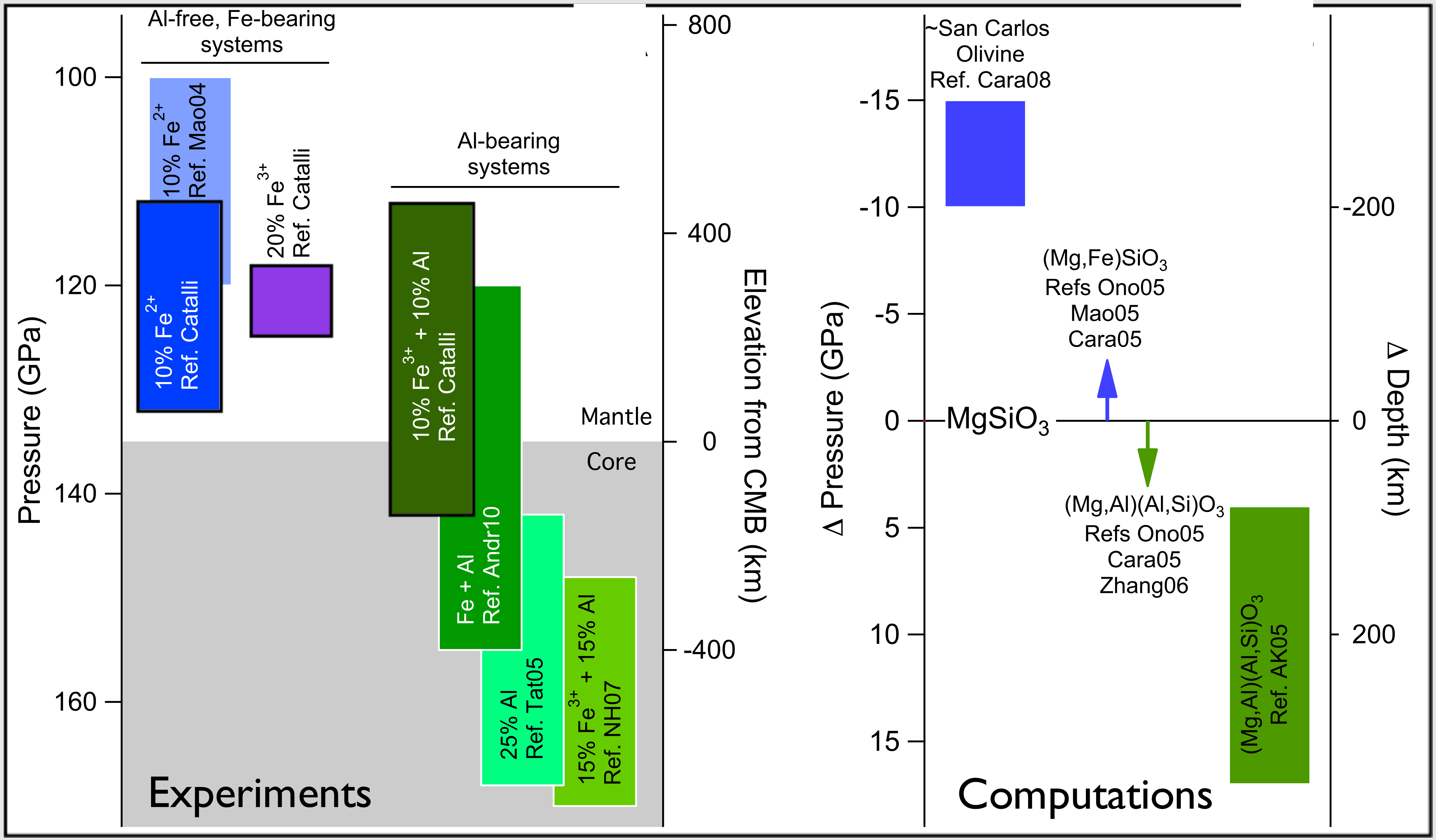

Summary of binary and ternary systems

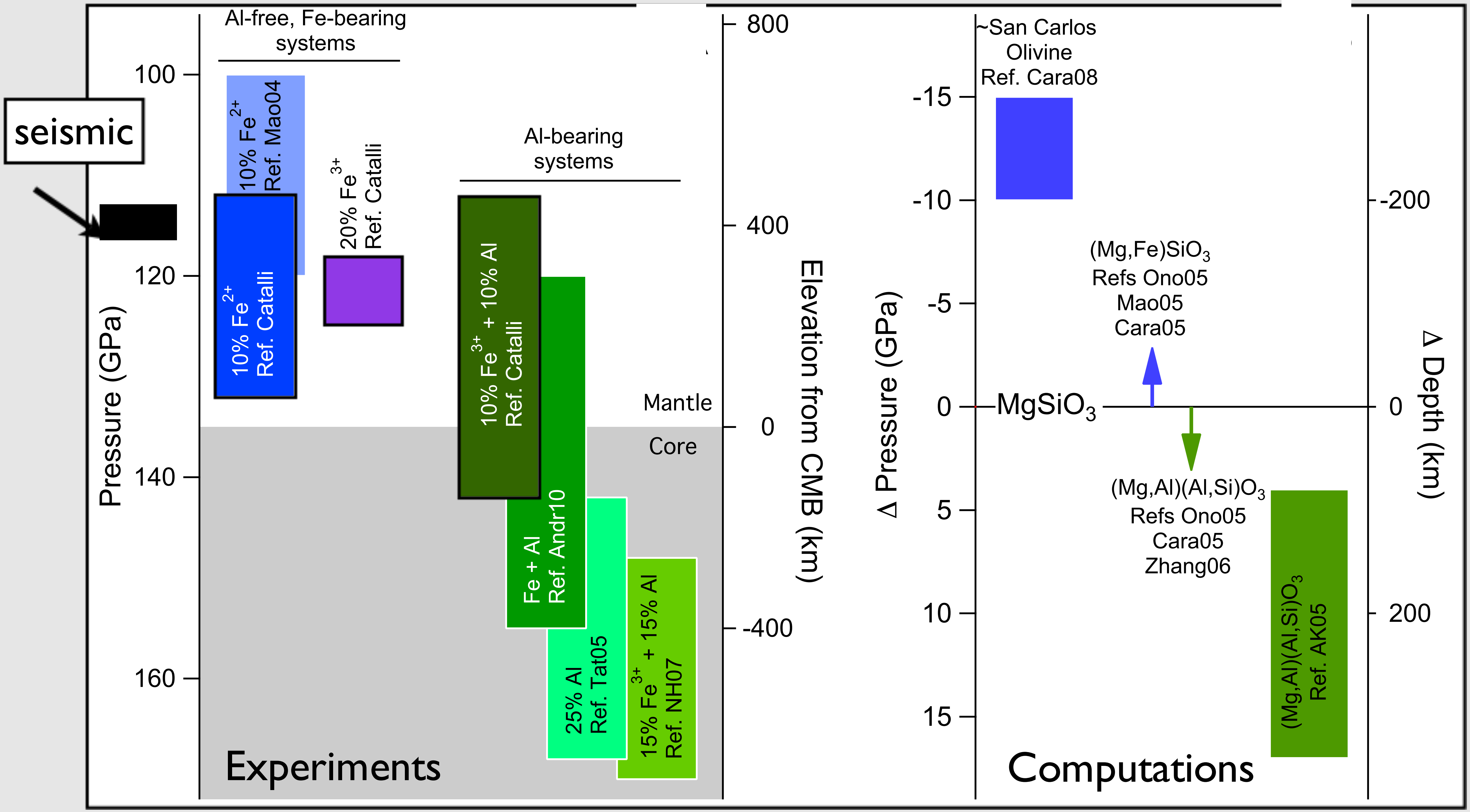

Seismically, the transition must occur over <70 km depth

Lay, 2008, GRL
Wysession et al., 1998

Pv → PPv

- Ternary and binary systems
- Multi-mineral systems

Partitioning effects

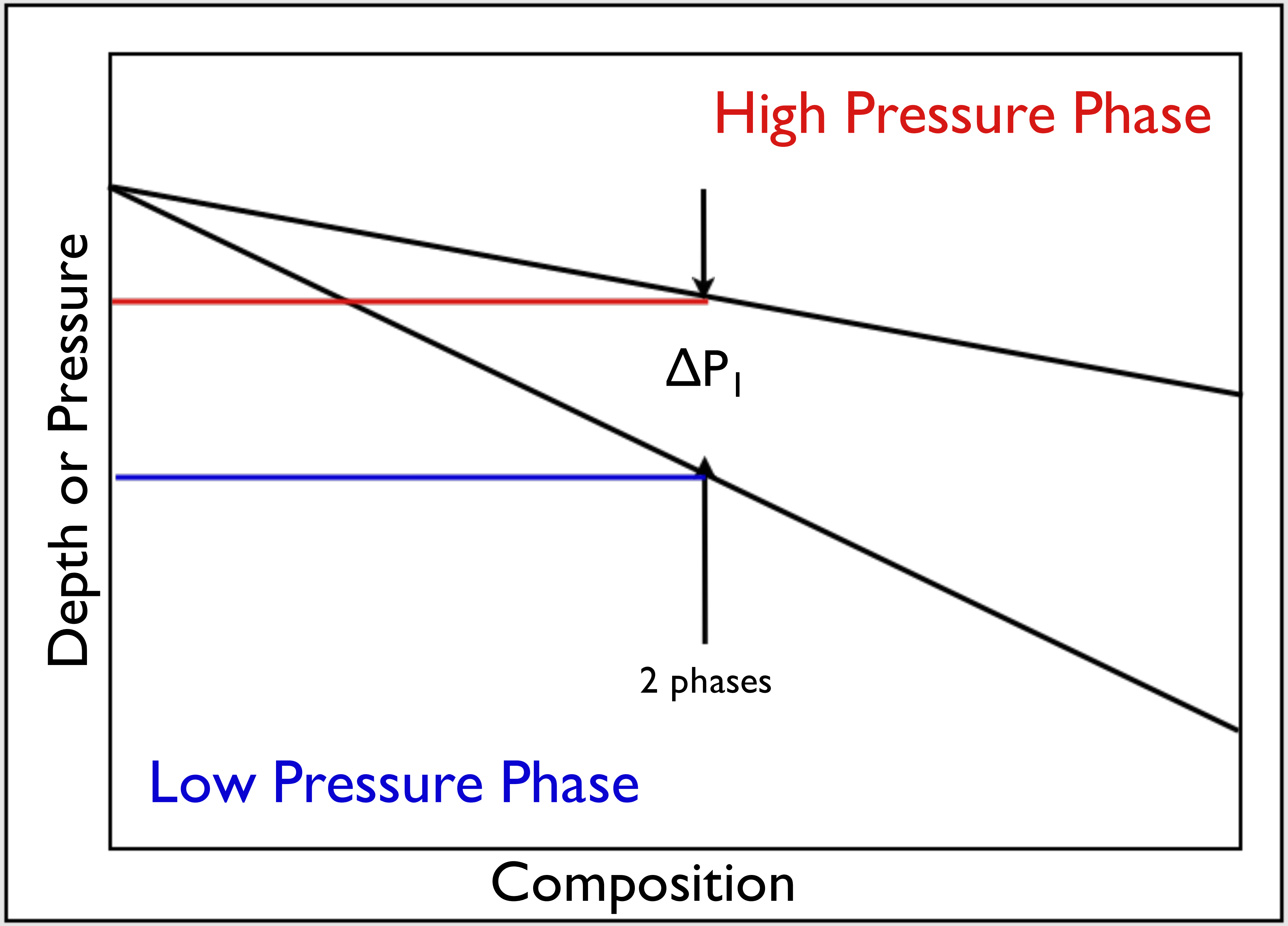

Unbuffered transition

Partitioning effects

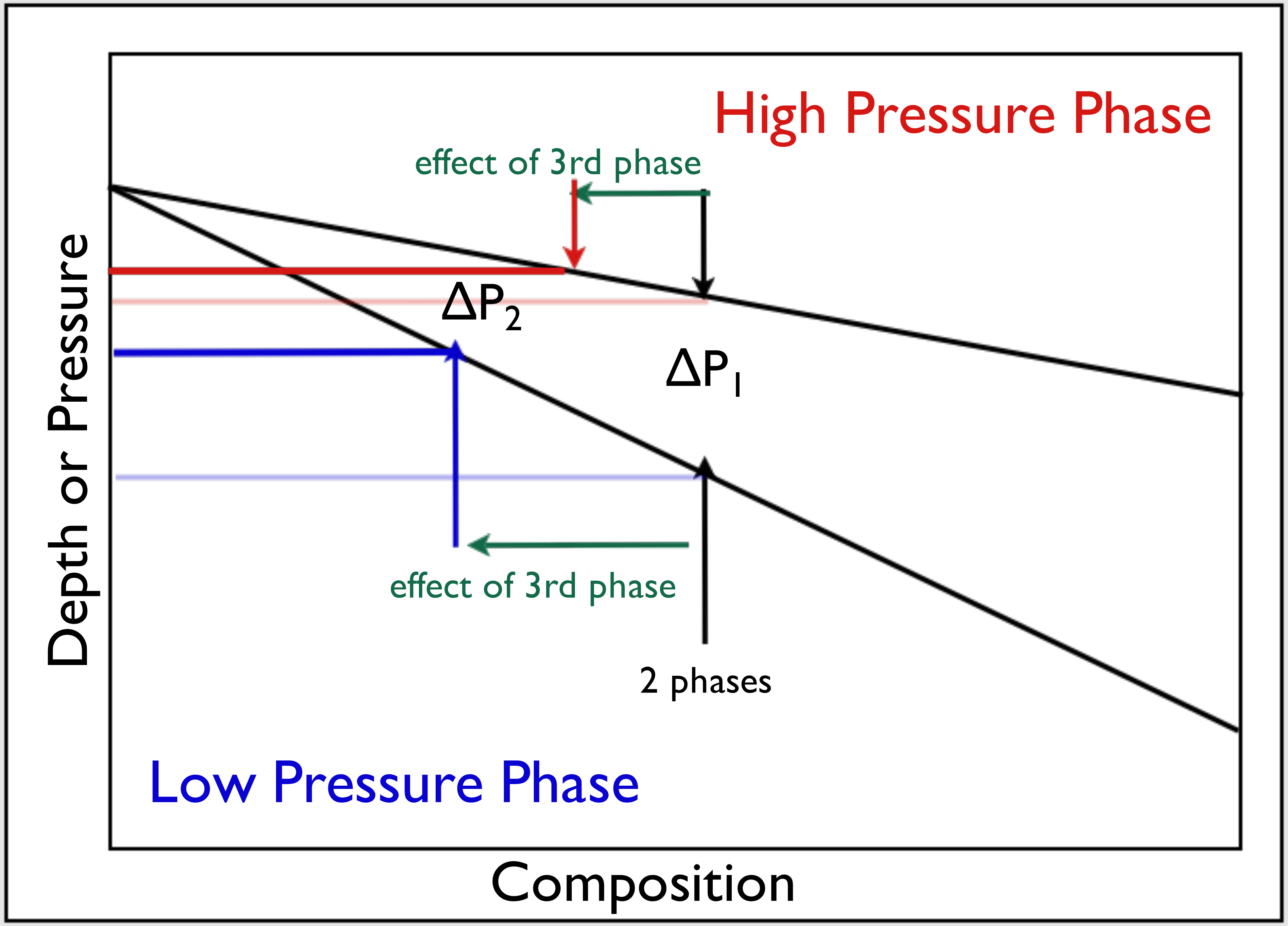

Buffered transition

Mineralogical effects: Element partitioning

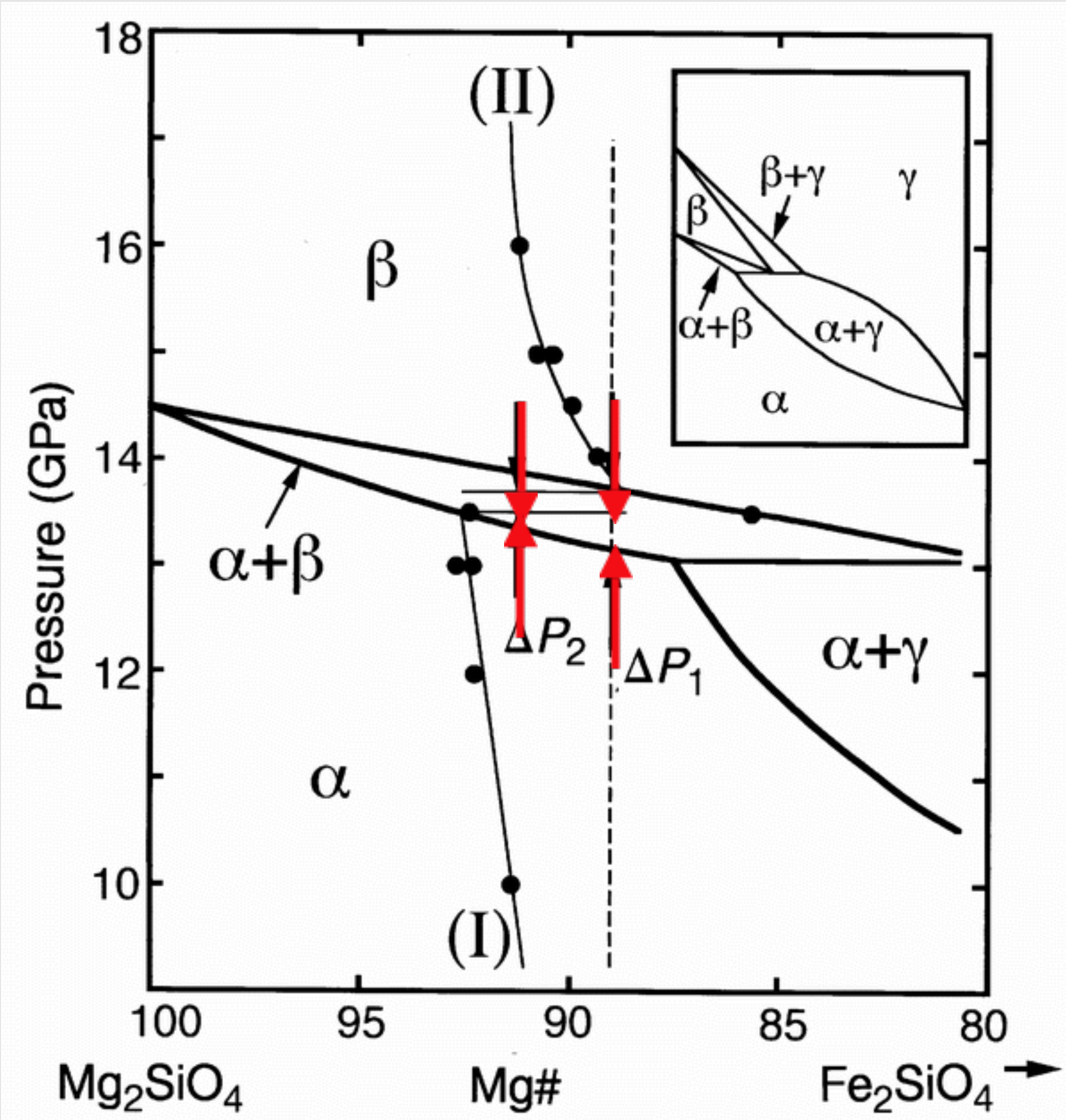

Irifune and Isshiki, 1998, Nature

- Background phases participate in the transition through element partitioning
- In the α→β transition, garnet sharpens the phase transition through partitioning of Fe

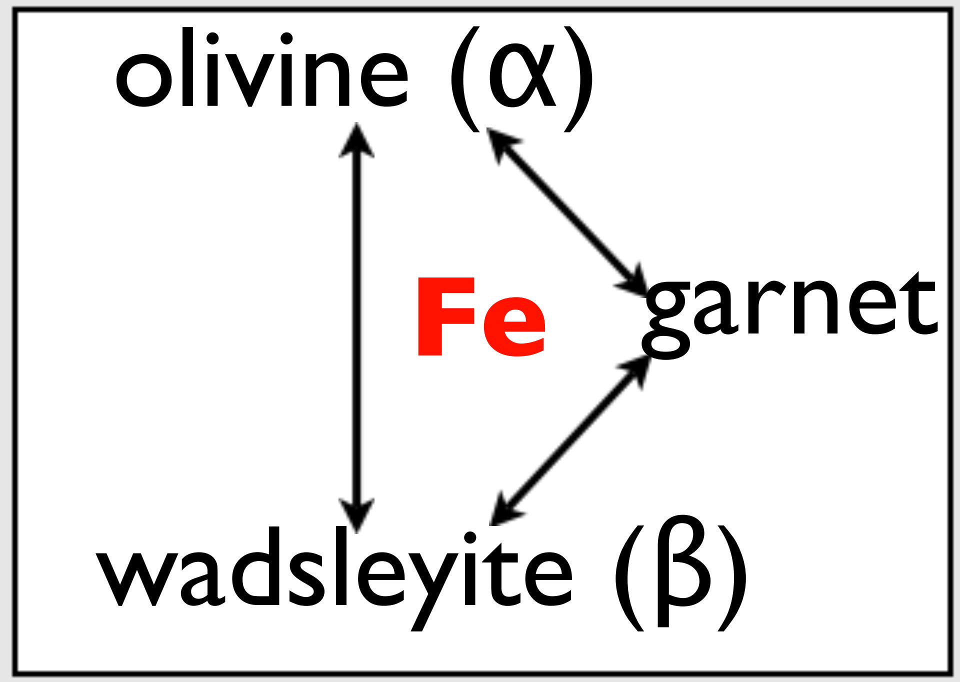

Plate tectonics

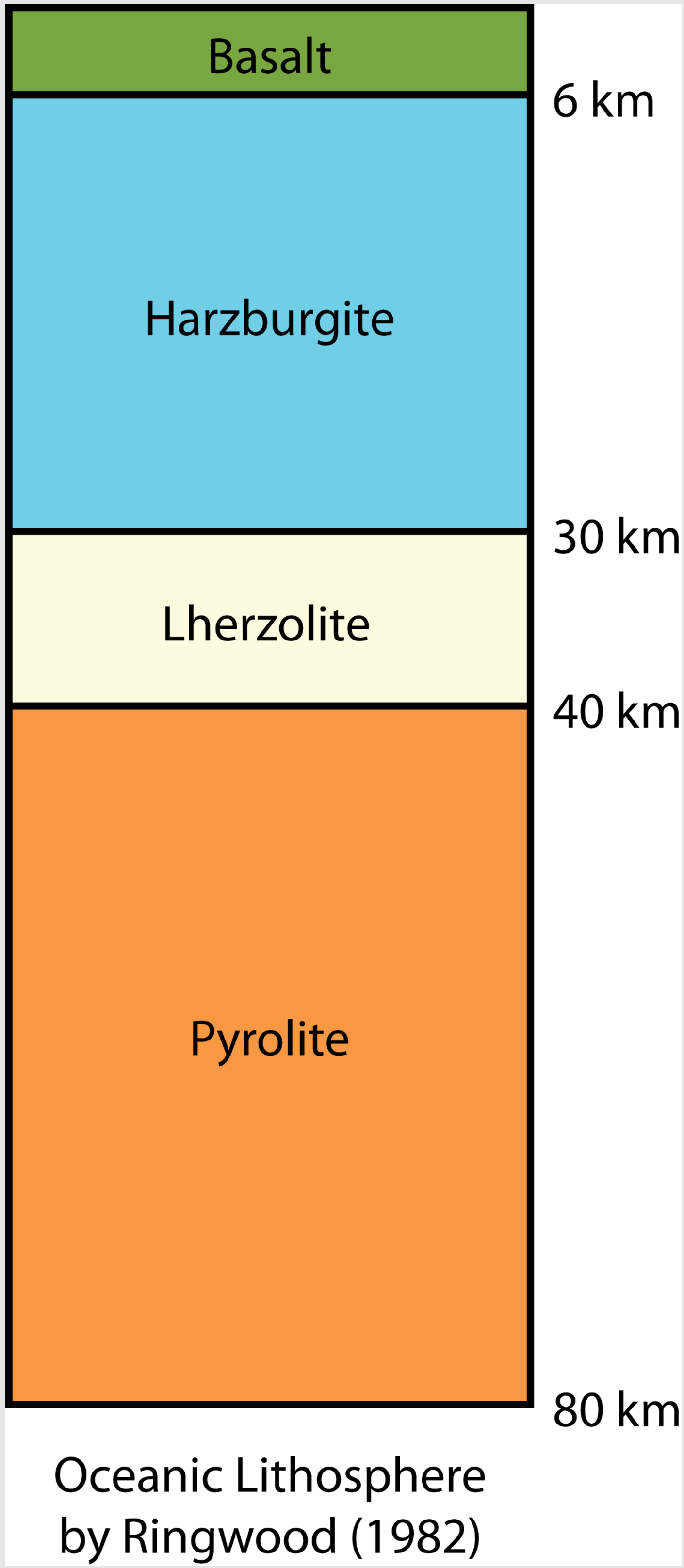

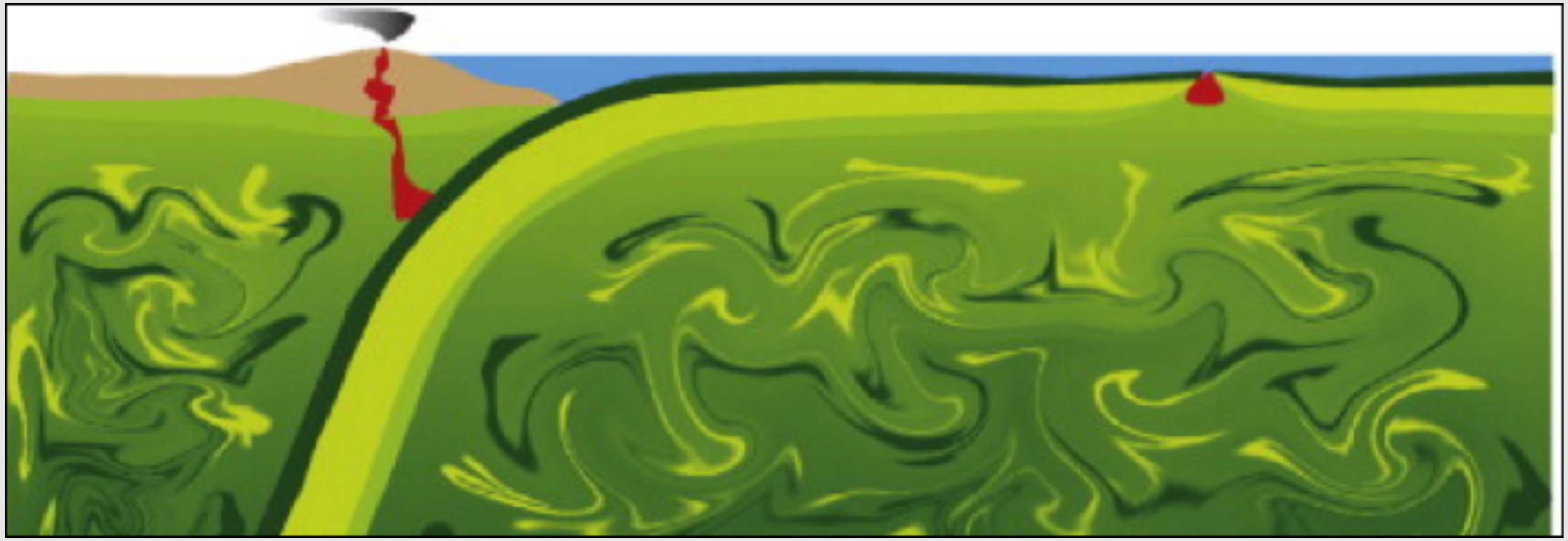

adapted from Xu et al., EPSL 2008

- Oceanic lithosphere is created at mid-ocean ridges through partial melting of the mantle
- It's colder (denser), causing it to subduct back into the mantle when it converges with continental crust

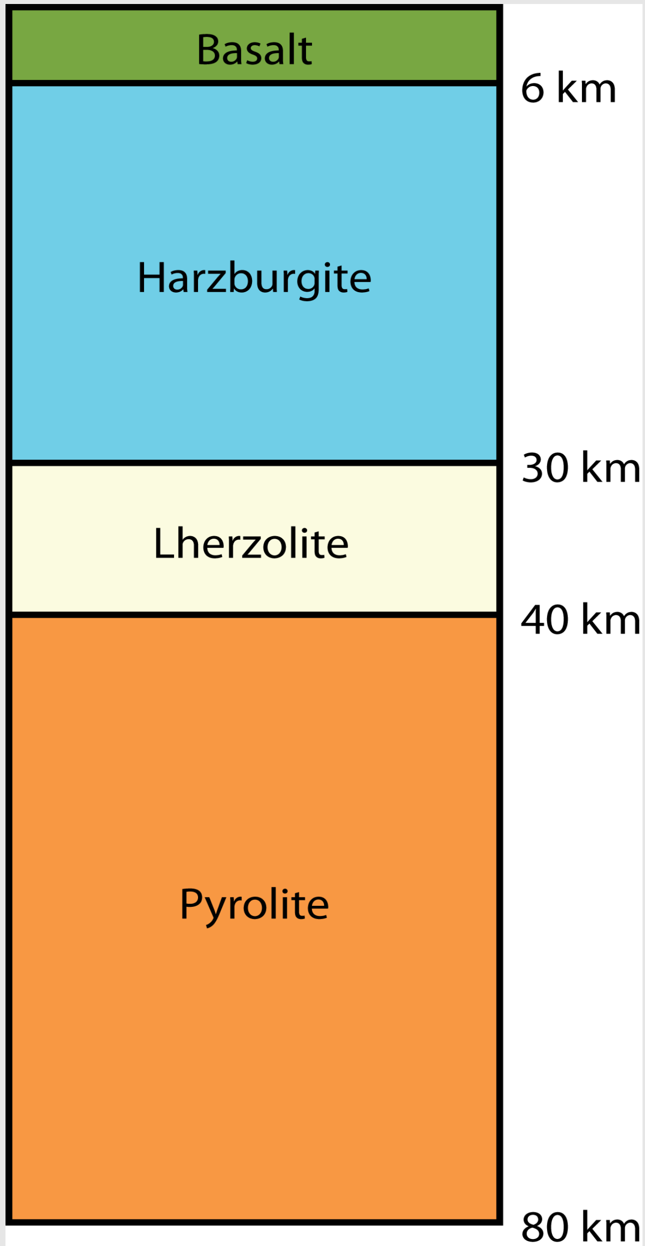

Oceanic Lithosphere
by Ringwood (1982)

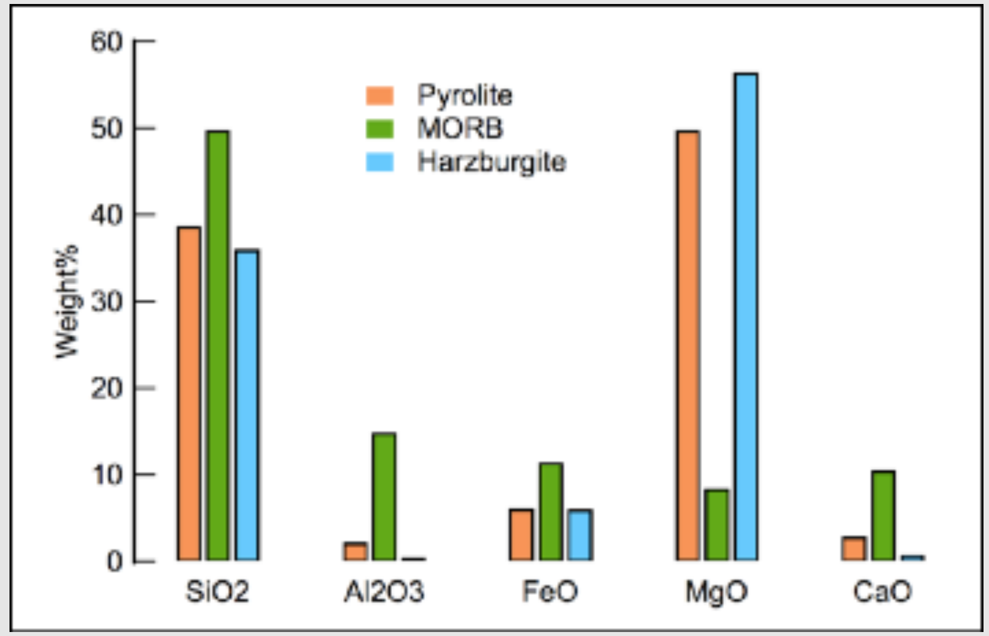

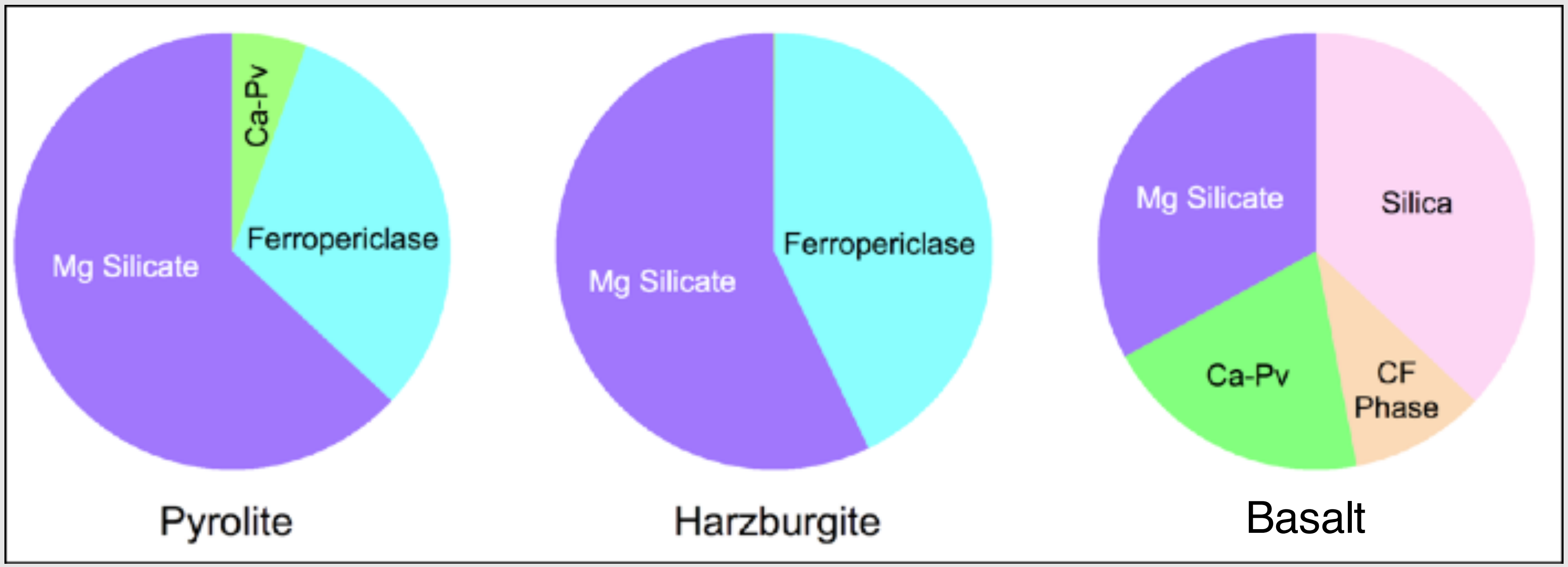

1. **Pyrolitic**: 5% Al, 6% Fe; no $CaSiO_3$ component

2. **San Carlos Olivine**: $(Mg_{0.89},Fe_{0.11})SiO_4$; ~50% ferropericlase

3. **Basaltic**: SiO_2-Al_2O_3-FeO-CaO-MgO-Na_2O

San Carlos olivine composition

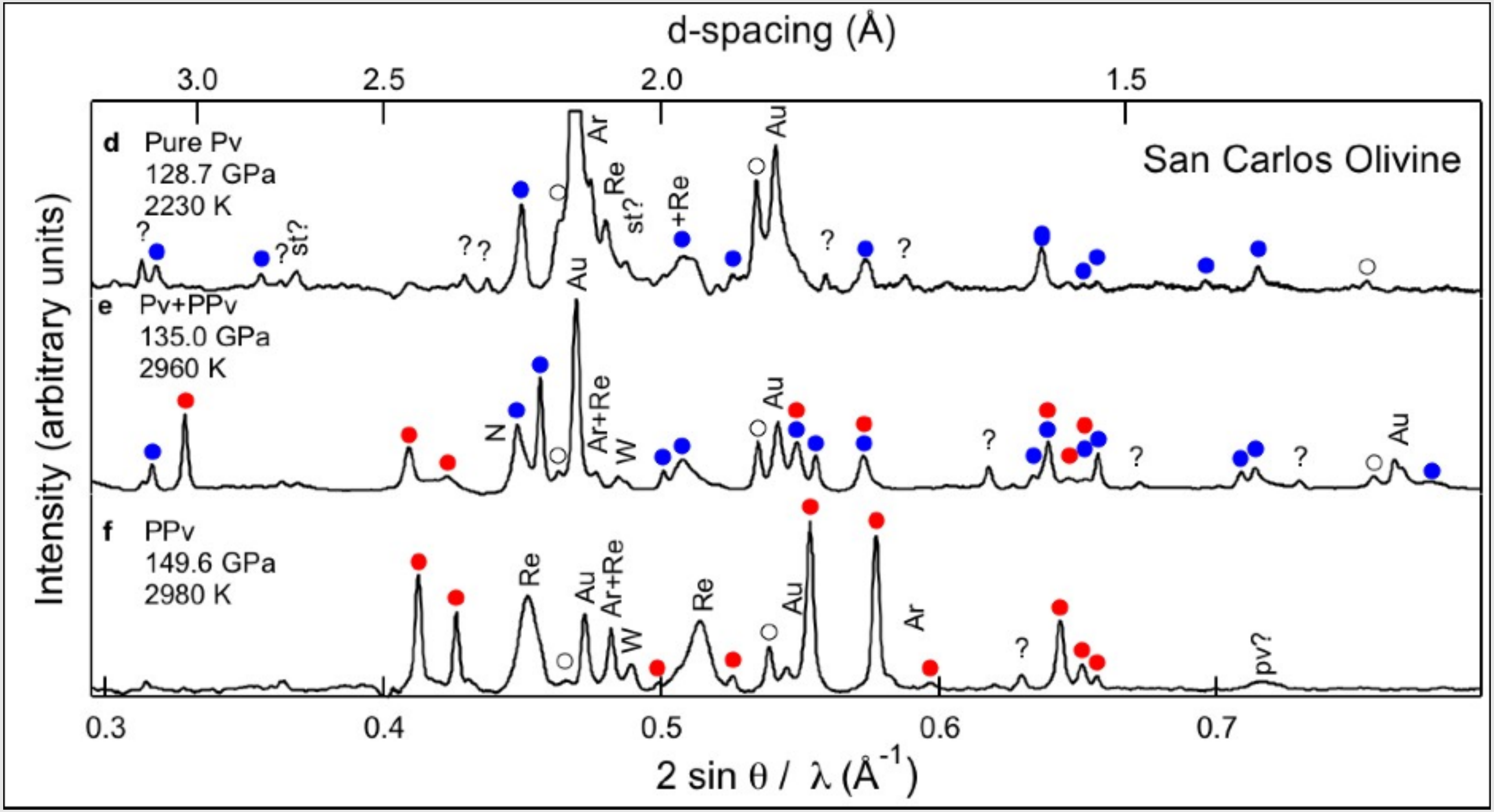

● post-perovskite ● perovskite ○ ferropericlase, (Mg,Fe)O

50% 50%

San Carlos olivine composition

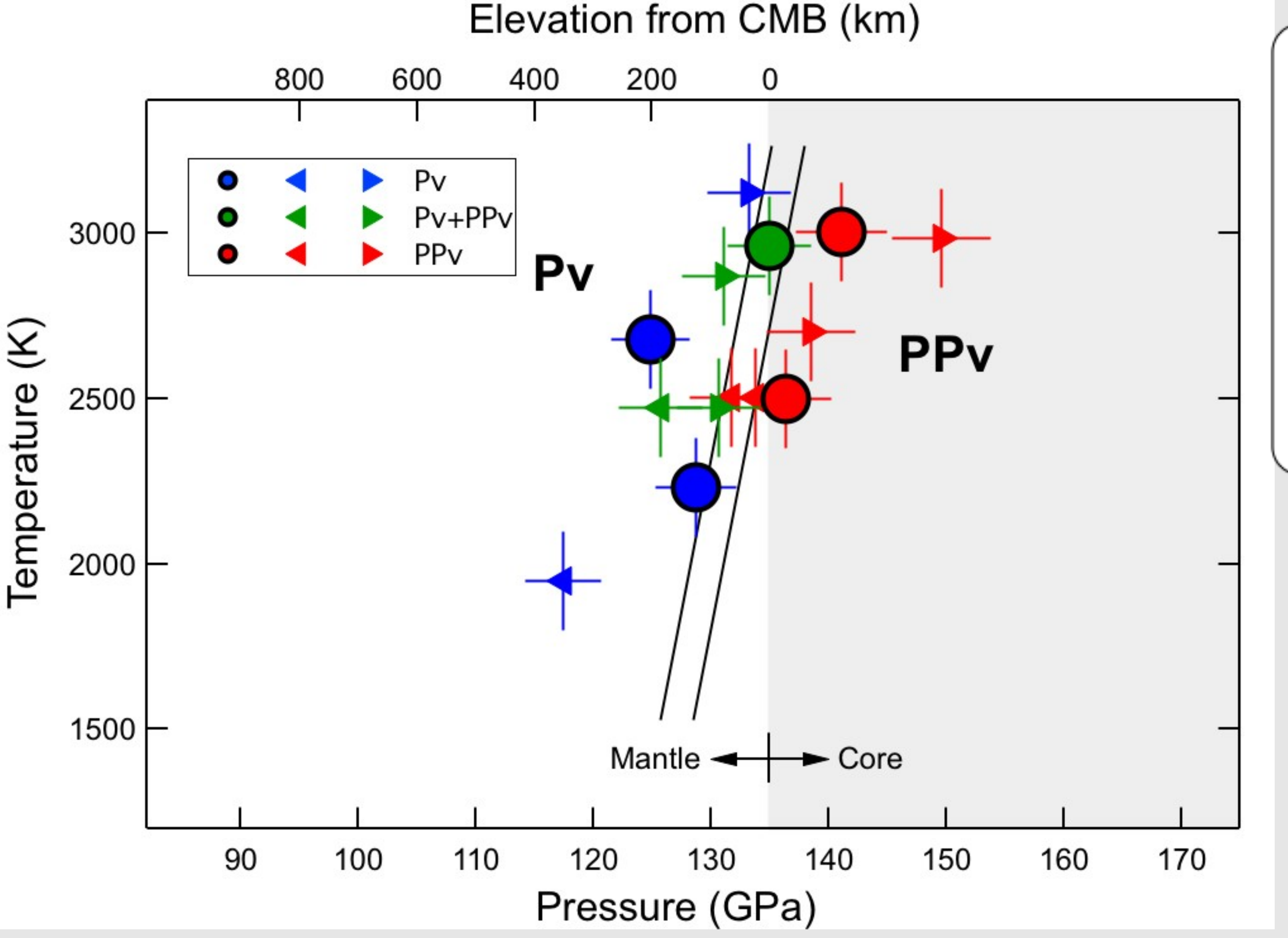

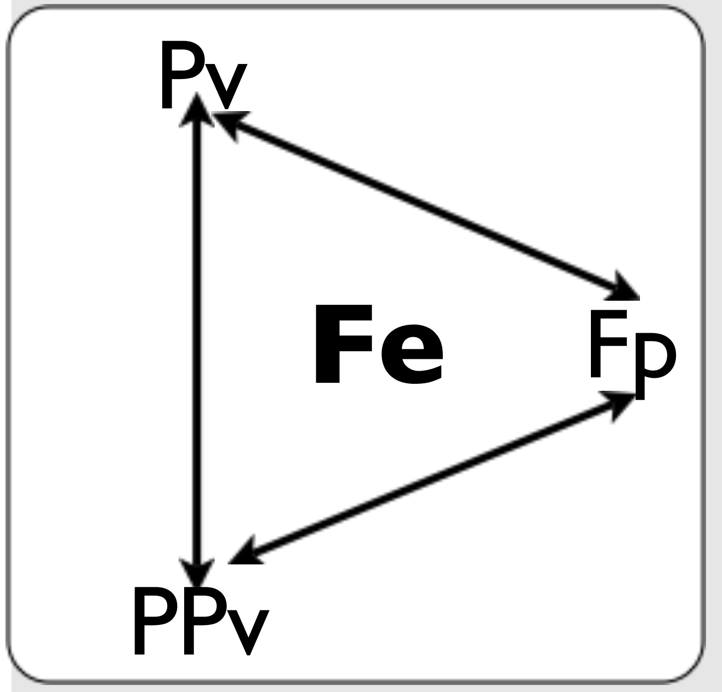

Pyrolitic composition

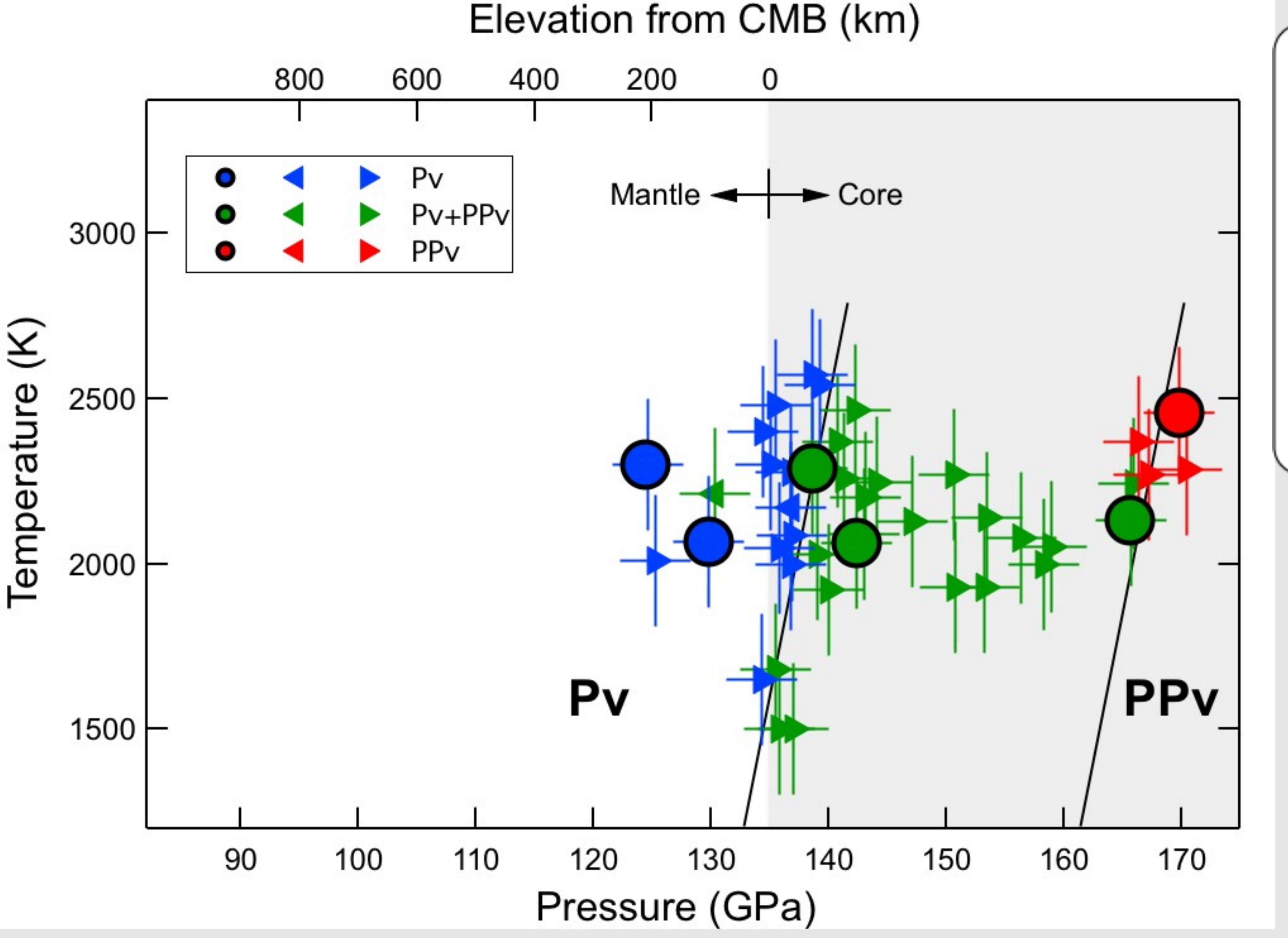

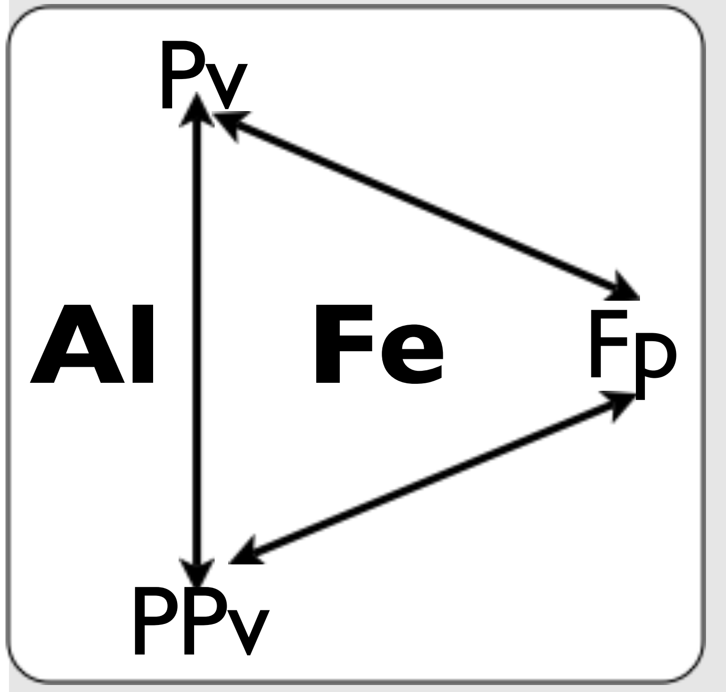

Basaltic composition

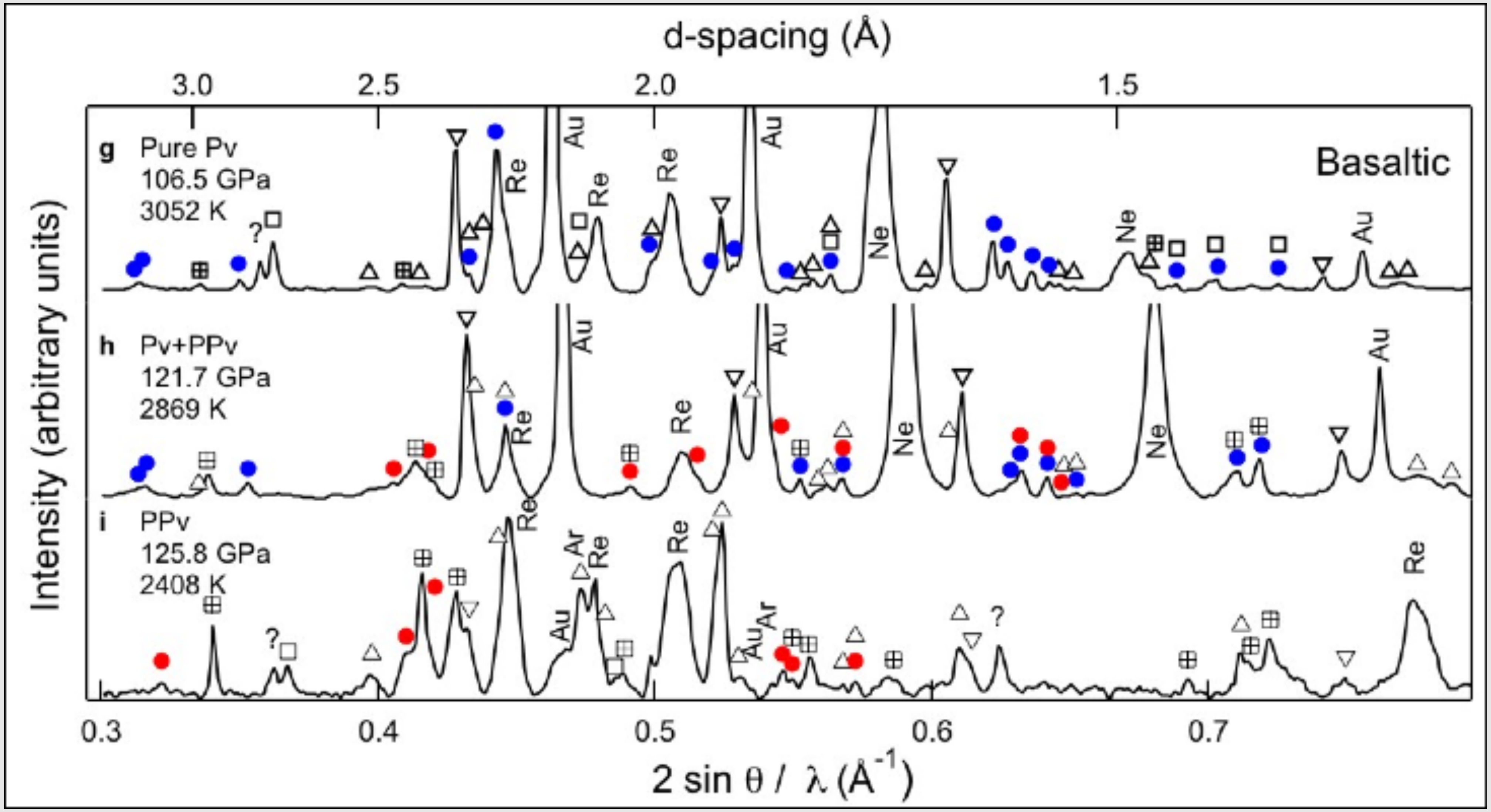

● post-perovskite ● perovskite		(with Fe, Al, and Na)
▽ $CaSiO_3$-perovskite		
□ $CaCl_2$-type SiO_2	⊞ α-PbO_2-type SiO_2	(with Al)
△ Ca-ferrite type, Na-bearing Al-rich silicate		(with Al, Na, Mg, Fe, Si)

Basaltic composition

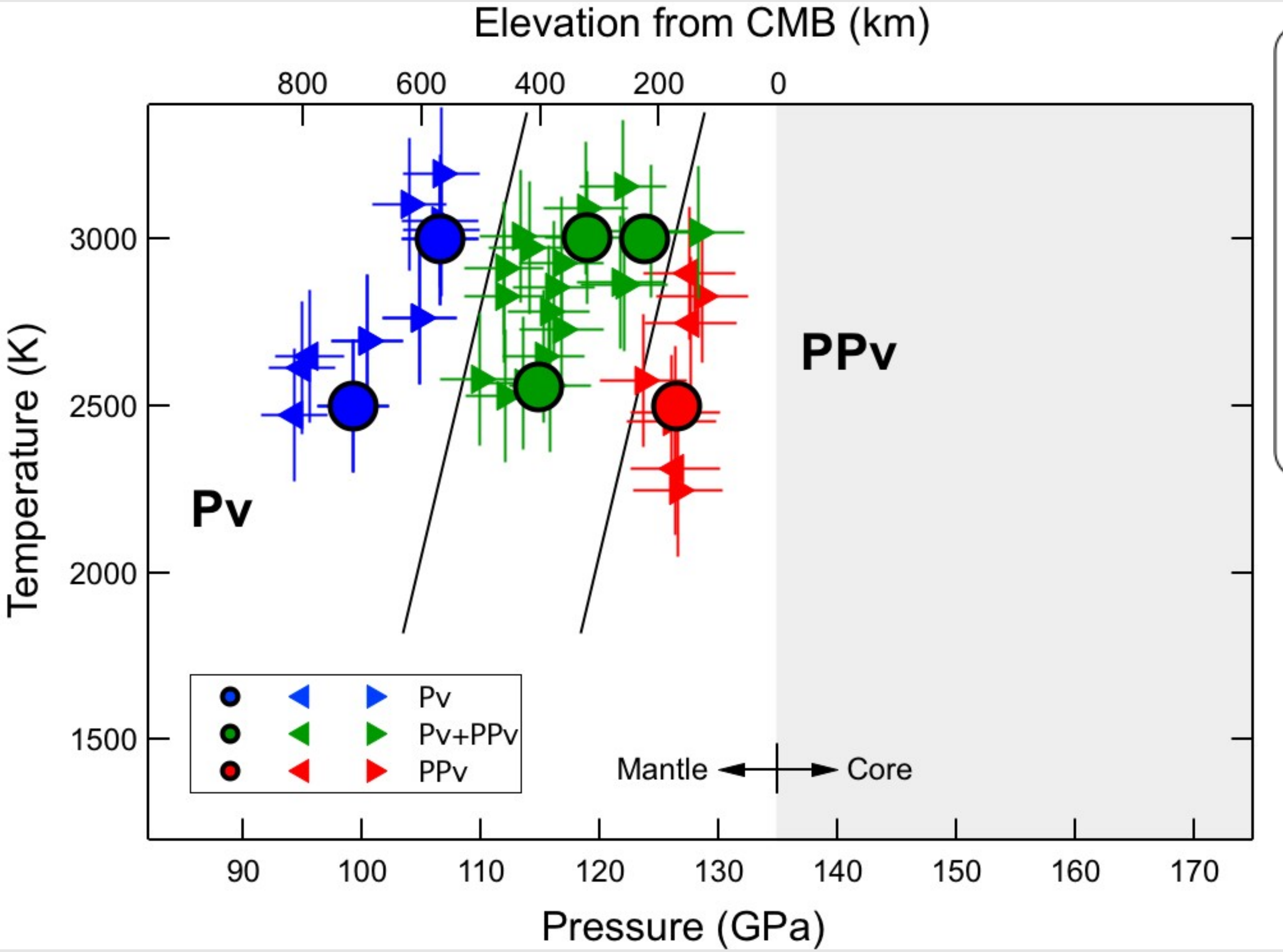

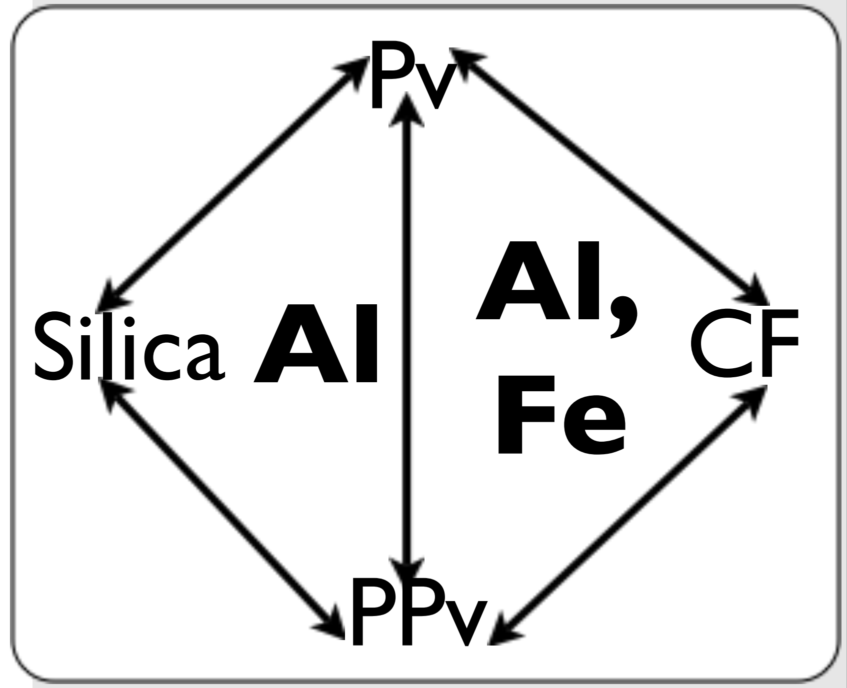

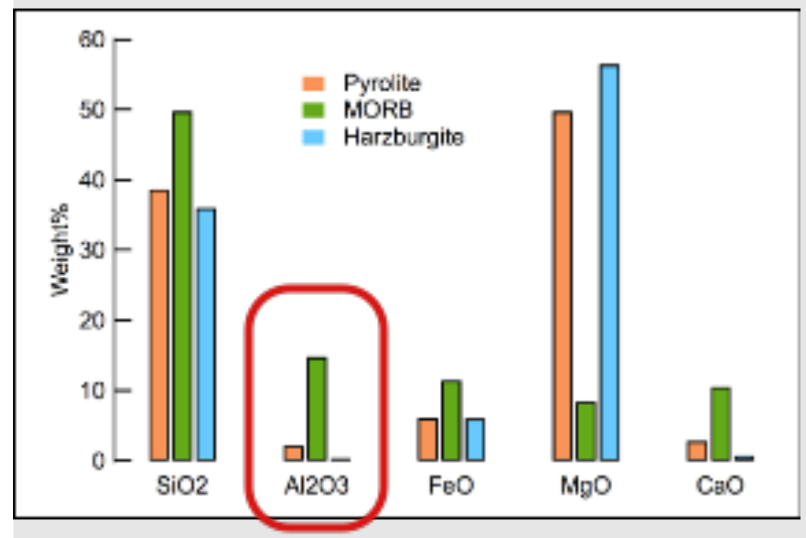

Summarizing the results . . .

2500 K

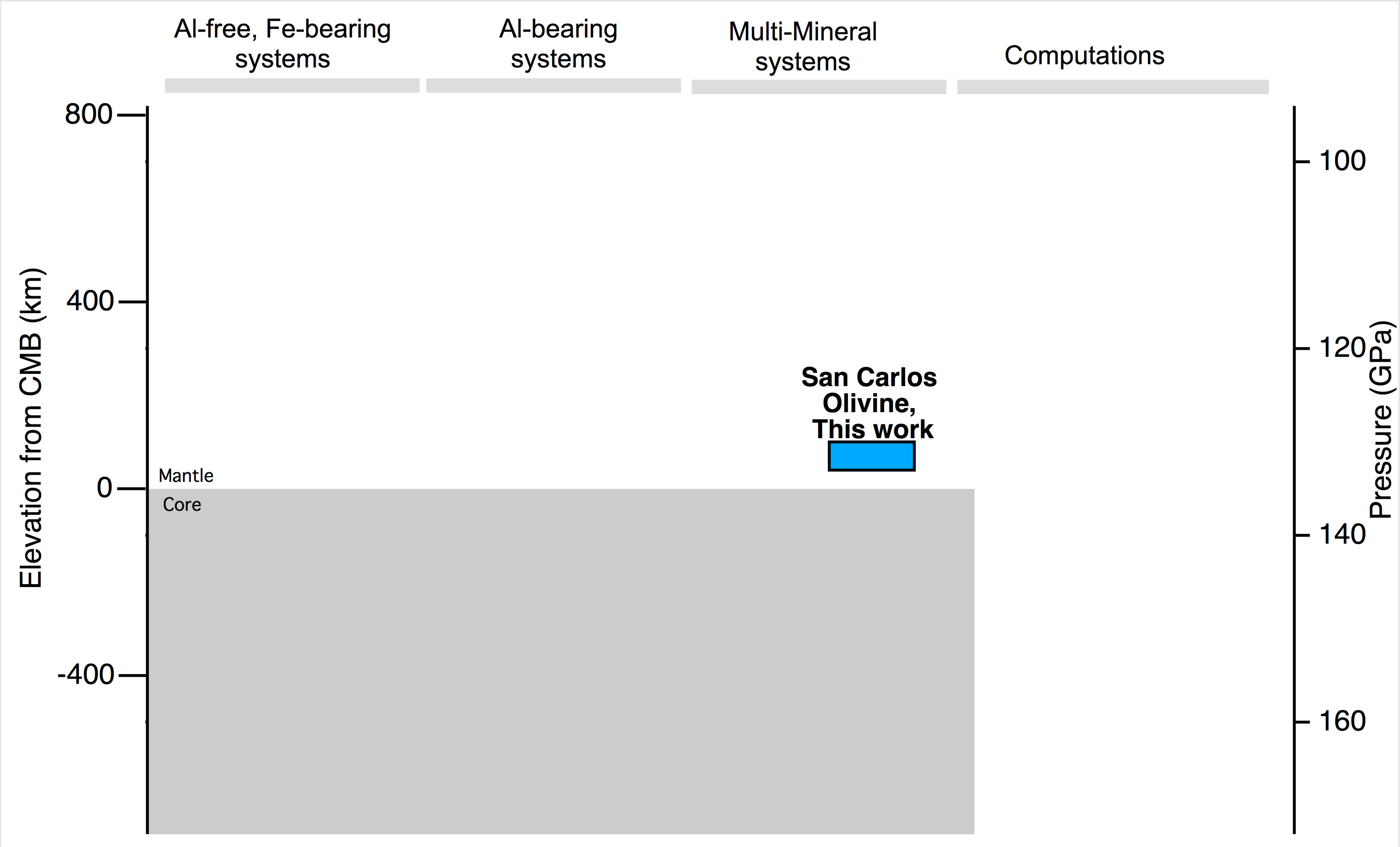

Effect of ferropericlase and iron

2500 K

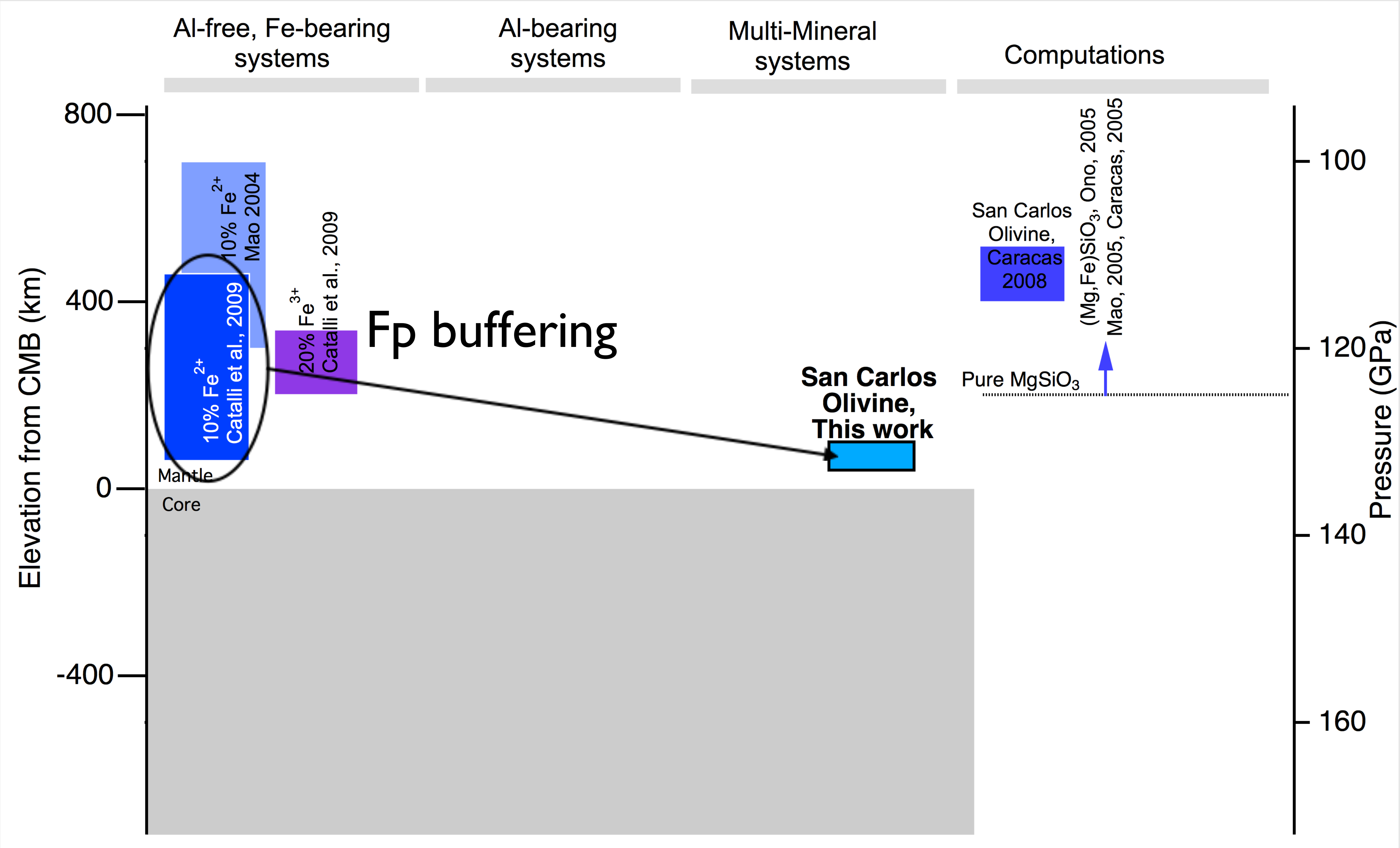

Ferropericlase deepens the Pv→Pv+PPv boundary and sharpens the mixed phase region

Effect of aluminum

2500 K

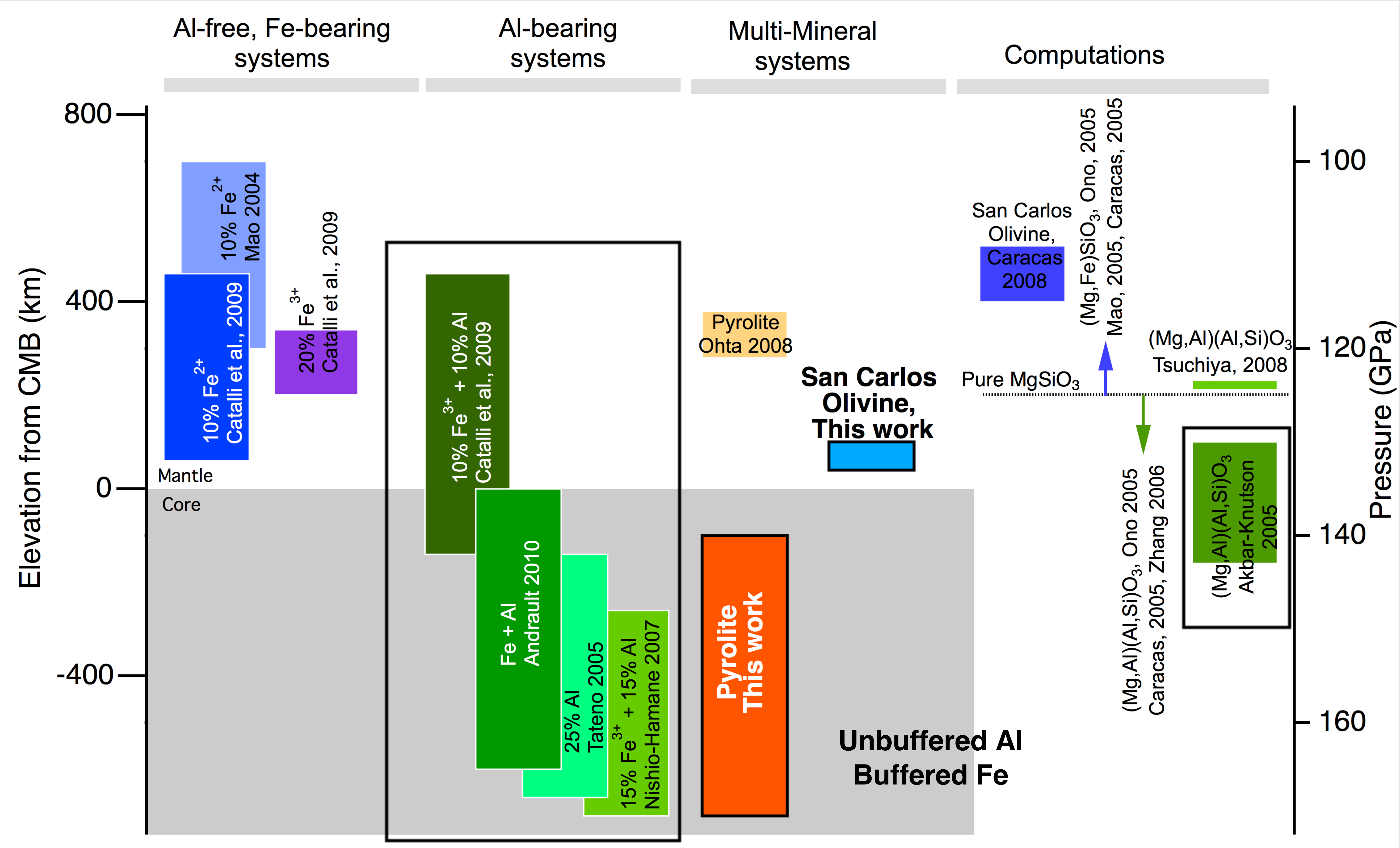

Aluminum broadens the mixed phase region and pushes the transition to higher pressure

2500 K

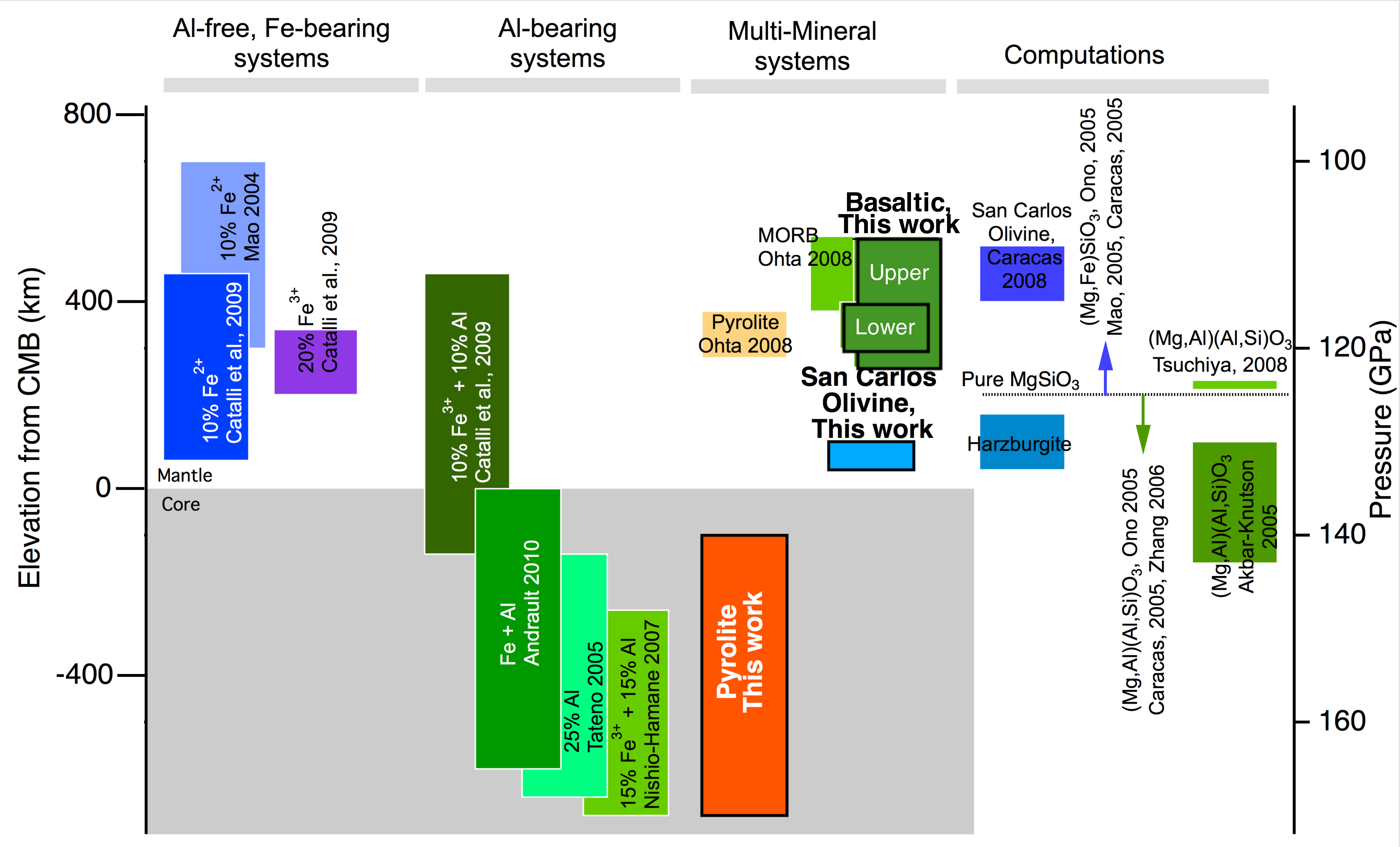

Basaltic and harzburgitic (calculation) compositions are good candidates to explain the D′′ discontinuity

2500 K

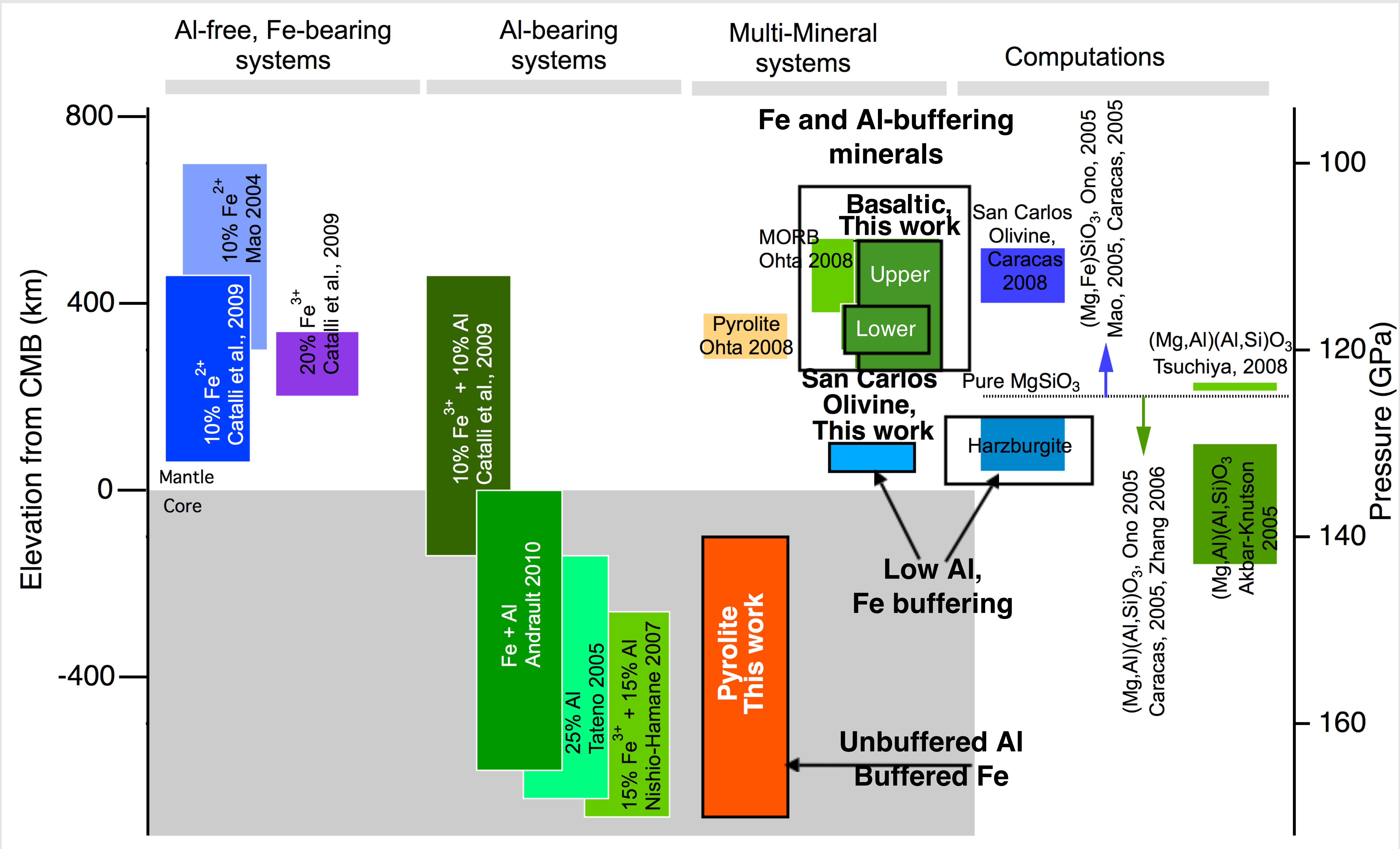

Basaltic and harzburgitic (calculation) compositions are good candidates to explain the D′′ discontinuity

2500 K

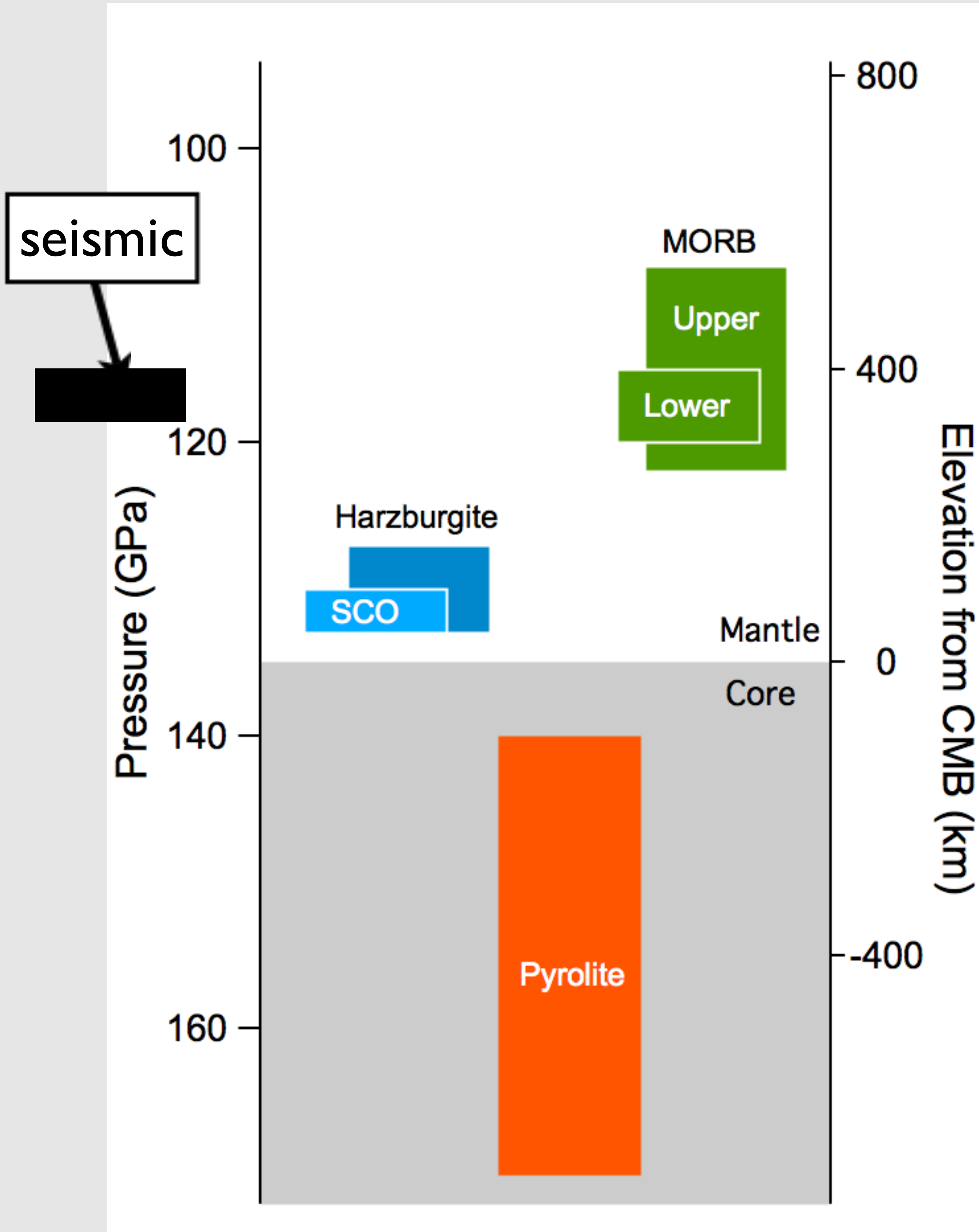

- Basaltic and harzburgitic compositions are good candidates to explain the D′′ discontinuity
- A homogenous mantle (pyrolite) is not

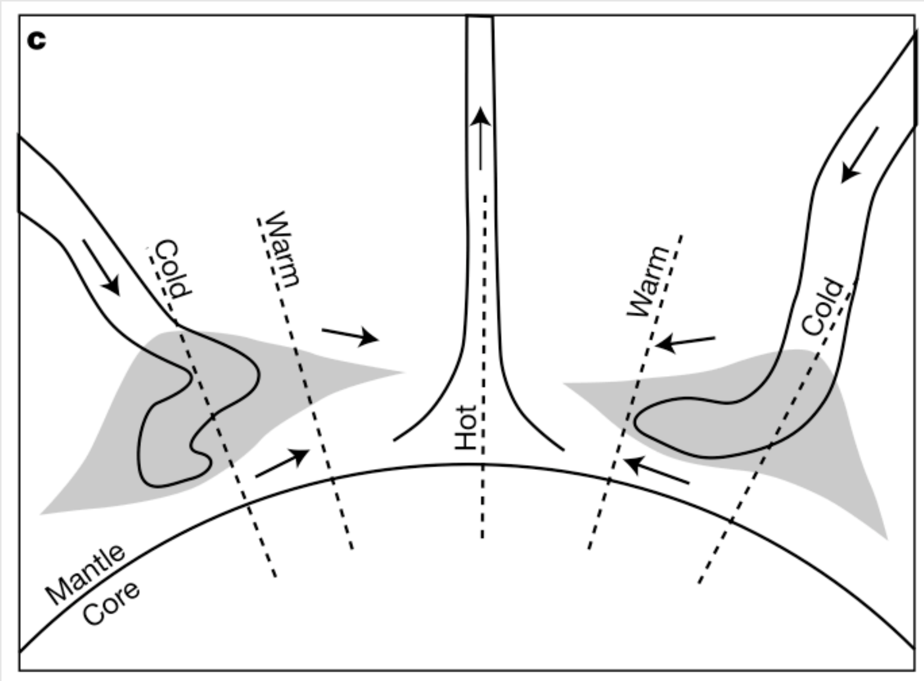

Hernlund et al. (2005) Nature

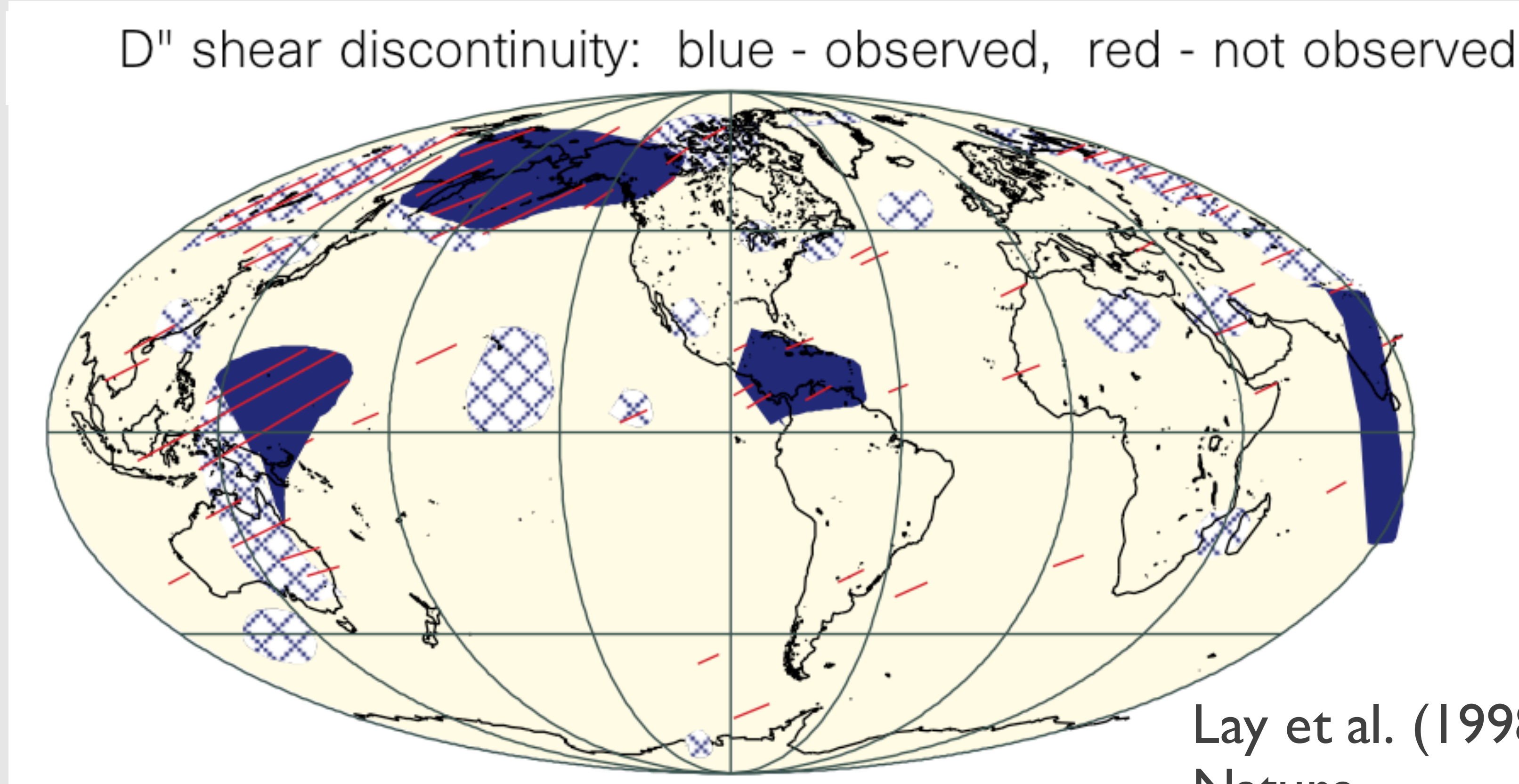

Lay et al. (1998) Nature

- A new hypothesis for the lateral variability in D′′ detection:
  - The Pv → PPv transition may only be detectable in areas where subducted slab materials have accumulated (presence of basaltic and/or harzburgitic compositions)
  - Pv → PPv transition is not sharp (and possibly does not occur at mantle conditions) in a pyrolitic composition

we know slabs penetrate the lowermost mantle

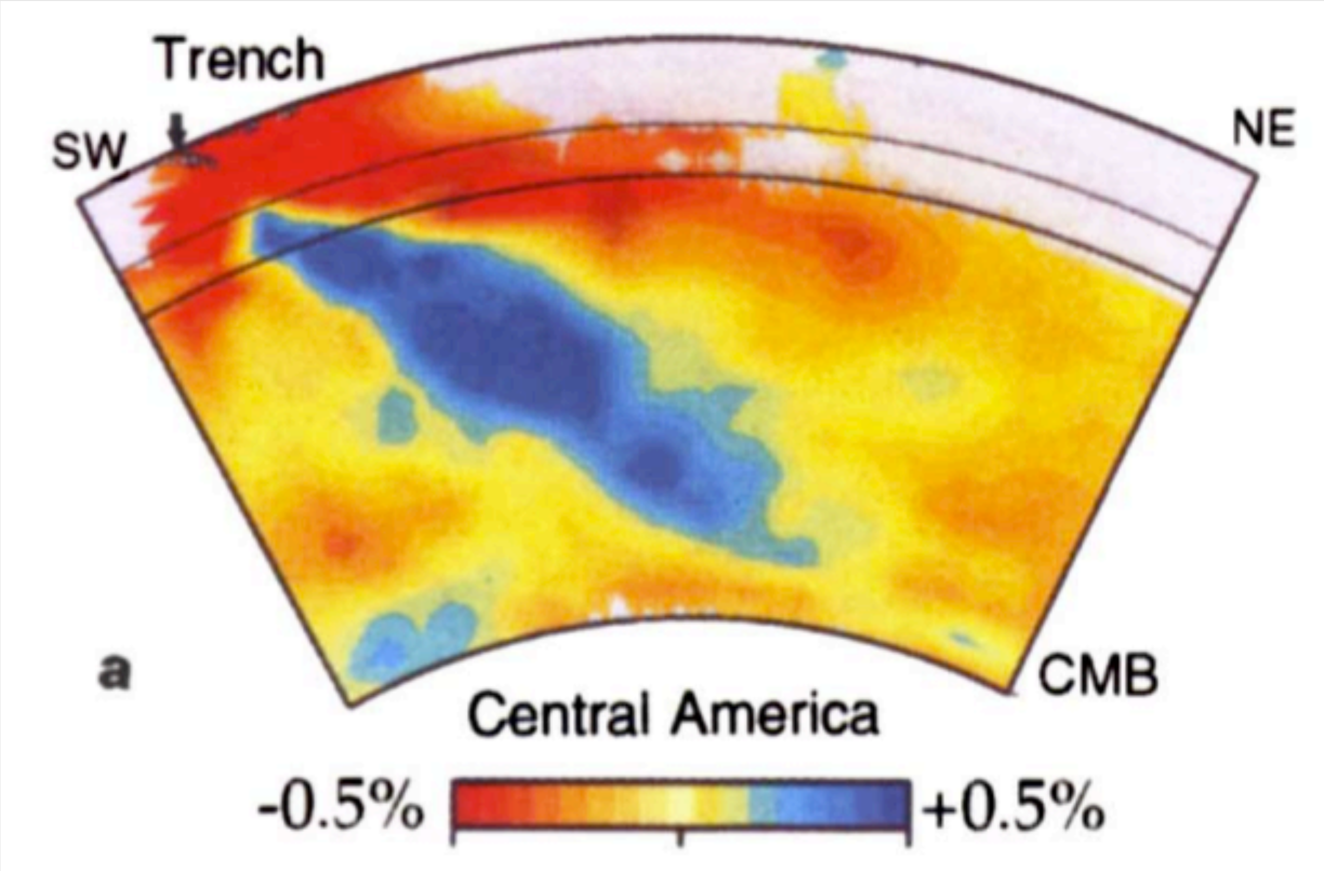

van der Hilst et al. (1997)
Nature

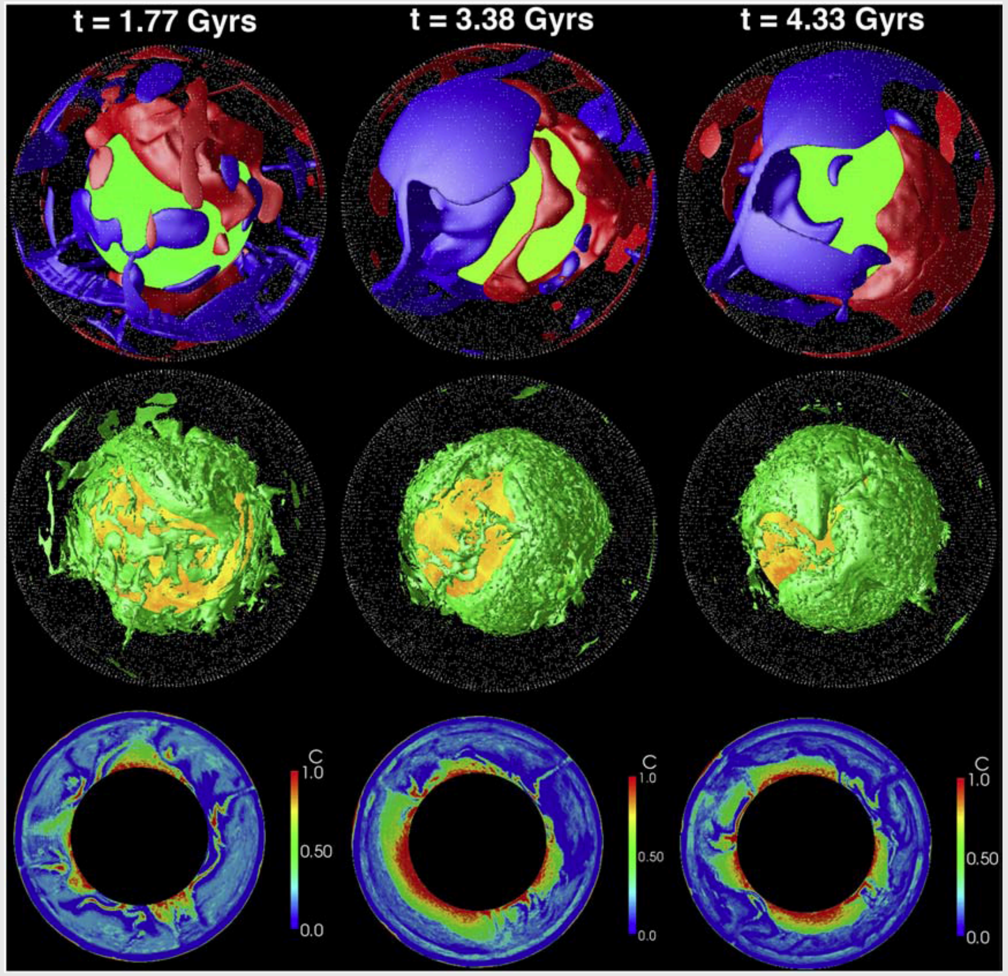

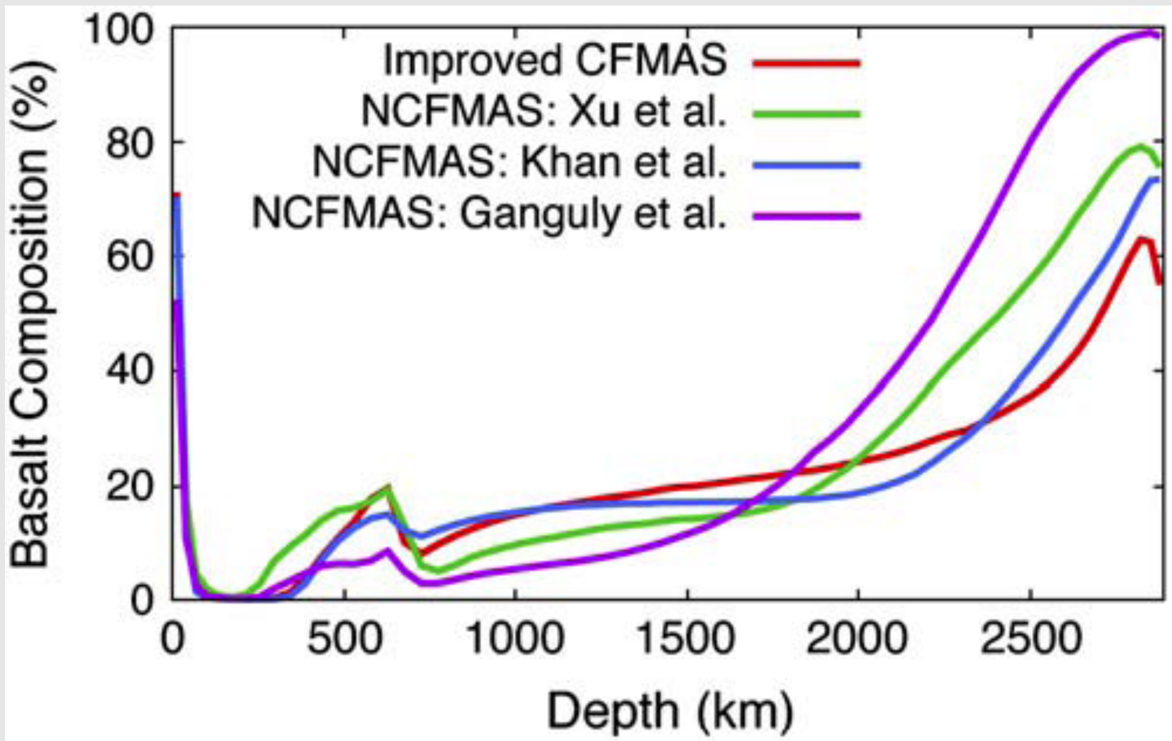

and modeling suggests the accumulation of basaltic material in the lowermost mantle

Nakagawa et al., 2010,
EPSL

Heterogeneous Mantle

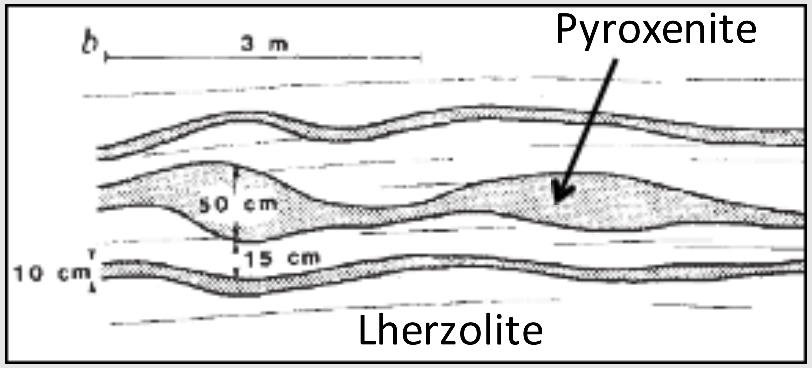

Marble Cake Mantle

Allègre and Turcotte (1984) Nature

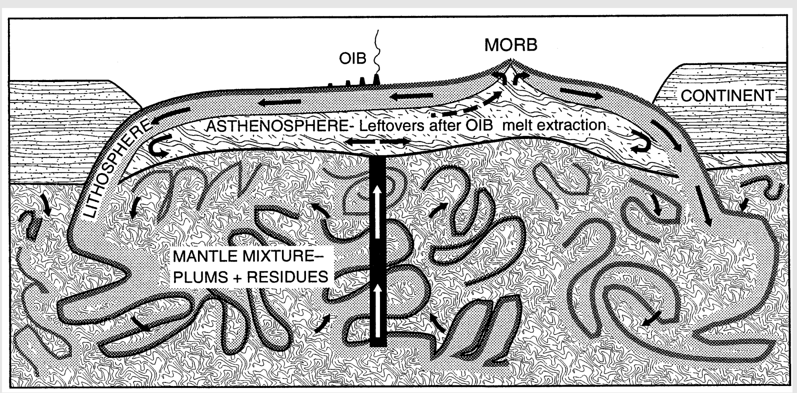

Plum Pudding Mantle

Morgan and Morgan (1999) EPSL

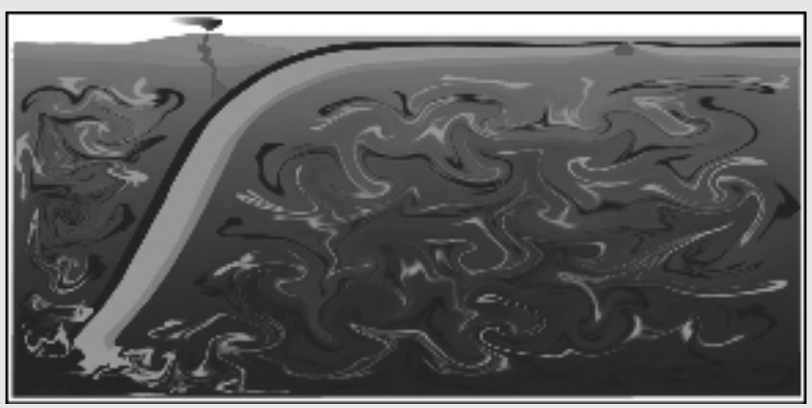

Mechanical Mixture Mantle

Xu et al. (2008) EPSL

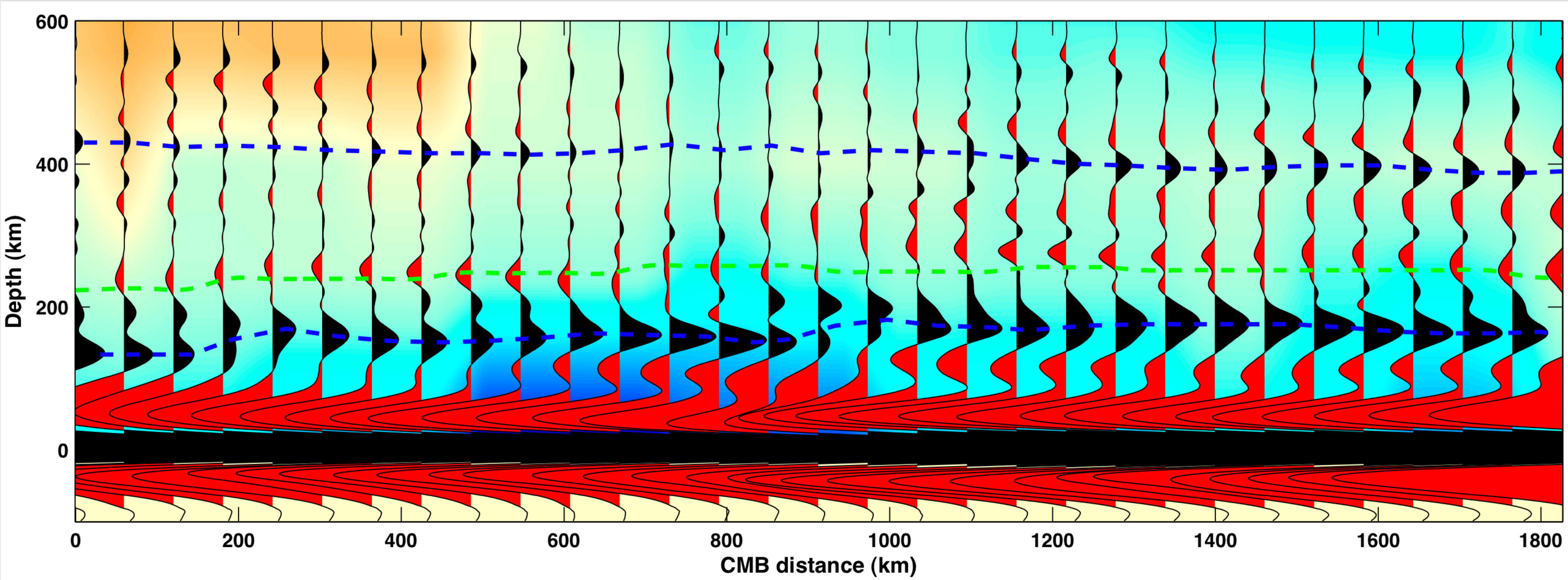

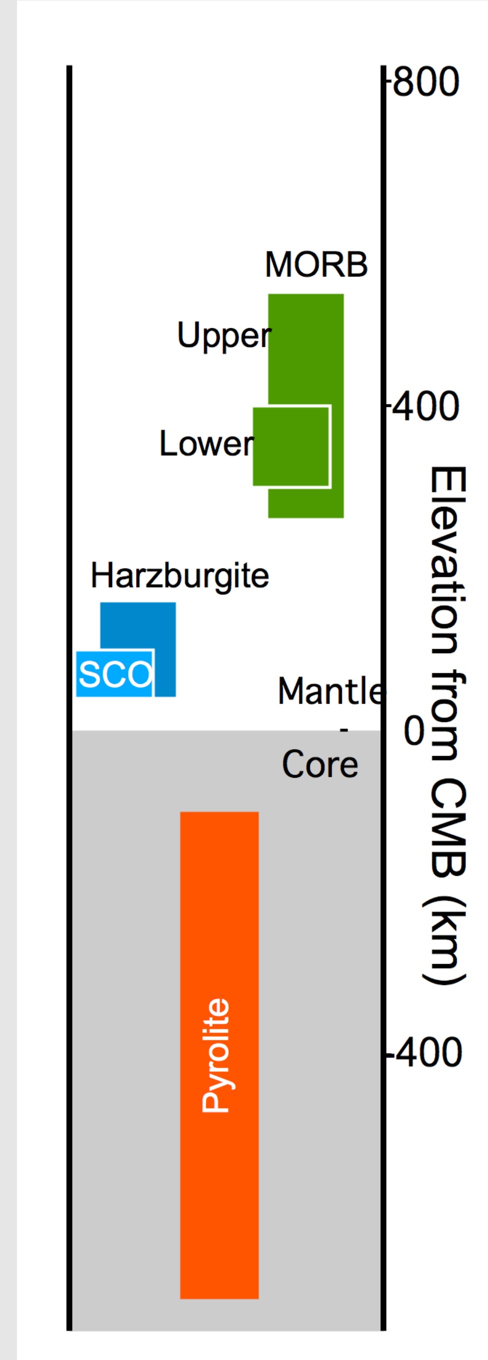

X. Shang, van der Hilst, and Shim, in review

Detailed seismic investigations of the lowermost mantle show multiple reflectors in the lowermost mantle

Summary

The depth and thickness of the post-perovskite boundary is highly dependent on composition/mineralogy

The D′′ discontinuity may only occur where subducted/differentiated materials have accumulated near the CMB

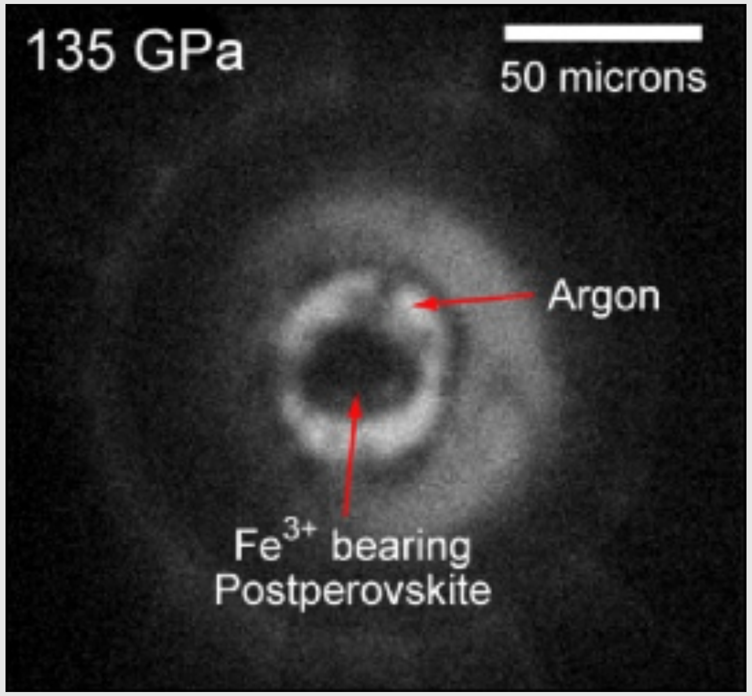

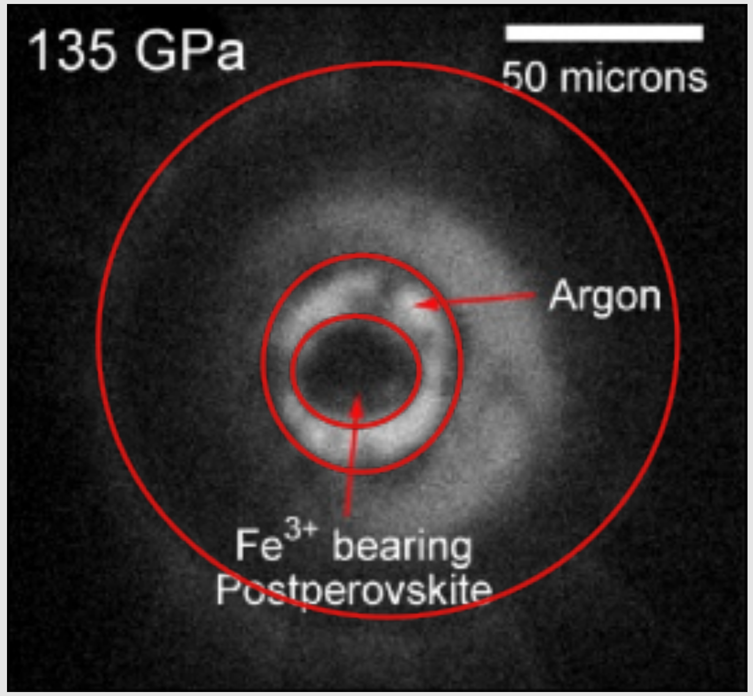

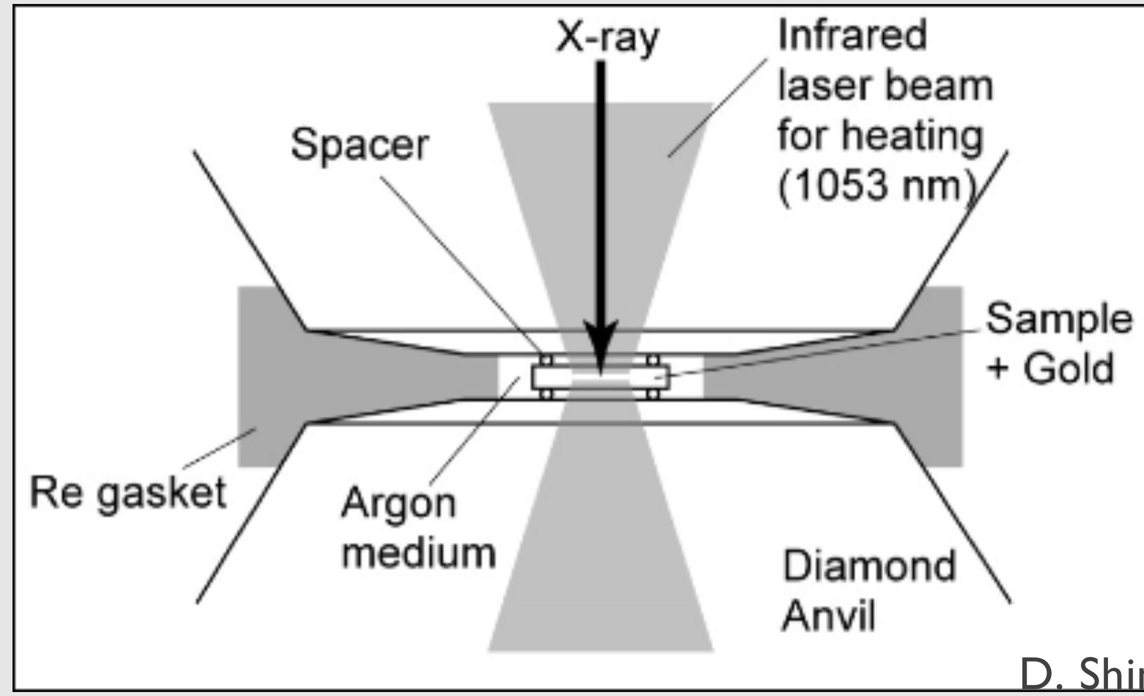

D. Shim

- Samples are powdered and mixed with 10 wt% gold for use as pressure standard
- Pressed into a platelet, ~5-10μm thick, 20-30 μm diameter
- Surrounded by Ar or Ne, pressure medium and thermal insulator
- Laser heated for long durations (1+ hours)

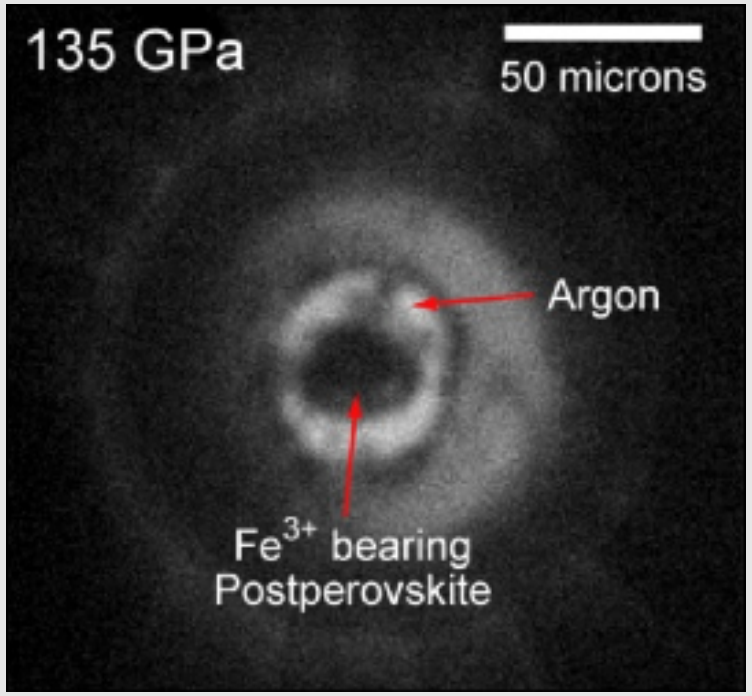

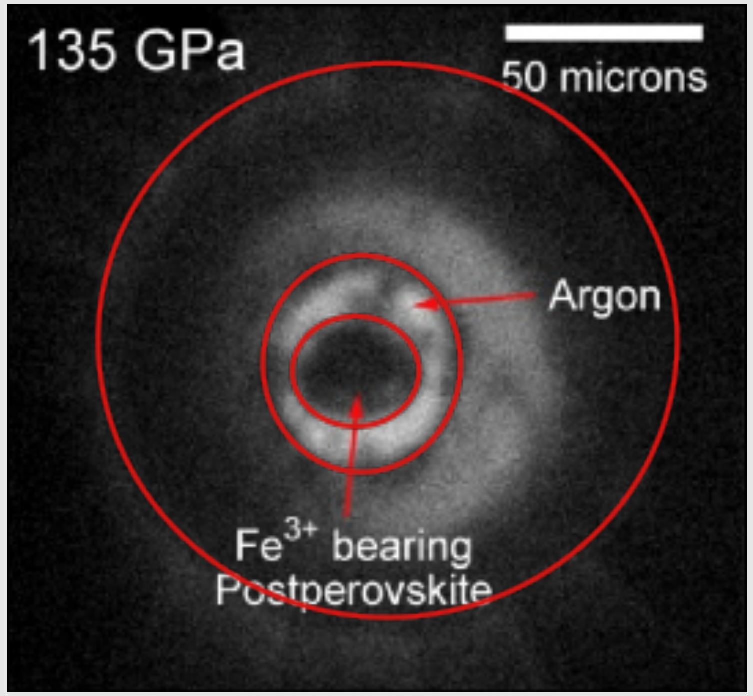

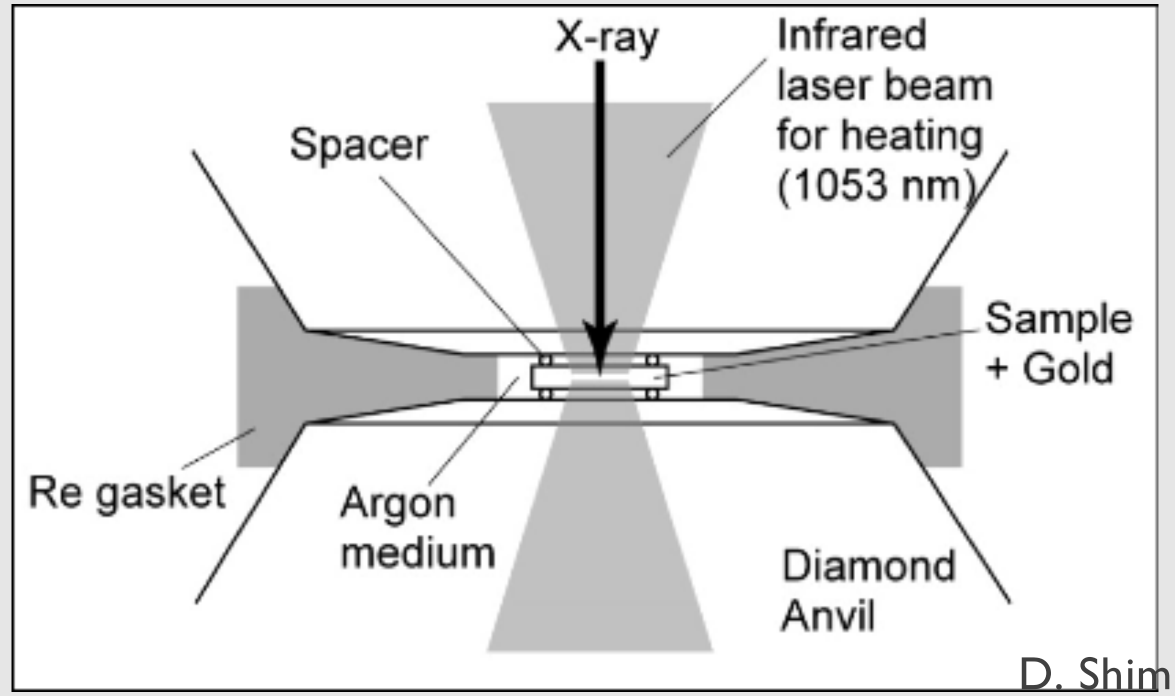

D. Shim

- 75-150 µm diamond culets depending on peak pressure
- 4 x 6 μm^2 X-ray beam spot
- λ = 0.3344 Å (E = 37.778 keV)
- 20 µm laser spot for heating

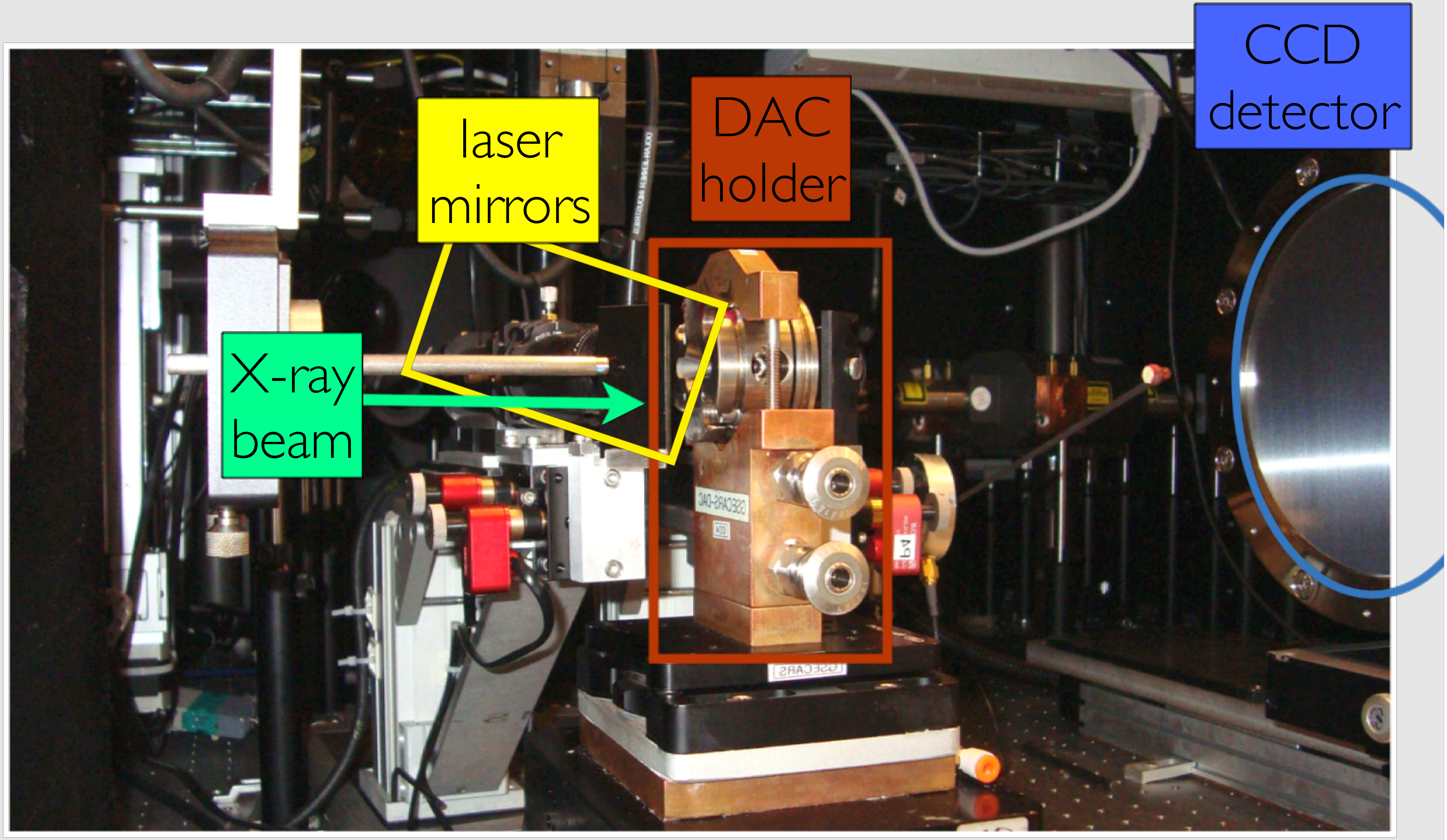

Photo courtesy B. Grocholski

Setup at GSECARS, 13IDD, Advanced Photon Source, Argonne National Lab

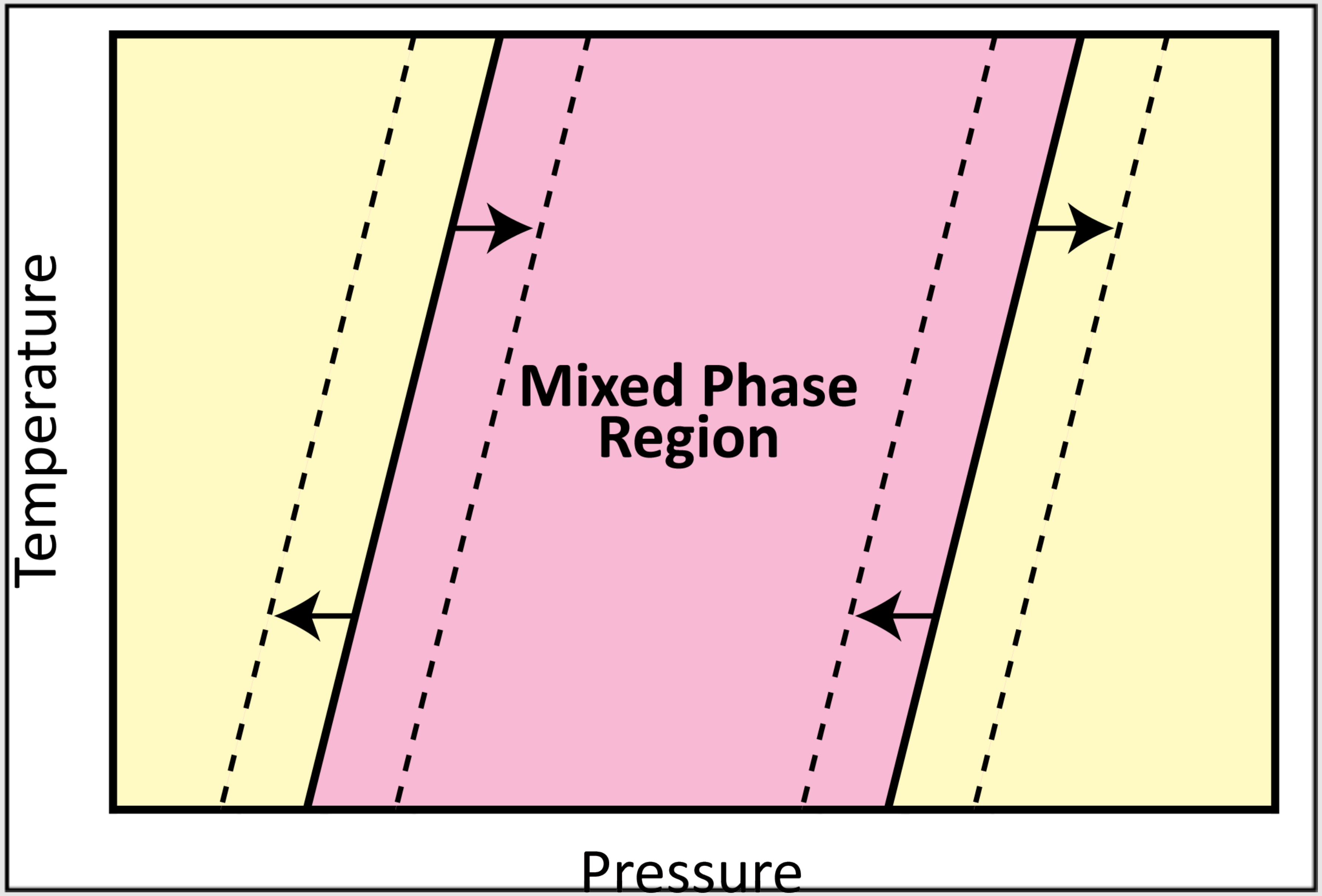

D. Shim

- Kinetic effects are reduced by:
  - long heating durations (1+ hours) and high temperatures (T = 2000~3000 K)
  - reversal measurements

Effect of ferropericlase, (Mg,Fe)O

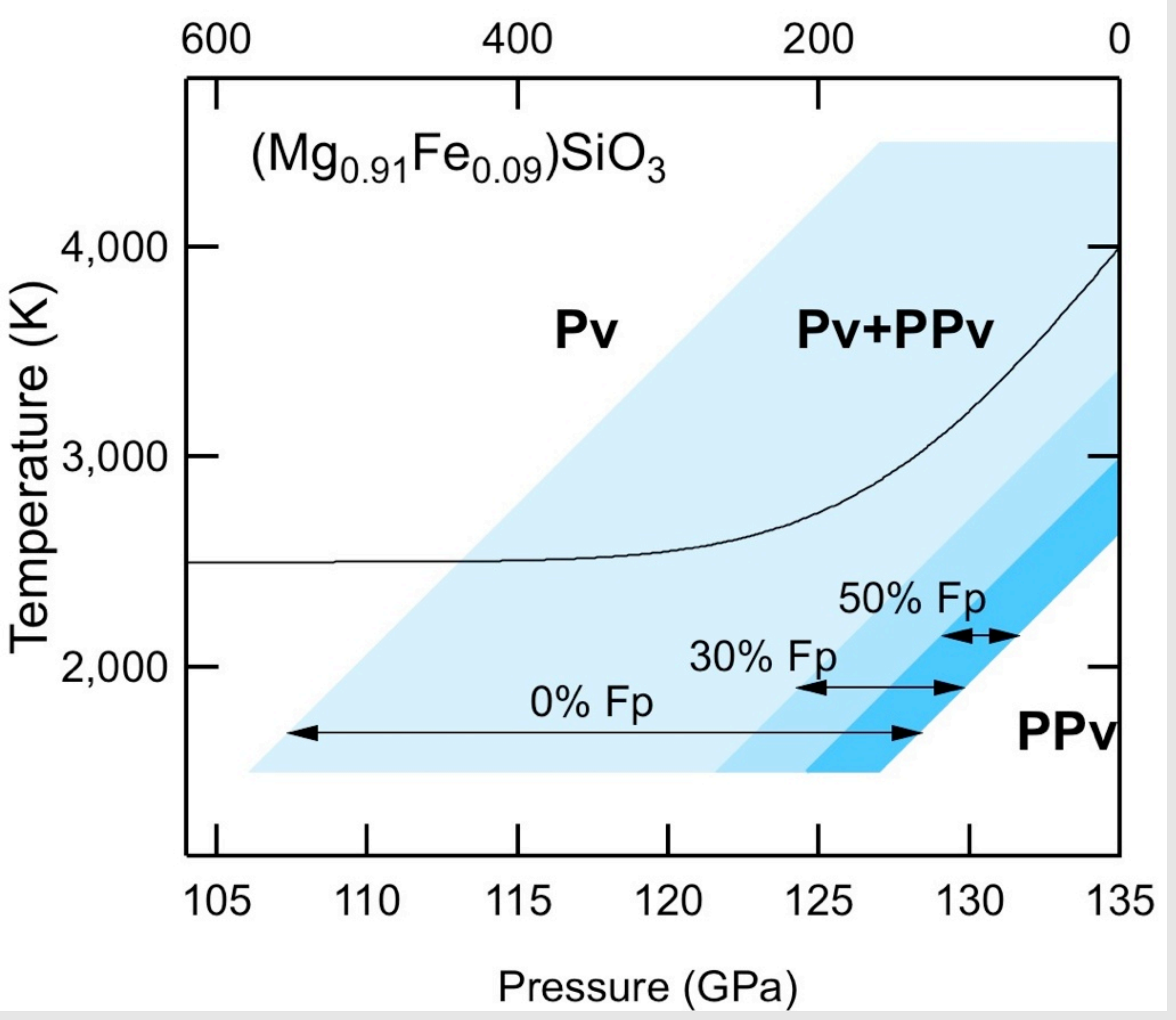

Catalli et al., 2009, Nature

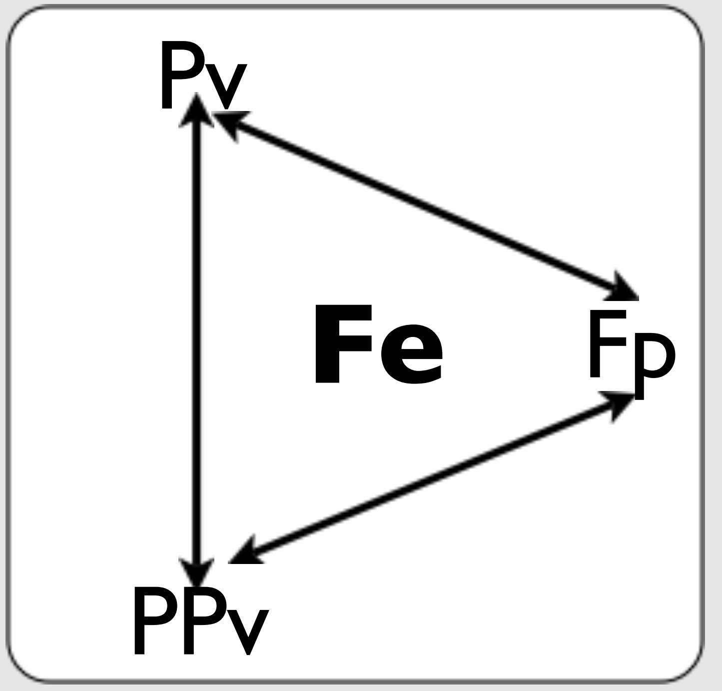

Thermodynamic calculations based on an ideal solution model using experimental partitioning coefficients

Detectability

- ↓ Composition
- ↑ Mineralogy
- ↑ Preferred orientation
- ↓ Temperature gradient
- ↑ Nonlinear phase fraction

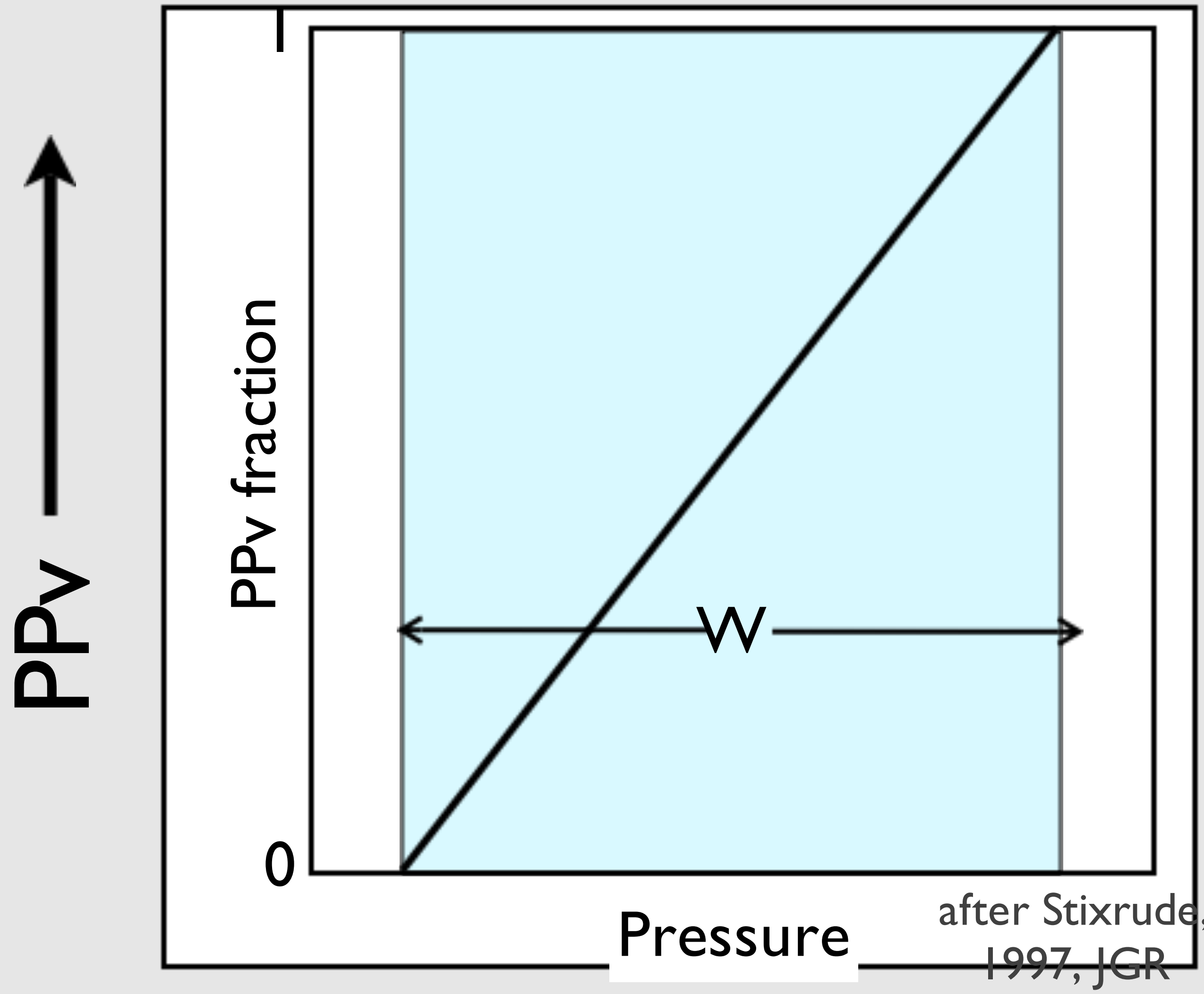

after Stixrude, 1997, JGR

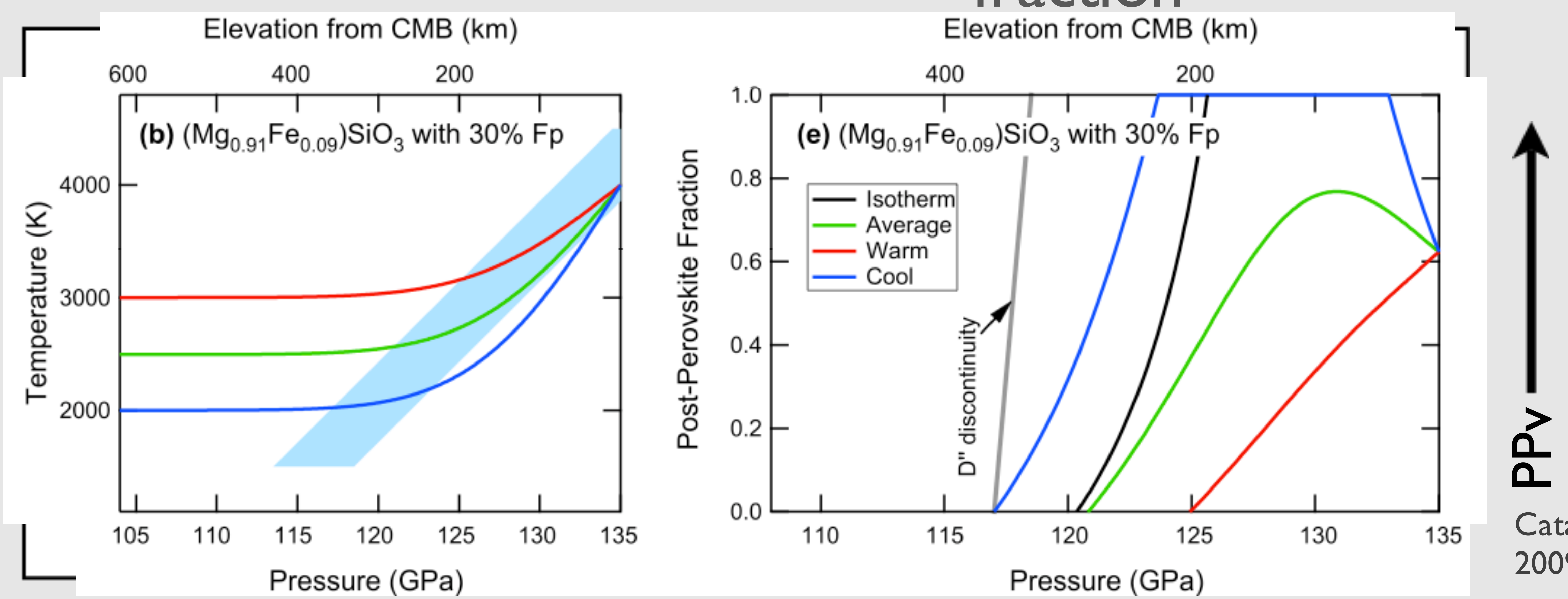

Catalli et al., 2009, Nature

Detectability

- ↓ Composition
- ↑ Mineralogy
- ↓ Temperature gradient
- ↑ Nonlinear phase fraction
- ↑ Preferred orientation

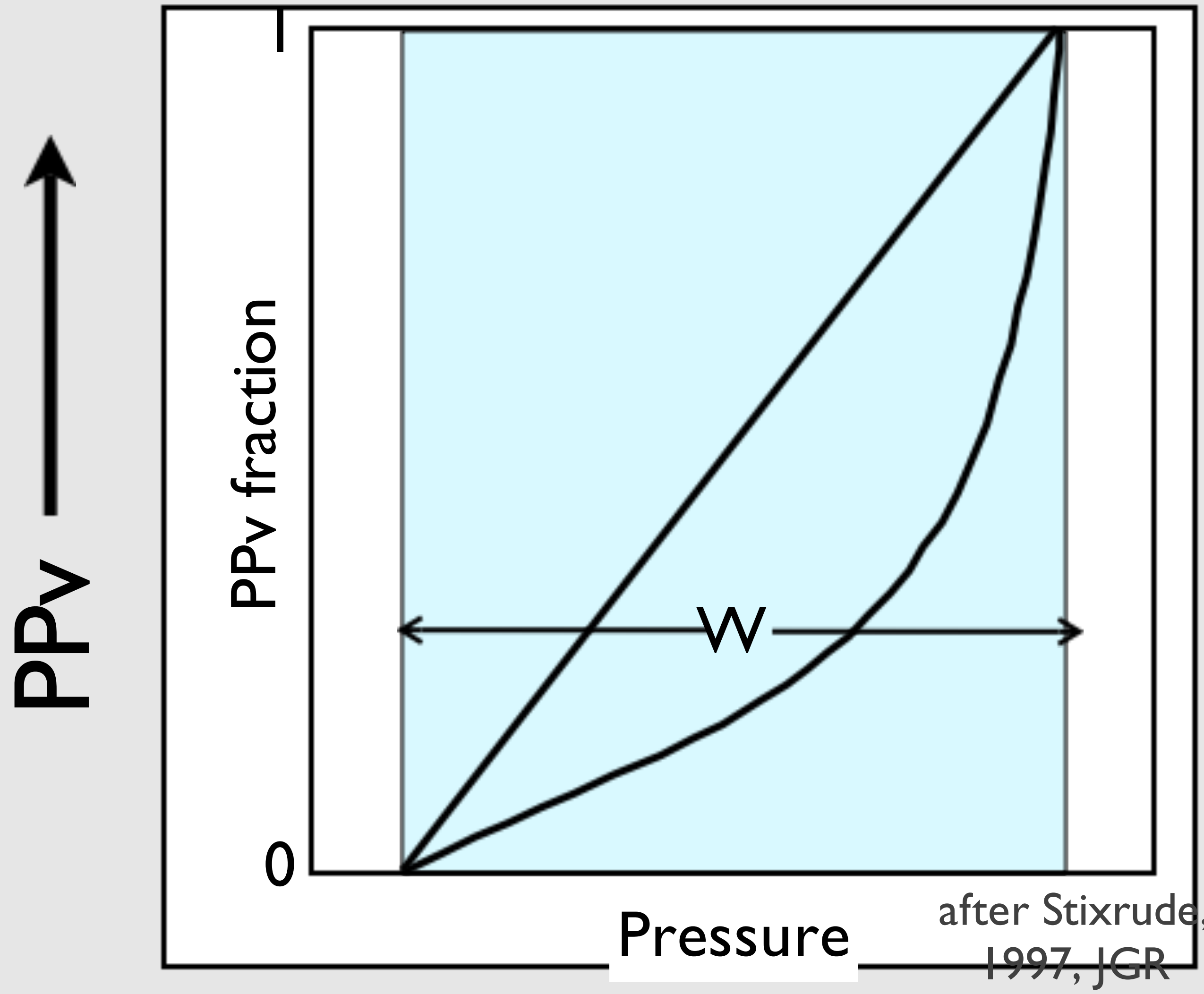

after Stixrude, 1997, JGR

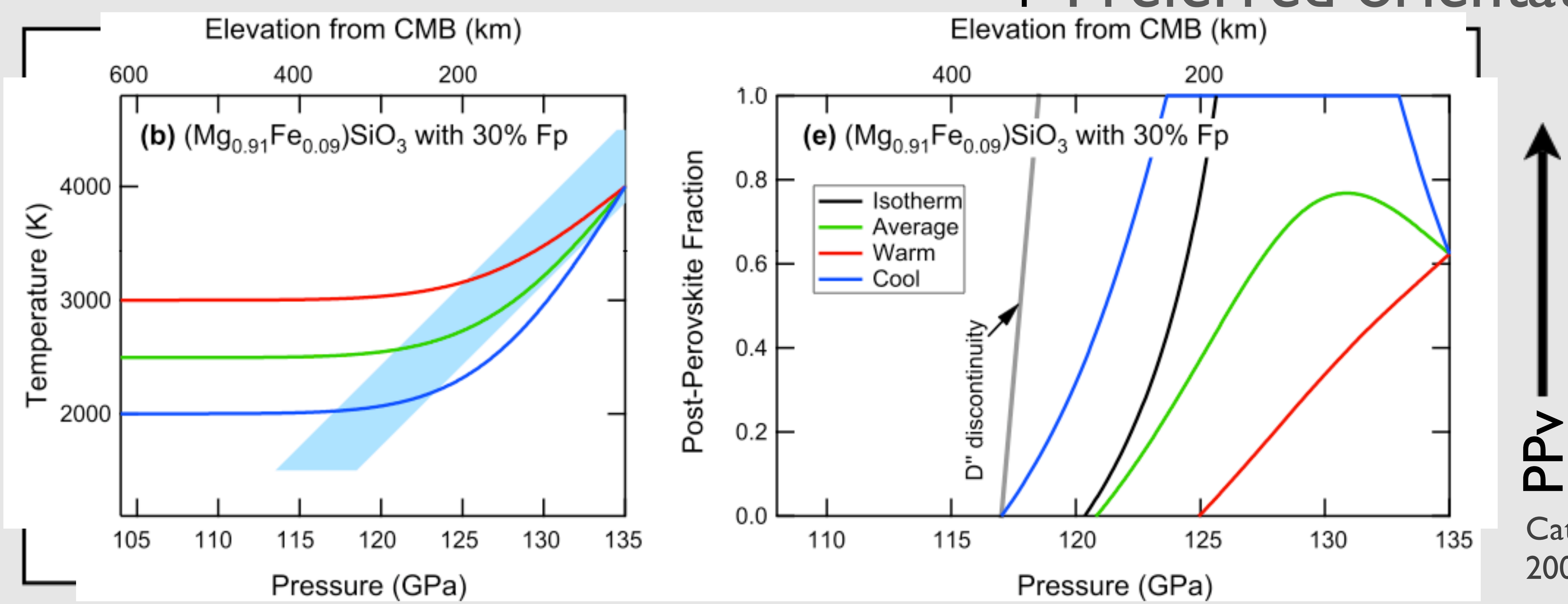

Catalli et al., 2009, Nature

Detectability

- ↓ Composition
- ↑ Mineralogy
- ↓ Temperature gradient
- ↑ Nonlinear phase fraction
- ↑ Preferred orientation

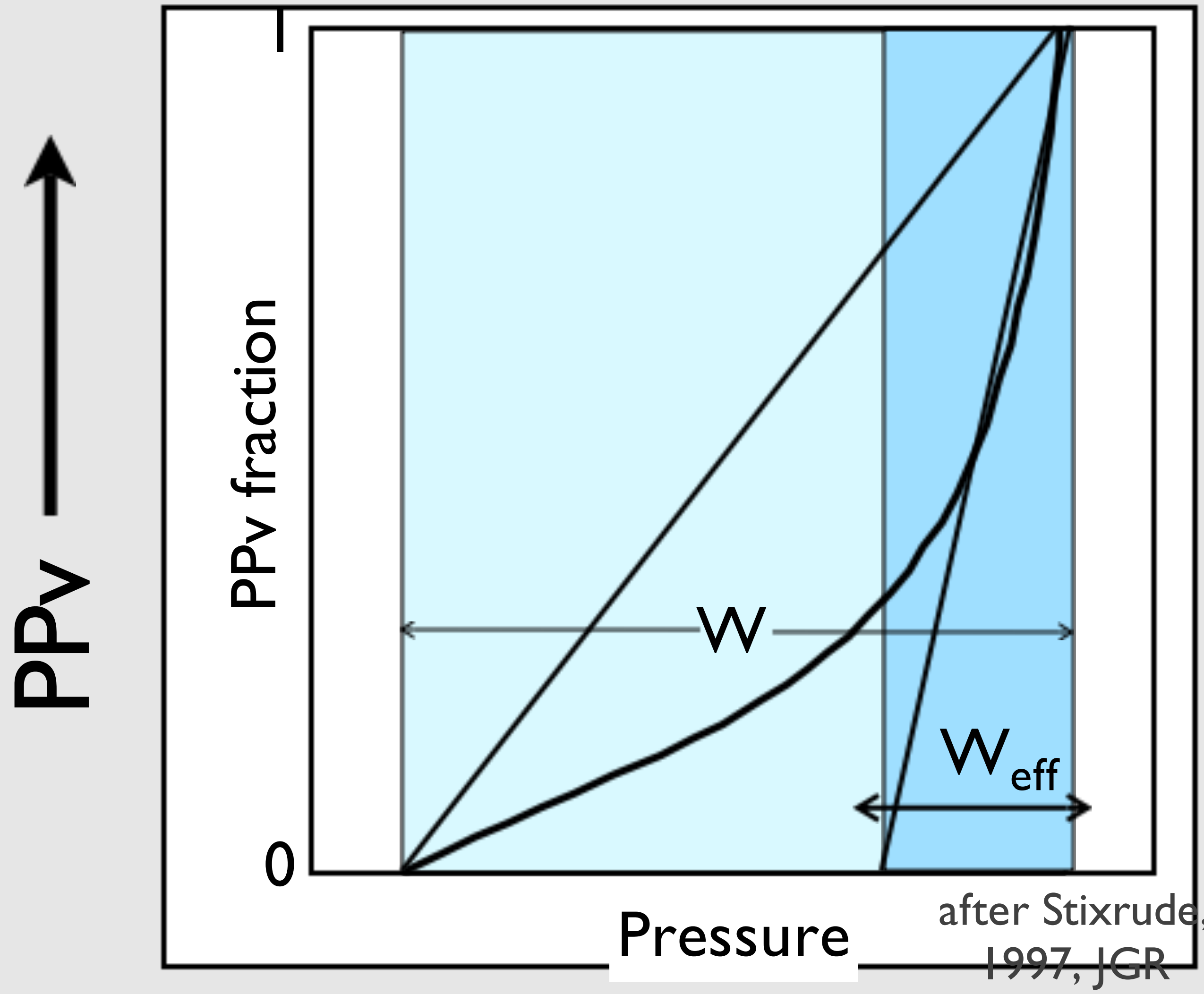

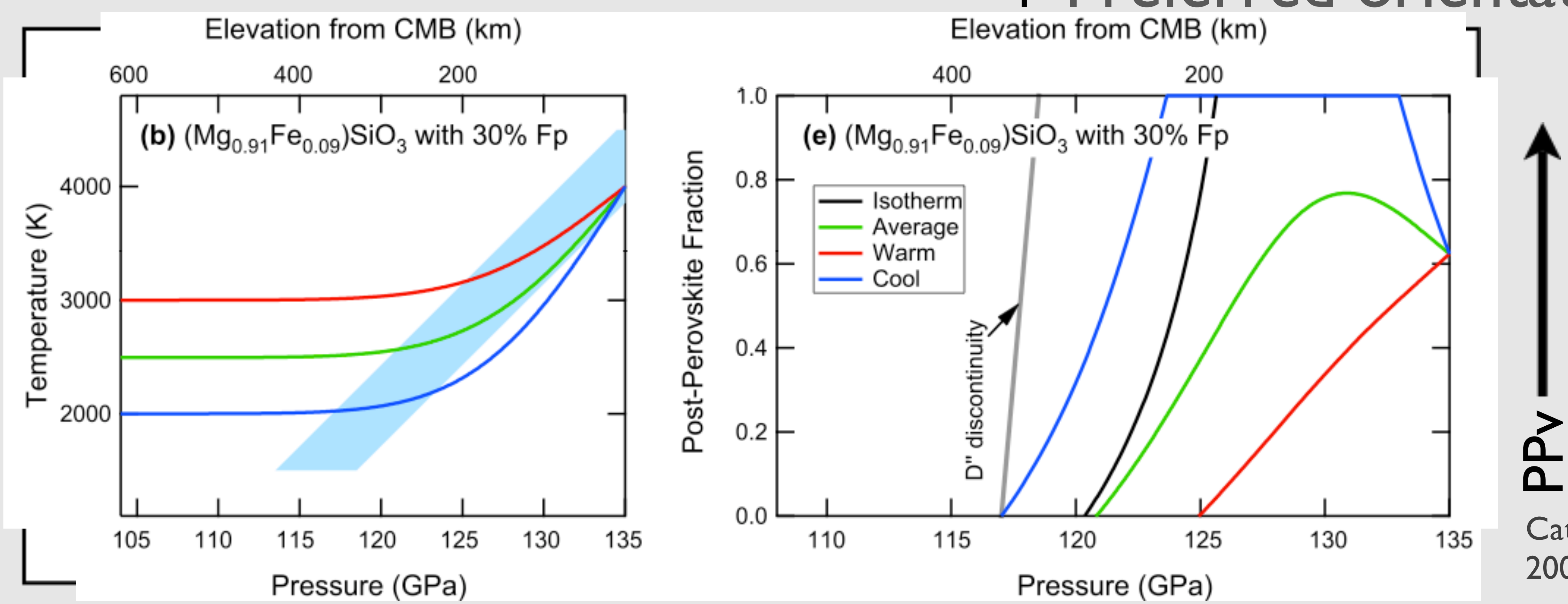

Catalli et al., 2009, Nature

Dynamic Earth

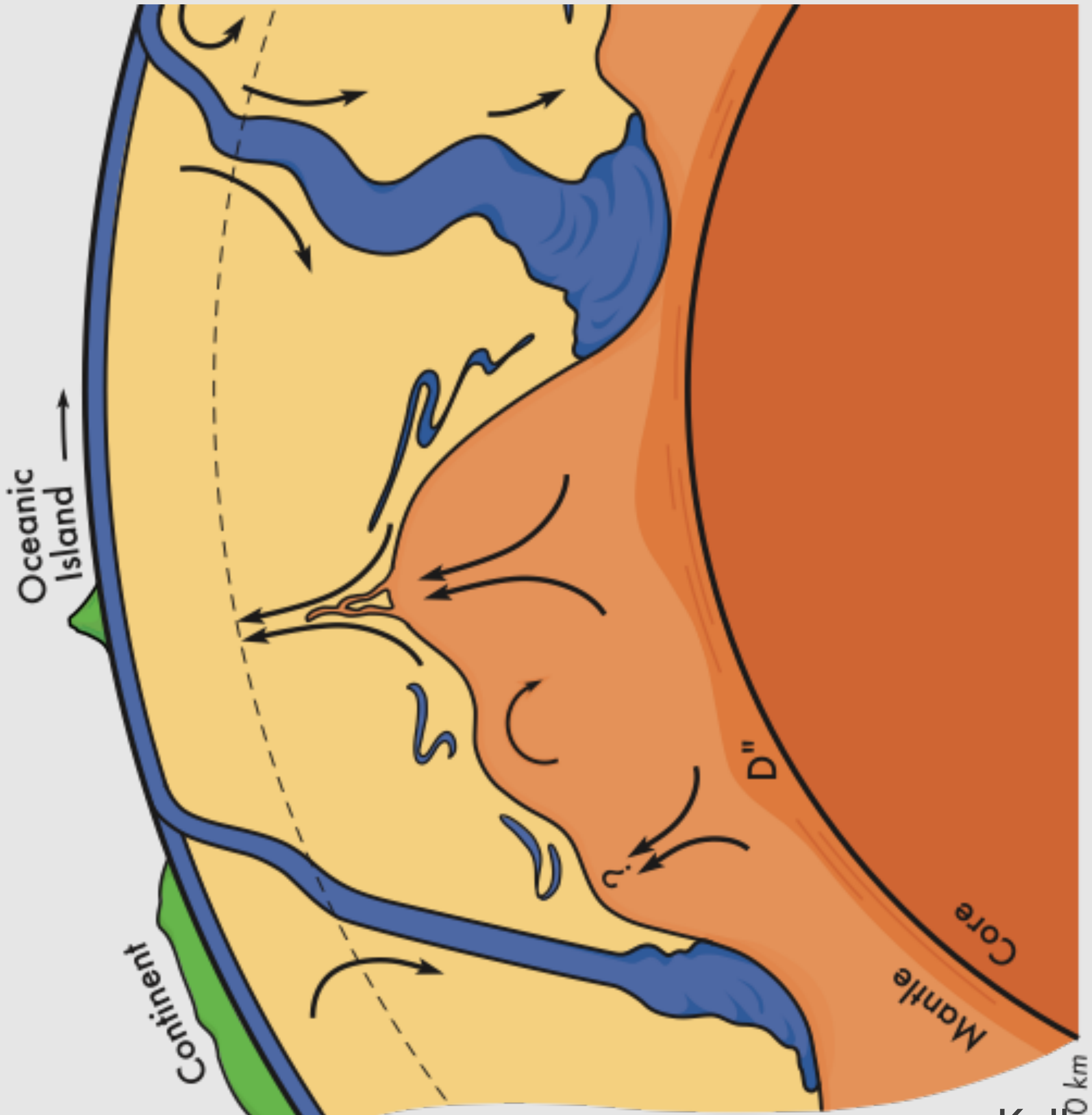

Kellogg et al., 1999, Science